Updating bounds on R-parity violating supersymmetry from meson oscillation data

Florian Domingo,[a,b,c] **Herbert K. Dreiner,**[a] **Jong Soo Kim,**[d] **Manuel E. Krauss,**[a] **Víctor Martín Lozano**[a] **and Zeren Simon Wang**[a]

[a]*Bethe Center for Theoretical Physics & Physikalisches Institut der Universität Bonn,*
Nußallee 12, 53115 Bonn, Germany

[b]*Instituto de Física Teórica (UAM/CSIC), Universidad Autónoma de Madrid,*
Cantoblanco, E-28049 Madrid, Spain

[c]*Instituto de Física de Cantabria (CSIC-UC),*
E-39005 Santander, Spain

[d]*National Institute for Theoretical Physics,*
School of Physics and Mandelstam Institute for Theoretical Physics,
University of the Witwatersrand, Johannesburg, Wits 2050, South Africa

E-mail: florian.domingo@csic.es, dreiner@uni-bonn.de,
jongsoo.kim@tu-dortmund.de, mkrauss@th.physik.uni-bonn.de,
lozano@th.physik.uni-bonn.de, wzeren@physik.uni-bonn.de

ABSTRACT: We update the bounds on R-parity violating supersymmetry originating from meson oscillations in the $B_{d/s}^0$ and K^0 systems. To this end, we explicitly calculate all corresponding contributions from R-parity violating operators at the one-loop level, thereby completing and correcting existing calculations. We apply our results to the derivation of bounds on R-parity violating couplings, based on up-to-date experimental measurements. In addition, we consider the possibility of cancellations among flavor-changing contributions of various origins, *e.g.* from multiple R-parity violating couplings or R-parity conserving soft terms. Destructive interferences among new-physics contributions could then open phenomenologically allowed regions, for values of the parameters that are naively excluded when the parameters are varied individually.

Contents

1 Introduction

Several years of operation of the LHC have (as yet) failed to reveal any conclusive evidence for physics beyond the Standard Model (SM) [1]. On the contrary, experimental searches keep placing ever stronger limits on hypothesized strongly [2–5] and even weakly-interacting [6] particles in the electroweak-TeV range. While this situation tends to leave the simpler models in an uncomfortable position, for the so-called "CMSSM" see for example ref. [7], it also advocates for a deeper study of more complicated scenarios, satisfying the central motivations of the original paradigm but also requiring more elaborate experimental investigations for testing.

Softly-broken supersymmetric (SUSY) extensions of the SM [8, 9] have long been regarded as a leading class of candidates for the resolution of the hierarchy problem [10], as well as a possible framework in view of understanding the nature of dark matter or the unification of gauge-couplings. The simplest of such models, the Minimal Supersymmetric Standard Model (MSSM), has thus been the focus of numerous studies in the past decades. An implicit ingredient of the usual MSSM is R-parity (R_p) [11], a discrete symmetry related to baryon and lepton number. In addition to the preservation of these quantum numbers, R_p is also invoked in order to justify the stability of the lightest SUSY particle, leaving it in a position of a dark-matter candidate [12].

Despite its attractive features, R_p conservation is not essential to the phenomenological viability of a SUSY model. R_p violation (RpV) — see [13, 14] for reviews — is viable as well; simply a different discrete (or gauge) symmetry is required [15–18]. It also leads to a distinctive phenomenology which is relevant to LHC searches [19, 20].

With experimental constraints now coming from both low-energy physics and the high-energy frontier, it seems justified to give the RpV-phenomenology a closer look, beyond the tree-level or single-coupling approximations that are frequently employed in the literature.

In this paper, we consider the most general RpV-model with minimal superfield content. The superpotential of the R_p-conserving MSSM is thus extended by the following terms [21]:

$$W_{\not{R}_p} = \mu_i H_u \cdot L_i + \frac{1}{2}\lambda_{ijk}L_i \cdot L_j \bar{E}_k + \lambda'_{ijk}L_i \cdot Q_j \bar{D}_k + \frac{1}{2}\lambda''_{ijk}\varepsilon_{abc}\bar{U}_i^a \bar{D}_j^b \bar{D}_k^c, \qquad (1.1)$$

where Q, $\bar{U}$, $\bar{D}$, L, $\bar{E}$ denote the usual quark and lepton superfields, $\cdot$ is the $SU(2)_L$ invariant product and ε_{abc} is the 3-dimensional Levi-Civita symbol. The indices i, j, k refer to the three generations of flavor, while a, b, c correspond to the color index. We note that symmetry-conditions may be imposed on the parameters λ_{ijk} and λ''_{ijk} without loss of generality: $\lambda_{ijk} = -\lambda_{jik}$, $\lambda''_{ijk} = -\lambda''_{ikj}$. The first three sets of terms of eq. (1.1) violate lepton-number and the last set of terms violates baryon-number.

The superpotential of eq. (1.1) contains several sources of flavor-violation, in both the lepton and the quark sectors. Such effects are steadily searched for in experiments, placing severe bounds on the parameter space of the model. The impact of lepton-flavor violating observables on the RpV-MSSM has been discussed extensively in the literature, see e.g. [22–46]. In the quark sector, observables such as leptonic B-decays or radiative $b \to s$ transitions [47–49] have been considered. Here, we wish to focus on neutral-meson mixing observables, ΔM_K, ΔM_d, ΔM_s, for K^0, B_d^0 and B_s^0 mesons, respectively. Such observables have been discussed in the R-parity conserving [50, 51] as well as in an RpV context in the past [47, 52–59]. Yet, diagrams beyond the tree-level and box contributions as well as sfermion or RpV-induced mixings have been routinely ignored. The purpose of this paper consists in addressing these deficiencies and proposing a full one-loop analysis of the meson-mixing observables in the RpV-MSSM.

From the experimental perspective, the measurements of B-meson oscillations by the ALEPH, DELPHI, L3, OPAL, CDF, D0, BABAR, Belle, ARGUS, CLEO and LHCb collaborations have been combined by the Heavy-Flavor Averaging Group [60], leading to the averages:

$$\Delta M_d^{exp} = 0.5065 \pm 0.0019 \text{ ps}^{-1}, \qquad (1.2a)$$

$$\Delta M_s^{exp} = 17.757 \pm 0.021 \text{ ps}^{-1}. \qquad (1.2b)$$

These values are in excellent agreement with the SM computations [61–63], resulting in tight constraints on new physics contributions. However, we note that the latest SM evaluation of ΔM_s [64] is in tension with eq. (1.2). This largely appears as a consequence of the new lattice evaluation of the non-perturbative parameter $f_{B_s}^2 B_{B_s}$ by ref. [65], with reduced uncertainties. While this situation interestingly favors effects beyond the SM, we prefer to remain conservative as long as the new value of $f_{B_s}^2 B_{B_s}$ is not confirmed by other studies. We thus assume that the uncertainties on the SM prediction are still of the order of the older computations.

For the $K^0 - \bar{K}^0$ system, the Particle Data Group [66] combines the experimental measurements as:

$$\Delta M_K^{exp} = (0.5293 \pm 0.0009) \cdot 10^{-2} \text{ ps}^{-1}. \tag{1.3}$$

Despite the precision of this result, constraints from $K^0 - \bar{K}^0$ mixing on high-energy contributions are considerably relaxed by the large theoretical uncertainties due to long-distance effects. Historically, estimates of the latter have been performed using the techniques of large N QCD — see e.g. ref. [67] — while lattice QCD collaborations such as [68] are now considering the possibility of evaluating these effects in realistic kinematical configurations. Ref. [69] settles for a long-distance contribution at the level of $(20 \pm 10)\%$ of the experimental value, and we follow this estimate below. Concerning short-distance contributions, ref. [70] performed a NNLO study of the charm-quark loops, resulting in a SM estimate of $\Delta M_K^{\text{SM, Short Dist.}} = (0.47 \pm 0.18) \cdot 10^{-2} \text{ ps}^{-1}$.

Beyond the mass differences, CP-violating observables are also available in the meson-mixing system. Although our study is valid for these as well, we will not discuss them in the following, since we do not wish to pay much attention to the new-physics phases.

The computation of the meson oscillation parameters is usually performed in a low-energy effective field theory (EFT), where short-distance effects intervene via the Wilson coefficients of dimension 6 flavor-changing ($\Delta F = 2$) operators [71]. This procedure ensures a resummation of large logarithms via the application of the renormalization group equations (RGE) from the matching high-energy (e.g. electroweak) scale down to the low-energy (meson-mass) scale where hadronic matrix elements should be computed [72]. In this work, we calculate the contributions to the Wilson coefficients arising in the RpV-MSSM up to one-loop order. The λ' couplings of eq. (1.1) already generate a tree-level diagram. Going beyond this, at one-loop order, diagrams contributing to the meson mixings involve both R-parity conserving and R-parity violating couplings. These are furthermore intertwined via RpV-mixing effects stemming for example from the bilinear term $\mu_i H_u \cdot L_i$. Our analysis goes beyond the approximations that are frequently encountered in the literature. We also find occasional differences with published results, which we point out accordingly.

In the following section, we present the general ingredients of our full one-loop analytical calculation of the Wilson coefficients of the $\Delta F = 2$ EFT (effective field theory) in the RpV-MSSM, referring to the appendices where the exact expressions are provided. In section 3, we discuss our implementation of these results employing the public tools SPheno [73, 74], SARAH [75–80], FlavorKit [81] and Flavio [82]. Finally, numerical limits on the RpV-couplings are presented in a few simple scenarios, before a short conclusion.

2 Matching conditions for the $\Delta F = 2$ EFT of the RpV-MSSM

We consider the $\Delta F = 2$ EFT relevant for the mixing of $(\bar{d}_i d_j)$-$(\bar{d}_j d_i)$ mesons — d_i corresponds to the down-type quark of ith generation (d, s or b). The EFT Lagrangian is written as

$$\mathcal{L}_{\text{EFT}} = \sum_{i=1}^{5} C_i O_i + \sum_{i=1}^{3} \tilde{C}_i \tilde{O}_i, \tag{2.1}$$

where we employ the following basis of dimension 6 operators:

$$O_1 = (\bar{d}_j \gamma^\mu P_L d_i)(\bar{d}_j \gamma_\mu P_L d_i), \qquad \tilde{O}_1 = (\bar{d}_j \gamma^\mu P_R d_i)(\bar{d}_j \gamma_\mu P_R d_i),$$
$$O_2 = (\bar{d}_j P_L d_i)(\bar{d}_j P_L d_i), \qquad \tilde{O}_2 = (\bar{d}_j P_R d_i)(\bar{d}_j P_R d_i), \qquad (2.2)$$
$$O_3 = (\bar{d}_j^a P_L d_i^b)(\bar{d}_j^b P_L d_i^a), \qquad \tilde{O}_3 = (\bar{d}_j^a P_R d_i^b)(\bar{d}_j^b P_R d_i^a),$$
$$O_4 = (\bar{d}_j P_L d_i)(\bar{d}_j P_R d_i), \qquad O_5 = (\bar{d}_j^a P_L d_i^b)(\bar{d}_j^b P_R d_i^a).$$

The superscripts $(a, b = 1, 2, 3)$ refer to the color indices when the sum is not trivially contracted within the fermion product. We have employed the usual four-component spinor notations above, with $P_{L,R}$ denoting the left- and right-handed projectors.

The Wilson coefficients C_i, $\tilde{C}_i$ associated with the operators of eq. (2.2) in the Lagrangian of the EFT — eq. (2.1) — are obtained at high-energy by matching the $d_i \bar{d}_j \to d_j \bar{d}_i$ amplitudes in the EFT and in the full RpV-MSSM. We restrict ourselves to the leading-order coefficients (in a QCD/QED expansion) on the EFT-side. On the side of the RpV-MSSM, we consider only short-distance effects, i.e. we discard QCD or QED loops. Indeed, the photon and gluon are active fields in the EFT, so that a proper processing of the corresponding effects would require a NLO matching procedure. Furthermore, both tree-level and one-loop contributions are considered in the RpV-MSSM: we stress that this does not induce a problem in power-counting, as the tree-level contribution is a strict RpV-effect, so that R_p-conserving (or violating) one-loop amplitudes are not (all) of higher QED order. Numerically speaking, one possibility is that the tree-level is dominant in the Wilson coefficients, in which case, the presence of the one-loop corrections does not matter. This case is essentially excluded if we consider the experimental limits on the meson-oscillation parameters. If, on the contrary, the tree-level contribution is of comparable (or subdominant) magnitude with the one-loop amplitudes, then the electroweak power-counting is still satisfied. Yet, one-loop contributions that are aligned with the tree-level always remain subdominant.

For our calculations in the RpV-MSSM, we employ the Feynman 't Hooft gauge [83] and dimensional regularization [84, 85]. For reasons of consistency with the tools that we employ for the numerical implementation, $\overline{DR}$-renormalization conditions will be applied. However, in the results that we collect in the appendix, the counterterms are kept in a generic form, which allows for other choices of renormalization scheme. We apply the conventions where the sneutrino fields do not take vacuum expectation values.[1] Moreover, the λ' couplings of eq. (1.1) are defined in the basis of down-type mass-states, i.e. a CKM matrix appears when the second index of λ' connects with an up-type field, but not when it connects to a down-type field [52]. Mixing among fields are considered to their full extent, including left/right and flavor squark mixings, charged-Higgs/slepton mixing, neutral-Higgs/sneutrino mixing, chargino/lepton mixing and neutralino/neutrino mixing. The details of our notation and the Feynman rules employed can be found in appendix A. As a crosscheck, we performed the calculation using two different approaches for the fermions: the usual four-component spinor description and the two-component description [88].

---

[1]For the general rotation to this basis see ref. [86]. See also ref. [87] for a discussion of this in terms of physics at the unification scale.

(a) Tree-level Feynman diagram (appendix B)

(b) Tree-level Feynman diagram with quark self-energies (appendix C)

(c) Tree-level Feynman diagram with scalar self-energies (appendix D)

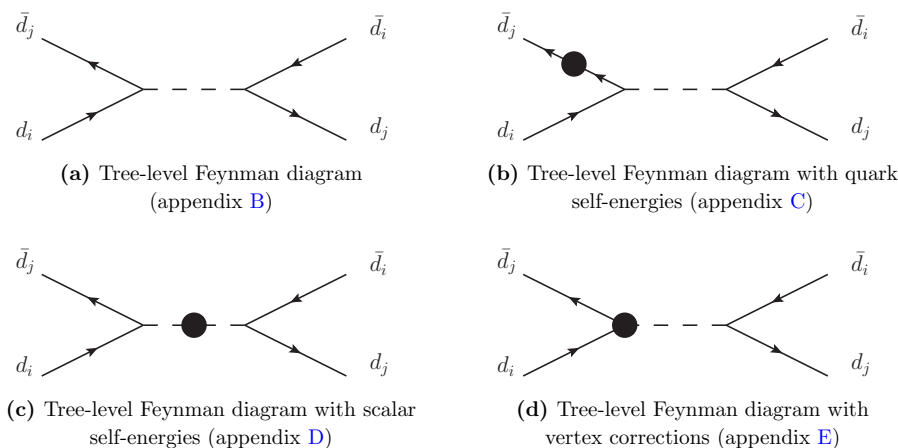**(d)** Tree-level Feynman diagram with vertex corrections (appendix E)

Figure 1. The tree level diagram and its one-loop corrections.

On the side of the EFT, the operators of eq. (2.2) each contribute four tree-level Feynman diagrams to the $d_i\bar{d}_j \to d_j\bar{d}_i$ amplitude. Half of these contributions are obtained from the other two by an exchange of the particles in the initial and final states: as the dimension 6 operators are symmetrical over the simultaneous exchange of both d_i's and both d_j's, we may simply consider two diagrams and double the amplitude. The two remaining diagrams correspond to an $(s \leftrightarrow t)$-channel exchange. We exploit these considerations to reduce the number of diagrams that we consider on the side of the RpV-MSSM to only one of the s/t-channels.

The tree-level contribution to the $d_i\bar{d}_j \to d_j\bar{d}_i$ amplitudes is due to the λ' couplings of eq. (1.1). It involves a sneutrino exchange where, however, sneutrino-flavor and sneutrino-Higgs mixing could occur. The appearance of RpV contributions at tree-level complicates somewhat a full one-loop analysis: one-loop contributions indeed depend on the renormalization of the $d_i\bar{d}_j$-sneutrino vertex (and of its external legs). In principle, one could define this vertex 'on-shell', i.e. impose that one-loop corrections vanish for on-shell d_i, d_j external legs — while the counterterm for the sneutrino field is set at momentum $p^2 = M_{K,B}^2 \simeq 0$. In such a case, one could restrict oneself to calculating the box-diagram contributions to $d_i\bar{d}_j \to d_j\bar{d}_i$. However, in any other renormalization scheme, self-energy and vertex-correction diagrams should be considered. Yet, if the λ' couplings contributing at tree-level are small, the impact of the vertex and self-energy corrections is expected to be limited, since these contributions retain a (at least) linear dependence on the tree-level λ'. These contributions are symbolically depicted in figure 1.

One-loop diagrams contributing to $d_i\bar{d}_j \to d_j\bar{d}_i$ include SM-like contributions (box diagrams with internal u, c, t quarks, W and Goldstone bosons), 2-Higgs-doublet-model-like contributions (box diagrams with internal u, c, t quarks, charged-Higgs bosons and possibly W or Goldstone bosons), R_p-conserving SUSY contributions (box diagrams with chargino/scalar-up, neutralino/sdown or gluino/sdown particles in the loop) and RpV-contributions (self-energy and vertex corrections, box diagrams with sneutrino/quark, slepton/quark, lepton/squarks, neutrino/squark or quark/squark internal lines). The RpV-
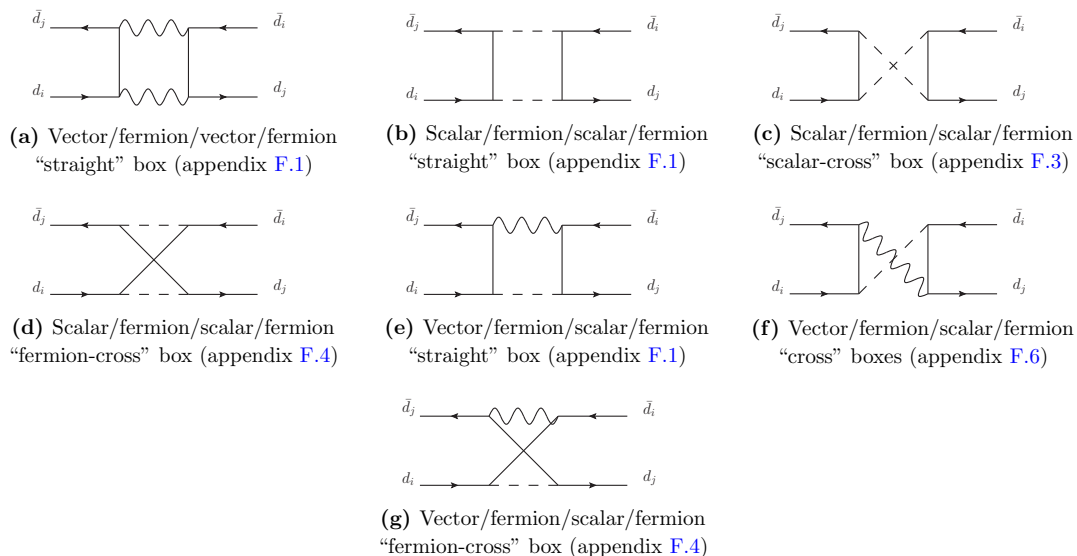
(a) Vector/fermion/vector/fermion "straight" box (appendix F.1)

(b) Scalar/fermion/scalar/fermion "straight" box (appendix F.1)

(c) Scalar/fermion/scalar/fermion "scalar-cross" box (appendix F.3)

(d) Scalar/fermion/scalar/fermion "fermion-cross" box (appendix F.4)

(e) Vector/fermion/scalar/fermion "straight" box (appendix F.1)

(f) Vector/fermion/scalar/fermion "cross" boxes (appendix F.6)

(g) Vector/fermion/scalar/fermion "fermion-cross" box (appendix F.4)

Figure 2. The topologies of box diagrams that appear in the neutral mesons mixing with the RpV-MSSM.

driven mixing further intertwines these contributions, so that the distinction among e.g. the R_p-conserving chargino/scalar-up and RpV lepton/scalar-up boxes becomes largely superfluous. For all these contributions, with exception of the self-energy diagrams on the external legs, we neglect the external momentum, as it controls effects of order $m_{d_{i,j}}$, which are subdominant when compared to the momentum-independent pieces of order M_W or M_{SUSY}. Yet, when a SM-fermion f appears in the loop, some pieces that are momentum-independent still come with a suppression of order $m_f/M_{W,\text{SUSY}}$. We keep such pieces even though they could be discarded in view of the previous argument.

The diagrams of figure 1 are calculated in appendix B (tree-level contribution), appendix C (d_i-quark self-energies), appendix D (scalar self-energy) and appendix E (vertex corrections). Figure 2 lists the various relevant topologies involved in box diagrams. The corresponding contributions are presented in appendix F. The relevant loop functions are provided in appendix A.3.

While we go beyond the usual assumptions employed to study the $\Delta F = 2$ Wilson coefficients in the RpV-MSSM, it is possible to compare the outcome of our calculation to partial results available in the literature. First, in the limit of vanishing RpV-parameters, we recover the well-known results in the R_p-conserving MSSM, which are summarized in e.g. the appendix of ref. [50]. Then, RpV-contributions from the tree-level and box-diagram topologies have been presented in ref. [47] in the no-mixing approximation. Taking this limit and neglecting further terms that are not considered by this reference, we checked that our results coincided, with the exception of the coefficient $c'^{\lambda'}_{LR}$ of ref. [47] (a piece of the contribution to C_5). Transcripted to our notations, the result of ref. [47] reads:

$$
\begin{aligned}
c'^{\lambda'}_{LR} = & -\frac{1}{64\pi^2} \lambda'^*_{i1k} \lambda'_{j2k} \lambda'_{im1} \lambda'^*_{jm2} D_2(m^2_{N_i}, m^2_{N_j}, m^2_{d_k}, m^2_{d_m}) \\
& -\frac{1}{64\pi^2} \lambda'^*_{i1k} \lambda'_{j2k} \lambda'_{im1} \lambda'^*_{jm2} D_2(m^2_{\nu_i}, m^2_{\nu_j}, m^2_{\bar{D}^k_R}, m^2_{\bar{D}^m_R}),
\end{aligned} \tag{2.3}
$$

while we obtain:

$$c_{LR}^{\prime\lambda'} = \frac{1}{32\pi^2} \lambda_{i1k}^{\prime*} \lambda_{j2k}' \lambda_{im1}' \lambda_{jm2}^{\prime*} D_2(m_{N_i}^2, m_{N_j}^2, m_{d_k}^2, m_{d_m}^2)$$
$$+ \frac{1}{32\pi^2} \lambda_{i1k}^{\prime*} \lambda_{j2k}' \lambda_{im1}' \lambda_{jm2}^{\prime*} D_2(m_{\nu_i}^2, m_{\nu_j}^2, m_{D_R^k}^2, m_{D_L^m}^2). \tag{2.4}$$

The mismatch lies in the prefactor and the sfermion chiralities. Another class of λ' boxes involving an electroweak charged current has been considered in the no-mixing limit in ref. [54]. There, we find agreement with our results. As self-energy and vertex corrections have not been considered before, the opportunities for comparison are more limited. Still, we checked that the scalar self-energies were consistent with the results of ref. [89]. Finally, our results can be controlled in another fashion, using the automatically generated results of public tools: we detail this in the following section.

3 Numerical implementation and tools

In order to determine limits from the meson oscillation measurements on the parameter space of the RpV-MSSM, we establish a numerical tool implementing the one-loop contributions to the $\Delta F = 2$ Wilson coefficients and deriving the corresponding theoretical predictions for $\Delta M_{K,d,s}$. To this end, we make use of the `Mathematica` package `SARAH` [75–80] to produce a customized spectrum generator based on `SPheno` [73, 74, 90]. `SPheno` calculates the complete supersymmetric particle spectrum at the one-loop order and includes all important two-loop corrections to the neutral scalar masses [91].

The routines performing the calculation of flavor observables are generated through the link to `FlavorKit` [81]. `FlavorKit` makes use of `FeynArts`/`FormCalc` [92–94] to calculate the leading diagrams to quark and lepton flavor violating observables. For the meson mass differences, the tree-level and box diagrams as well as the double-penguin contributions are included per default. However, as parameters within `SPheno` are defined in the $\overline{DR}$ scheme, it is in principle necessary to implement the self-energy and vertex corrections. We added the vertex corrections via `PreSARAH` [81], which enables the implementation of new operators into `FlavorKit` within certain limits. As the scalar self-energies cannot be generated in this fashion, we incorporated these by hand.

The Wilson coefficients computed by `FlavorKit` and `PreSARAH` at the electroweak matching scale are stored in analytical form in the `Fortran` output of `FlavorKit`. We compared these expressions with our results of the previous section; we found explicit agreement in almost all cases — and adapted the code to match our results in the few cases where it proved necessary.[2]

After the Wilson coefficients at the electroweak matching scale are computed, further steps are necessary in order to relate them to the observables $\Delta M_{K,d,s}$. The `FlavorKit` output includes a theoretical prediction for these observables, however the hadronic input

---

[2] In rare cases, we identified seemingly minor — but numerically important — differences between our computation and the `FlavorKit` code, namely in a few tree-level contributions to C_5 (which should be absent), as well as in $\tilde{C}_{2,3}$ and $C_{2,3}$ for a few one-loop box diagrams. We fixed those appearances in the code as well as the relative sign between tree and one-loop contributions after correspondence and cross-checking with the `FlavorKit` authors.

parameters are more up-to-date in the more recently-developed code `Flavio` [82], which shares an interface with `FlavorKit` using the FLHA standards [95]. We hence use `Flavio` to process the Wilson coefficients as calculated by `FlavorKit`. First, the Wilson coefficients must be run to a low-energy scale using the QCD RGE's of the EFT [72]. In the case of the $K^0 - \bar{K}^0$ system, the impact of the charm loop is sizable [70]: we upgraded the NLO coefficient η_{cc} coded within `Flavio` to the NNLO value 1.87(76) [70] and $\eta_{ct} = 0.496(47)$ [96]. For consistency, the charm mass in the loop functions is set to the $\overline{\text{MS}}$ value $m_c(m_c) \simeq 1.28\,\text{GeV}$. Then, the hadronic dynamics encoded in the dimension 6 operators must be interpreted at low-energy in the form of hadronic mixing elements: this step gives rise to "bag-parameters", which are evaluated in lattice QCD. Here, `Flavio` employs the bag parameters of ref. [97] for the $K^0 - \bar{K}^0$ system and of ref. [65] for the $B_d^0 - \bar{B}_d^0$ and $B_s^0 - \bar{B}_s^0$ systems. In addition, the CKM matrix elements within `Flavio` are derived from the four inputs $|V_{us}|$, $|V_{ub}|$, $|V_{cb}|$ and γ. We set these to the fit-results of ref. [66]: $|V_{us}| \simeq 0.22506$, $|V_{ub}| \simeq 3.485 \cdot 10^{-3}$, $|V_{cb}| \simeq 4.108 \cdot 10^{-2}$ and $\gamma \simeq 1.236$. Moreover, we changed the B_d^0 decay constant to a numerical value of $186\,\text{MeV}$ [98]. Finally, we added the observable ΔM_K to Flavio (based on pre-included material) and made sure that the predicted SM short-distance prediction was consistent with the theoretical SM estimate given by ref. [70].

A quantitative comparison of the predicted $\Delta M_{K,d,s}$ with the experimental results of eqs. (1.2) and (1.3) requires an estimate of the theoretical uncertainties. The Wilson coefficients have been obtained at leading order, which implies higher-order corrections of QCD-size. In the case of the SM-contributions, large QCD logarithms are resummed in the evolution of the RGEs between the matching electroweak scale and the low-energy scale. However, for the new-physics contributions, further logarithms between the new-physics and the electroweak scale could intervene — `FlavorKit` computes the new-physics contributions to the Wilson coefficients at the electroweak scale, hence missing such logarithms. Therefore, the higher-order uncertainty is larger for contributions beyond the SM and can be loosely estimated as $O\left(\frac{\alpha_S}{\pi} \log \frac{\mu_{\text{NP}}^2}{\mu_{\text{EW}}^2}\right)$, where μ_{NP} and μ_{EW} represent the new-physics and electroweak scales, respectively. Further sources of uncertainty are the RGE evolution in the EFT and the evaluation of hadronic matrix elements. For the SM matrix elements, the uncertainties on η_{cc}, η_{ct} and η_{tt} are of order 30% [70], 10% [96] and 1% [99], respectively, leading to a large SM uncertainty in ΔM_K and a smaller one in $\Delta M_{d,s}$. For the $K^0 - \bar{K}^0$ system, the bag-parameters are known with a precision of $\sim 3\%$ in the case of $B_K^{(1)}$ and $\sim 7\%$ for the other operators [97]. For the $B_d^0 - \bar{B}_d^0$ system, the uncertainty is of order 10% [65] — and even 20% for $B_{B_d}^{(3)}$. For the $B_s^0 - \bar{B}_s^0$, the bag parameters are known at about 7% accuracy [65] — 14% for $B_{B_s}^{(3)}$. Finally, CKM matrix elements contribute to the uncertainty at the level of a few percent. To summarize, we decided to estimate the theoretical uncertainties of our predictions for the meson oscillation parameters in the RpV-MSSM as follows:

- $40\% \times \left[|\Delta M_K^{\text{SM, Short. Dist.}}| + |\Delta M_K^{\text{RpV-MSSM, Short. Dist.}} - \Delta M_K^{\text{SM, Short. Dist.}}| \right]$ for the short-distance contribution to ΔM_K. As explained above, we will employ the estimate of ref. [69] for the long-distance contribution: $\Delta M_K^{\text{SM, Long Dist.}} \simeq (20 \pm 10)\% \times \Delta M_K^{exp}$.

- $15\% \times |\Delta M_{d,s}^{\text{SM}}| + 30\% \times |\Delta M_{d,s}^{\text{RpV-MSSM}} - \Delta M_{d,s}^{\text{SM}}|$ for the evaluation of $\Delta M_{d,s}$.

These uncertainty estimates restore the magnitude of the SM uncertainties [61–63, 70]. Concerning the new-physics part, we stress that the calculation employs a (QCD/QED) LO matching and misses running effects between the SUSY and the matching scales, which motivates conservative estimates.

Finally, we note that our calculation of the Wilson coefficients for the $\Delta F = 2$ transition also provides access to CP-violating observables such as ϵ_K. These would grant complementary constraints on the parameter space, in particular when the RpV-parameters of eq. (1.1) are considered as complex degrees of freedom. Obviously, in the presence of e.g. a large RpV tree-level contribution to the $d_i \bar{d}_j \to d_j \bar{d}_i$ amplitude, it is always possible to choose the phases of the λ'-parameters such that, amongst others, ϵ_K is in agreement with the experimental measurement (within uncertainties that are dominated by the theoretical evaluation [70]). On the other hand, it is less trivial whether such an adjustment would be possible within the magnitude of the NP contributions that is compatible with ΔM's. For simplicity — keeping in mind that our numerical studies are strictly illustrative in purpose and do not aim at conveying an exhaustive picture of possible RpV-effects associated to the meson-oscillation parameters —, we restrict ourselves to real values of the RpV-parameters and do not consider the CP-violating observables below. In practice, the R_p-conserving contributions beyond the SM in the scenarios that we consider in the following section are always subleading to RpV effects, so that any deviation of the CP-violating observables from the SM predictions (caused by the CKM phase) is proportional to the RpV parameters and could be compensated via the corresponding RpV phases. Of course, if one chooses not to exploit this degree of freedom, the scenario with real RpV parameters itself would be subject to stronger limits when the CP-violating observables are also taken into account.

4 Numerical results

We are now in a position to study the limits on RpV-parameters that are set by the meson-oscillation parameters. However, it makes limited sense to scan blindly over the RpV-MSSM parameter space imposing only constraints from the ΔM's. Comparable analyses of all the relevant observables for which experimental data is available would be necessary. We will thus restrict ourselves to a discussion of the bounds over a restricted number of parameters and in a few scenarios. The input parameters that we mention below correspond to the SPheno input defined at the M_Z scale.

We first consider the case where no explicit source of flavor violation appears in the R_p-conserving parameters. The flavor transition is thus strictly associated to the CKM matrix or to the RpV-effects. The latter can intervene in several fashions:

- Flavor violation in the λ' couplings could lead to tree-level contributions to the ΔM's. The relevant combinations — in the absence of sneutrino mixing — are of the form $\lambda'_{fIJ} \lambda'^*_{fJI}$, where (I, J) are the indices of the valence quarks of the considered meson — i.e. $(1, 2)$, $(1, 3)$ and $(2, 3)$ for ΔM_K, ΔM_d and ΔM_s respectively — and f is the flavor of the sneutrino mediator.

Scenario	M_A/TeV	μ/TeV	$\tan\beta$	$m_{\tilde{q}}/\mathrm{TeV}$	$M_{1,2}/\mathrm{TeV}$	M_3/TeV
SM-like	3.5	2	10	2	2	2
2HDM	0.8	2	10	2	2	2
SUSY-RpV(a)	1.2	0.6	10	$\simeq 2$	0.5	2
SUSY-RpV(b)	1.2	0.3	10	$\simeq 2\&1_{\tilde{t},\tilde{b}}$	0.5	2

Table 1. Input parameters for various scenarios under consideration. With $2\&1_{\tilde{t},\tilde{b}}$ we imply $m_{\tilde{q}_{1,2}} = 2\,\mathrm{TeV}$ while keeping a lighter third generation, $m_{\tilde{q}_3} = 1\,\mathrm{TeV}$.

- Flavor violation in the λ' couplings could also intervene at the loop-level only. This happens when, for instance, one product of the form $\lambda'_{mnI}\lambda'^*_{mnJ}$ or $\lambda'_{mIn}\lambda'^*_{mJn}$ is non-zero — again, (I, J) corresponds to the valence quarks of the meson; m and n are internal to the loop.

- Finally, the flavor transition can be conveyed by the λ'' couplings, in which case it appears only at the loop level in the ΔM's. Possible coupling combinations include $\lambda''_{m12}\lambda''_{m23}$, $\lambda''_{m12}\lambda''_{m13}$ or $\lambda''_{m13}\lambda''_{m23}$.

Below, we first consider these three cases separately, before we investigate possible interferences between tree- and loop-level generated diagrams for several non-zero λ' couplings. However, we avoid considering simultaneously non-zero $LQ\bar{D}$ and $\bar{U}\bar{D}\bar{D}$ couplings: then, discrete symmetries no longer protect the proton from decay, so that the phenomenology would rapidly come into conflict with associated bounds. Still, we note that some diagrams contributing to the meson mixing parameters would combine both types of couplings: these are also provided in the appendix.

Then, flavor transitions can also be mediated by R_p-conserving effects. In this case, flavor violation could originate either in the CKM matrix, as in the Minimal Flavor Violation scenario [100], or in new-physics parameters, such as the soft squark bilinear and trilinear terms. We briefly discuss possible interferences with RpV-contributions.

For simplicity, we consider only the case of real $\lambda'^{(\prime)}$ and disregard the bilinear R-parity violating terms (though they are included in our analytical results in the appendix).

4.1 Bounds on a pair of simultaneously non-zero $LQ\bar{D}$ couplings

4.1.1 Tree level contributions

Let us begin with the case where only two $LQ\bar{D}$ couplings are simultaneously non-vanishing and contribute to the ΔM's at tree-level. For doing so, we choose a spectrum of the form of an effective SM at low mass, where we have fixed the squark, higgsino and gaugino masses to $2\,\mathrm{TeV}$, while varying all the slepton masses simultaneously in the range $0.2 - 2\,\mathrm{TeV}$. The important parameter values are listed in the first line of table 1. In addition, the stop trilinear coupling A_t, of order $3\,\mathrm{TeV}$ (without endangering (meta)stability of the potential however[3]), is adjusted so that the lighter Higgs mass satisfies $m_h \approx 125\,\mathrm{GeV}$ (within

---

[3]The stability of the electroweak minimum was tested for individual points. To this end, we generated a model file allowing for non-vanishing squark VEVs with SARAH and tested it through the numerical code Vevacious [101], interfaced with CosmoTransitions [102]. A parameter point is deemed unstable on cosmological time-scales, and therefore ruled out, if the mean tunnelling time is smaller than 21.7% of the age of the Universe.
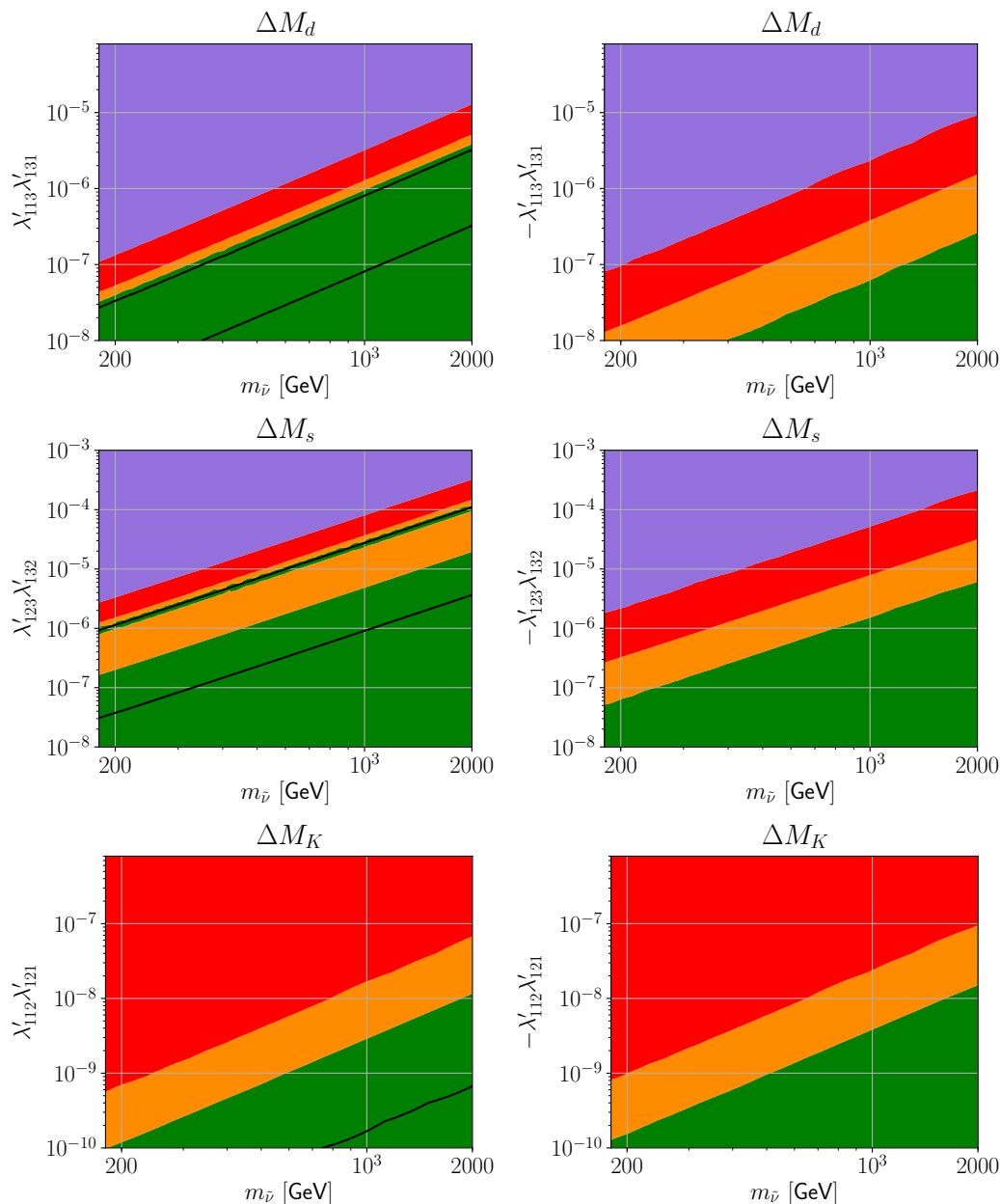
Figure 3. Constraints from the ΔM's on scenarios with RpV-mediated flavor violation contributing at tree-level, as a function of the sneutrino mass. The plots on the left correspond to the upper limit on positive $\lambda' \cdot \lambda'$; those on the right to lower limits on negative $\lambda' \cdot \lambda'$ combinations. The green, orange, red and purple colors represent regions within $[0, 1\sigma]$, $[1\sigma, 2\sigma]$, $[2\sigma, 3\sigma]$ and $> 3\sigma$ bounds, respectively. The experimental central value is exactly recovered on the black lines. For these plots, the parameter set of the scenario SM-like of table 1 has been employed.

3 GeV). We also considered several other scenarios, listed in table 1, e.g. involving lighter charged Higgs or lighter squarks of the third generation, but the general properties of the constraints remained qualitatively unchanged. In fact, the predicted values of ΔM's in the R_p-conserving limit only differ at the percent level (a barely noticeable variation in view of the uncertainties) between these four scenarios, which can be placed into the perspective of the systematic suppression of the SUSY R_p-conserving loops due to the high squark masses. As the R_p-conserving contributions do not depend on the parameters that we vary in this subsection, the $n\,\sigma$-boundaries ($n = 0, \cdots, 3$) are only shifted by an imperceptible amount in parameter space when comparing the various scenarios of table 1. Therefore, we only present the results in the SM-like scenario here. All the input is defined at the electroweak scale, so that we can discuss the various classes of RpV-contributions to the ΔM's without the blurring effect due to the propagation of flavor-violation via RGE's between a high-energy scale and the electroweak scale.

In figure 3, we present the limits set by ΔM_d, ΔM_s and ΔM_K on the tree-level flavor violating contributions. The plots in the first column are obtained for a positive product $\lambda' \cdot \lambda'$, while those in the second column correspond to negative $\lambda' \cdot \lambda'$. For each observable, the most relevant $\lambda' \cdot \lambda'$ combination, leading to a tree-level contribution, was selected. The individual sub-figures depict the extension of the $0, 1, 2, 3\,\sigma$ regions in the plane defined by the corresponding flavor-violating $\lambda' \cdot \lambda'$ product and the slepton mass. The colors in figure 3 are chosen such that purple regions are excluded at three standard deviations or more; red regions are excluded at $\geq 2\,\sigma$ — which is the limit that we apply later on, in order to decide whether a point in parameter space is excluded or allowed experimentally; the orange regions correspond to a prediction of the ΔM within 1 and $2\,\sigma$; finally, the green areas are consistent with the experimental measurement within $1\,\sigma$, while the black curves reproduce the central values exactly. Experimental and theoretical uncertainties are added in quadrature to define the total uncertainty $U_{\text{tot}} = \sqrt{U_{\text{theo}}^2 + U_{\text{exp}}^2}$. In the case of ΔM_K, the theoretical uncertainties from long-distance and short-distance contributions are also combined quadratically. Since experimentally one cannot tell apart the two mass eigenstates of $B_{d/s}^0$, we simply consider the absolute value of $\Delta M_{d/s}$ in our evaluation. When we plot $\Delta M_{d,s}$, this feature may result in a doubling of the solutions for the central value or of the $1\,\sigma$-allowed regions, such as in the upper-left and middle-left plots of figure 3. For K^0, instead, the mass ordering, and hence the sign of ΔM_K is known.

The limits that we obtain on the λ' couplings contributing at tree-level are relatively tight. In the scenarios of figure 3, the 2σ bounds read approximately:

$$\begin{cases} \lambda'_{i13}\lambda'_{i31} \lesssim 1.6 \times 10^{-6} \left(\frac{m_{\tilde{\nu}_i}}{1\,\text{TeV}}\right)^2, & -\lambda'_{i13}\lambda'_{i31} \lesssim 4 \times 10^{-7} \left(\frac{m_{\tilde{\nu}_i}}{1\,\text{TeV}}\right)^2, \\ \lambda'_{i23}\lambda'_{i32} \lesssim 3.6 \times 10^{-5} \left(\frac{m_{\tilde{\nu}_i}}{1\,\text{TeV}}\right)^2, & -\lambda'_{i23}\lambda'_{i32} \lesssim 8 \times 10^{-6} \left(\frac{m_{\tilde{\nu}_i}}{1\,\text{TeV}}\right)^2, \\ |\lambda'_{i12}\lambda'_{i21}| \lesssim 2.2 \times 10^{-8} \left(\frac{m_{\tilde{\nu}_i}}{1\,\text{TeV}}\right)^2, & \end{cases} \tag{4.1}$$

where we assume that only one lepton flavor, namely i, has non-vanishing RpV-couplings — therefore the bounds only depend on the mass of the corresponding sneutrino $\tilde{\nu}_i$. Alternatively, with degenerate sneutrinos, we could sum over the index i on the left-hand

side of eq. (4.1). Limits on these products of couplings have been presented in ref. [103] for a SUSY mass of $100\,\text{GeV}$ and in [59] for a mass of $500\,\text{GeV}$ — as explained above, our limits can be confronted to the bounds applying on $\sum_i \lambda'_{i13}\lambda'_{i31}$, etc., in these references. In comparison, the bounds that we obtain in figure 3 are somewhat stronger, at least by a factor ~ 3. This result should be put mainly in the perspective of the reduction of the experimental uncertainty in the recent years.

4.1.2 1-loop contributions to flavor transition

Next, we turn to the case where a pair of $LQ\bar{D}$ couplings mediate the flavor transition only at the loop-level and we focus on coupling combinations of the form $\lambda'_{mnI}\lambda'^*_{mnJ}$ or $\lambda'_{mIn}\lambda'^*_{mJn}$ (with I, J the valence quarks of the meson). In principle we could consider other combinations, such as $\lambda'_{mnI}\lambda'^*_{\tilde{m}nJ}$, $\lambda'_{mnI}\lambda'^*_{m\tilde{n}J}$, $\lambda'_{mIn}\lambda'^*_{\tilde{m}Jn}$ or $\lambda'_{mIn}\lambda'_{mJ\tilde{n}}$ (with $m \neq \tilde{m}$, $n \neq \tilde{n}$). However, either the associated contributions are CKM suppressed or they would require several $\lambda' \cdot \lambda'$ products to be simultaneously non-zero or non-degenerate scalar / pseudoscalar sneutrino fields. We thus restrict ourselves to the two types mentioned above. For these, we note that the limits are independent of the flavor m of the slepton field. In this context, RpV-effects in ΔM's are dominated by diagrams involving the comparatively light (charged or neutral) sleptons. We thus concentrate on these below. We can distinguish two types of contributions:

- If one of the pair of non-vanishing $LQ\bar{D}$ couplings is one of those involved for the tree-level exchange diagram — i.e. if it contains the two flavor indices of the valence quarks of the meson — we find that quark self-energy corrections on the tree-level diagram can be comparable to or even dominant over box contributions.

- If neither of the non-vanishing $LQ\bar{D}$ couplings participates in the tree-level diagrams, box diagrams are the main contributions.

This difference impacts both the magnitude of the resulting bounds and their dependence on the slepton mass, as we shall see below.

The spectrum that we focus on in this subsection (and later on) is described in the third row of table 1. The choice of the scenario SUSY-RpV(a) instead of SM-like is motivated by the wish not to systematically suppress the loop diagrams associated with charginos/neutralinos. We will also comment on the mild differences that we obtain in the other scenarios of table 1.

In figure 4, we consider non-vanishing $\lambda'_{121}\lambda'_{123}$, $\lambda'_{112}\lambda'_{113}$ and, finally, $\lambda'_{113}\lambda'_{123}$. In these cases, the box diagrams dominate over the fermionic self-energy corrections. For each scenario, the limits from the ΔM's essentially originate in one of the three observables ΔM_d, ΔM_s or ΔM_K. The corresponding limits approximately read:

$$\begin{cases} |\lambda'_{i21}\lambda'_{i23}| \lesssim 3.4 \times 10^{-2} \left(\frac{m_{\tilde{l}_i}}{1\,\text{TeV}} \right), \\ |\lambda'_{i12}\lambda'_{i13}| \lesssim 1.6 \times 10^{-1} \left(\frac{m_{\tilde{l}_i}}{1\,\text{TeV}} \right), \\ |\lambda'_{i13}\lambda'_{i23}| \lesssim 6.3 \times 10^{-2} \left(\frac{m_{\tilde{l}_i}}{1\,\text{TeV}} \right), \end{cases} \qquad (4.2)$$
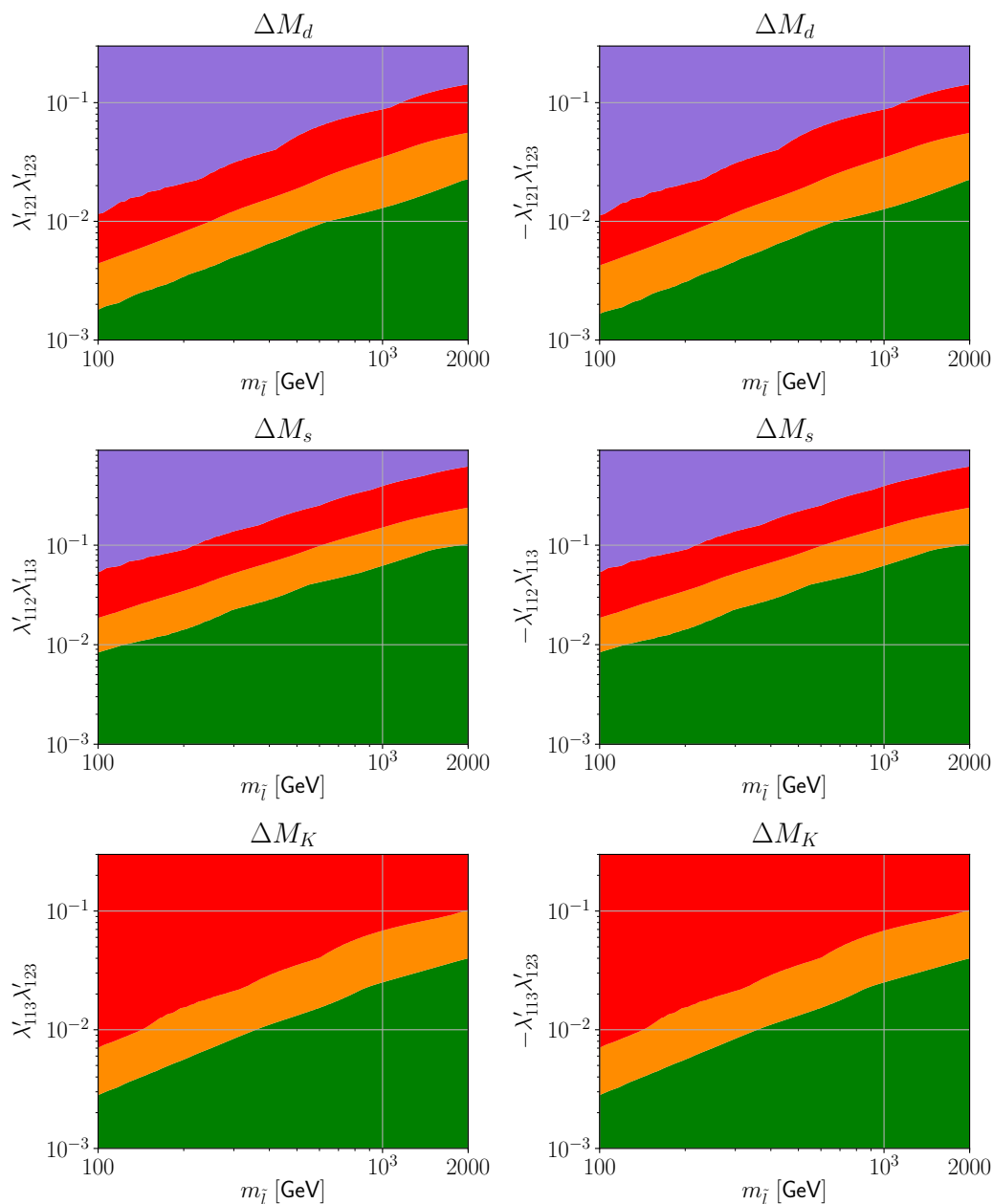
Figure 4. Constraints from the ΔM's on scenarios with RpV-mediated flavor violation of $LQ\bar{D}$-type, where the RpV-violating contribution is dominated by a box diagram. The limits are plotted against the slepton mass and follow the same color-code as figure 3. For these plots, the parameter set of the scenario SUSY-RpV(a) of table 1 has been employed.

where $m_{\tilde{l}_i}$ denotes the mass of the degenerate sneutrinos and charged sleptons. Here, we note that the mass dependence of the form $(\lambda' \cdot \lambda')^2 < c \cdot m_{\tilde{\ell}}^2$ differs from that appearing when the RpV-contribution intervenes at tree-level. It is characteristic of the leading RpV-diagrams in the considered setup, corresponding to the box formed out of two charged sleptons and two up-type quarks in the internal lines and to the box consisting of two sneutrinos and two down-type quarks: these diagrams roughly scale as $(\lambda' \cdot \lambda')^2/m_{\tilde{\ell}}^2$. As a consequence, the limits for positive and negative $\lambda' \cdot \lambda'$ products are comparable. In addition, the bounds on $\lambda' \cdot \lambda'$ now scale about linearly with the sparticle mass.

Expectedly, the limits are much weaker in these box-dominated scenarios than in the case where the flavor transition appears at tree-level. Refs. [54, 55, 59] presented limits on the corresponding coupling-combinations for a sfermion mass of 100 or 500 GeV. The bounds that we derive are of the same order. Similarly to the case where the RpV-contribution to the flavor transition is mediated at tree-level, the investigation of the various scenarios of table 1 results in very little variations.

Finally, we turn to the case where one of the non-vanishing λ' involves both flavors of the valence quarks of the K^0, $B_{d,s}^0$ meson while the other is flavor-diagonal (and contains only one of the valence flavors). Then, the dominant diagrams are of the form of figure 1b: one $\Delta F = 1$ transition is mediated by the non-vanishing λ' with both valence-flavor indices, while the second $\Delta F = 1$ transition appears at the loop level — typically through a SM loop (W/up-type quark), i.e. in association with the CKM matrix. We stress that such contributions were dismissed in previous analyses and are considered here for the first time.

Corresponding scenarios are displayed in figure 5, where ΔM_{B_d}, ΔM_{B_s} and ΔM_K are plotted against $\lambda'_{131} \cdot \lambda'_{133}$, $\lambda'_{132} \cdot \lambda'_{133}$ and $\lambda'_{121} \cdot \lambda'_{122}$, respectively. The bounds have a comparable scaling to that appearing in the scenario with tree-level sneutrino exchange, but the constraints are far weaker. At $2\,\sigma$:

$$\begin{cases} \lambda'_{i31}\lambda'_{i33} \lesssim 6 \times 10^{-4} \left(\frac{m_{\tilde{\nu}_i}}{1\,\text{TeV}}\right)^2, & -\lambda'_{i31}\lambda'_{i33} \lesssim 2.7 \times 10^{-3} \left(\frac{m_{\tilde{\nu}_i}}{1\,\text{TeV}}\right)^2, \\ \lambda'_{i32}\lambda'_{i33} \lesssim 1.4 \times 10^{-2} \left(\frac{m_{\tilde{\nu}_i}}{1\,\text{TeV}}\right)^2, & -\lambda'_{i32}\lambda'_{i33} \lesssim 3 \times 10^{-3} \left(\frac{m_{\tilde{\nu}_i}}{1\,\text{TeV}}\right)^2, \\ |\lambda'_{i21}\lambda'_{i22}| \lesssim 1.5 \times 10^{-3} \left(\frac{m_{\tilde{\nu}_i}}{1\,\text{TeV}}\right)^2, \end{cases} \qquad (4.3)$$

where $-\lambda'_{i31}\lambda'_{i33}, -\lambda'_{i32}\lambda'_{i33} > 0$. Due to the inclusion of the missing and obviously relevant self-energy diagrams, the bounds that we report are accordingly tighter than in the literature [54, 55, 59]. If we compare the various scenarios of table 1, we again observe little change at the qualitative level. However, the exact position of the $n\,\sigma$ ($n = 0, \cdots, 3$) boundaries is shifted by a numerical prefactor of order unity, homogeneous in the whole range of scanned parameters of figure 5. This prefactor is characteristic of the magnitude R_p-conserving loop entering the off-diagonal quark self-energy. For example, the upper-bounds on $\lambda'_{131}\lambda'_{133}$ are stronger by a factor ~ 2 in the SM-like scenario, as compared to the scenario SUSY-RPV(a) (shown in the plots), by a factor ~ 1.3 in the scenario 2HDM and by a factor ~ 1.6 in the scenario SUSY-RPV(b). Other numbers (of the same order) intervene for the two other considered sets of $\lambda' \cdot \lambda'$.
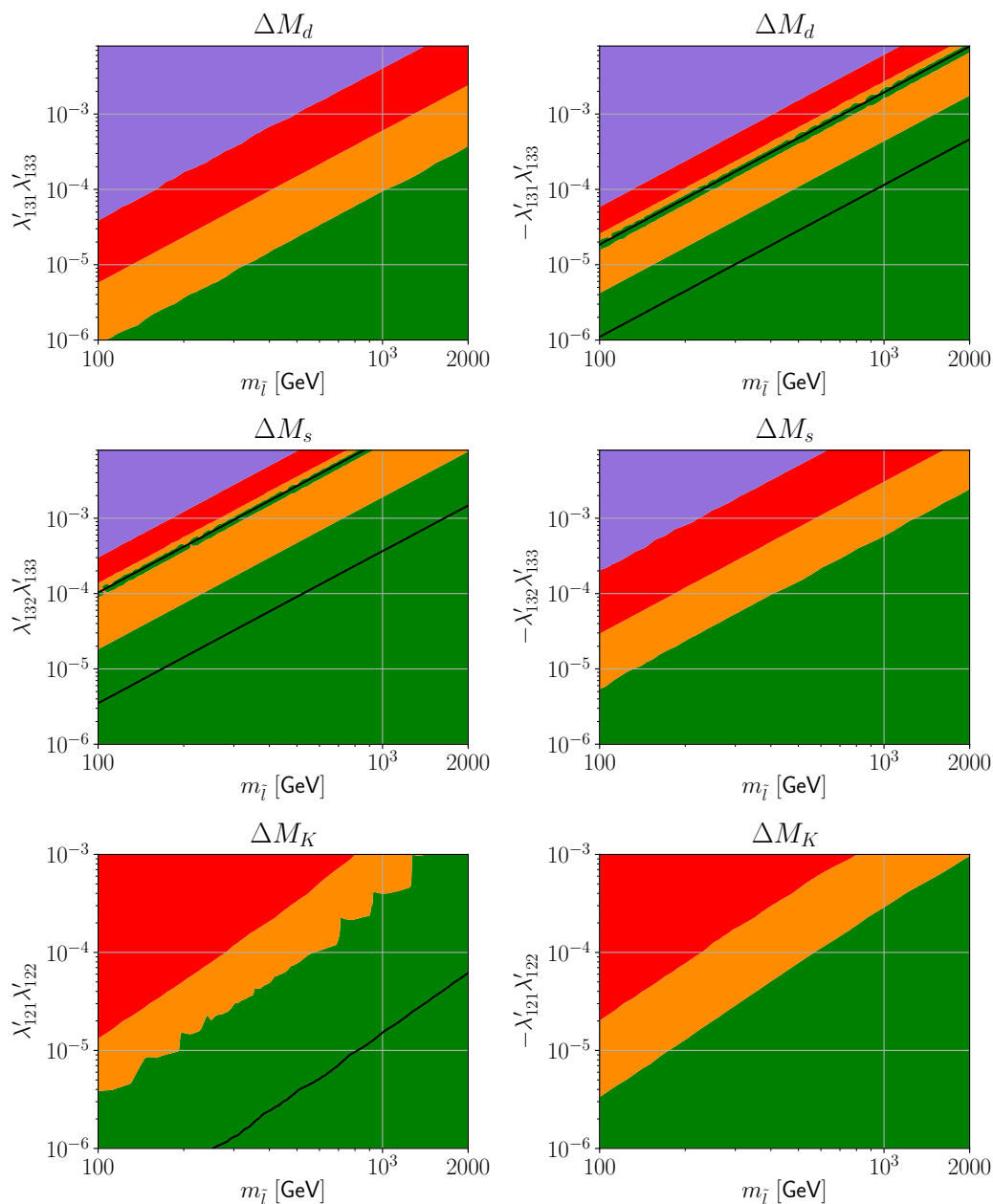
Figure 5. Constraints from the ΔM's on scenarios with RpV-mediated flavor violation of $LQ\bar{D}$-type, where the dominant RpV-diagram involves a one-loop quark self-energy. The limits are plotted against the sneutrino mass and follow the color code of figure 3. For these plots, the parameter set of the scenario SUSY-RpV(a) of table 1 has been employed.

$\Delta m_{B_d^0}$		$\Delta m_{B_s^0}$		Δm_{K^0}	
$|\lambda'_{ijk} \cdot \lambda'_{imn}|$	2σ bound	$|\lambda'_{ijk} \cdot \lambda'_{imn}|$	2σ bound	$|\lambda'_{ijk} \cdot \lambda'_{imn}|$	2σ bound
$(i31)(i13)^{(\mathrm{T})}$	1.6×10^{-6}	$(i32)(i23)^{(\mathrm{T})}$	3.6×10^{-5}	$(i12)(i21)^{(\mathrm{T})}$	2.2×10^{-8}
$(i11)(i13)^{(\mathrm{S})}$	1.8×10^{-3}	$(i22)(i23)^{(\mathrm{S})}$	9.5×10^{-3}	$(i12)(i11)^{(\mathrm{S})}$	1.5×10^{-3}
$(i21)(i13)^{(\mathrm{S})}$	$[2.8 \times 10^{-4}]$	$(i12)(i23)^{(\mathrm{S})}$	$[4.2 \times 10^{-2}]$	$(i22)(i21)^{(\mathrm{S})}$	1.5×10^{-3}
$(i31)(i23)^{(\mathrm{S})}$	0.15	$(i32)(i13)^{(\mathrm{S})}$	0.33	$(i12)(i31)^{(\mathrm{S})}$	9×10^{-6}
$(i31)(i33)^{(\mathrm{S})}$	2.7×10^{-3}	$(i32)(i33)^{(\mathrm{S})}$	1.4×10^{-2}	$(i32)(i21)^{(\mathrm{S})}$	4.2×10^{-5}
$(i21)(i23)^{(\mathrm{B})}$	3.4×10^{-2}	$(i12)(i13)^{(\mathrm{B})}$	0.16	$(i32)(i11)^{(\mathrm{B})}$	0.64
$(i21)(i33)^{(\mathrm{B})}$	0.64	$(i22)(i33)^{(\mathrm{B})}$	0.74	$(i22)(i31)^{(\mathrm{B})}$	0.24
$(i11)(i33)^{(\mathrm{B})}$	0.64	$(i12)(i33)^{(\mathrm{B})}$	4	$(i22)(i11)^{(\mathrm{B})}$	4
$(i11)(i23)^{(\mathrm{B})}$	N/A	$(i22)(i13)^{(\mathrm{B})}$	N/A	$(i32)(i31)^{(\mathrm{B})}$	0.01
$(i12)(i31)^{(\mathrm{S})}$	$[0.012]$	$(i23)(i31)^{(\mathrm{S})}$	N/A	$(i21)(i11)^{(\mathrm{S})}$	5×10^{-3}
$(i13)(i32)^{(\mathrm{S})}$	$[0.73]$	$(i22)(i32)^{(\mathrm{S})}$	0.23	$(i22)(i12)^{(\mathrm{S})}$	5.8×10^{-3}
$(i13)(i33)^{(\mathrm{B})}$	0.05	$(i23)(i33)^{(\mathrm{S})}$	0.24	$(i23)(i12)^{(\mathrm{S})}$	2.2×10^{-2}
$(i11)(i31)^{(\mathrm{B})}$	0.07	$(i21)(i32)^{(\mathrm{S})}$	$[2.25]$	$(i21)(i13)^{(\mathrm{S})}$	2.3×10^{-4}
$(i12)(i32)^{(\mathrm{B})}$	0.05	$(i21)(i31)^{(\mathrm{B})}$	0.21	$(i23)(i13)^{(\mathrm{B})}$	6.3×10^{-2}

Table 2. Compilation of the latest bounds on relevant couplings of $LQ\bar{D}$ operators, coming from the considered meson oscillation observables. These limits were established with the spectrum defined in the row SUSY-RpV(a) of table 1, with slepton and sneutrino masses of $1\,\mathrm{TeV}$. The precise 2σ boundary obviously depends on the sign of the non-vanishing $\lambda' \cdot \lambda'$ product: we always apply the most conservative (weakest) limit. In the list of couplings, the comment "(T)/(S)/(B)" indicates that the coupling product is dominated by a tree-level/quark self-energy/box contribution. "N/A" means that we did not identify upper-limits on the couplings below 4π (a rough limit from perturbativity considerations). Above the horizontal line, the non-vanishing coupling combinations select right-handed external quarks. Below this line, the external quarks are left-handed. The scaling with the sneutrino/slepton mass is roughly quadratic for all $\lambda' \cdot \lambda'$ products that contain both valence flavors in (at least) one of the non-vanishing λ', linear otherwise: see more precise explanation in the main body of the text. Some combinations contribute to two observables, such as $\lambda'_{i13}\lambda'_{i32}$, relevant for both ΔM_d and ΔM_s. In such a case, the square brackets identify the weaker limit.

In table 2, we compile the 2σ bounds on $\lambda' \cdot \lambda'$ products that we derive for $1\,\mathrm{TeV}$ sleptons in the scenario SUSY-RpV(a) of table 1 (the limits depend only weakly on the chosen scenario). In this list, the pairs $\lambda' \cdot \lambda'$ are taken non-zero only one at a time and, in particular, for a unique (s)lepton flavor i. As explained above, the scaling with the slepton/sneutrino mass depends on the choice of non-vanishing λ': essentially quadratic if at least one of the non-vanishing λ' contains both valence-flavors of the decaying meson, linear otherwise. One of the ΔM's is usually more sensitive to a specific $\lambda' \cdot \lambda'$ product than the other two. etc.

4.2 Bounds on a pair of simultaneously non-zero $\bar{U}\bar{D}\bar{D}$ couplings

We proceed with our analysis and now consider baryonic RpV, i.e. non-zero $\bar{U}\bar{D}\bar{D}$ couplings. The corresponding RpV-effects appear only at the radiative level and are dominated by box diagrams. Contrarily to existing analyses [47], we always consider heavy gluinos (as
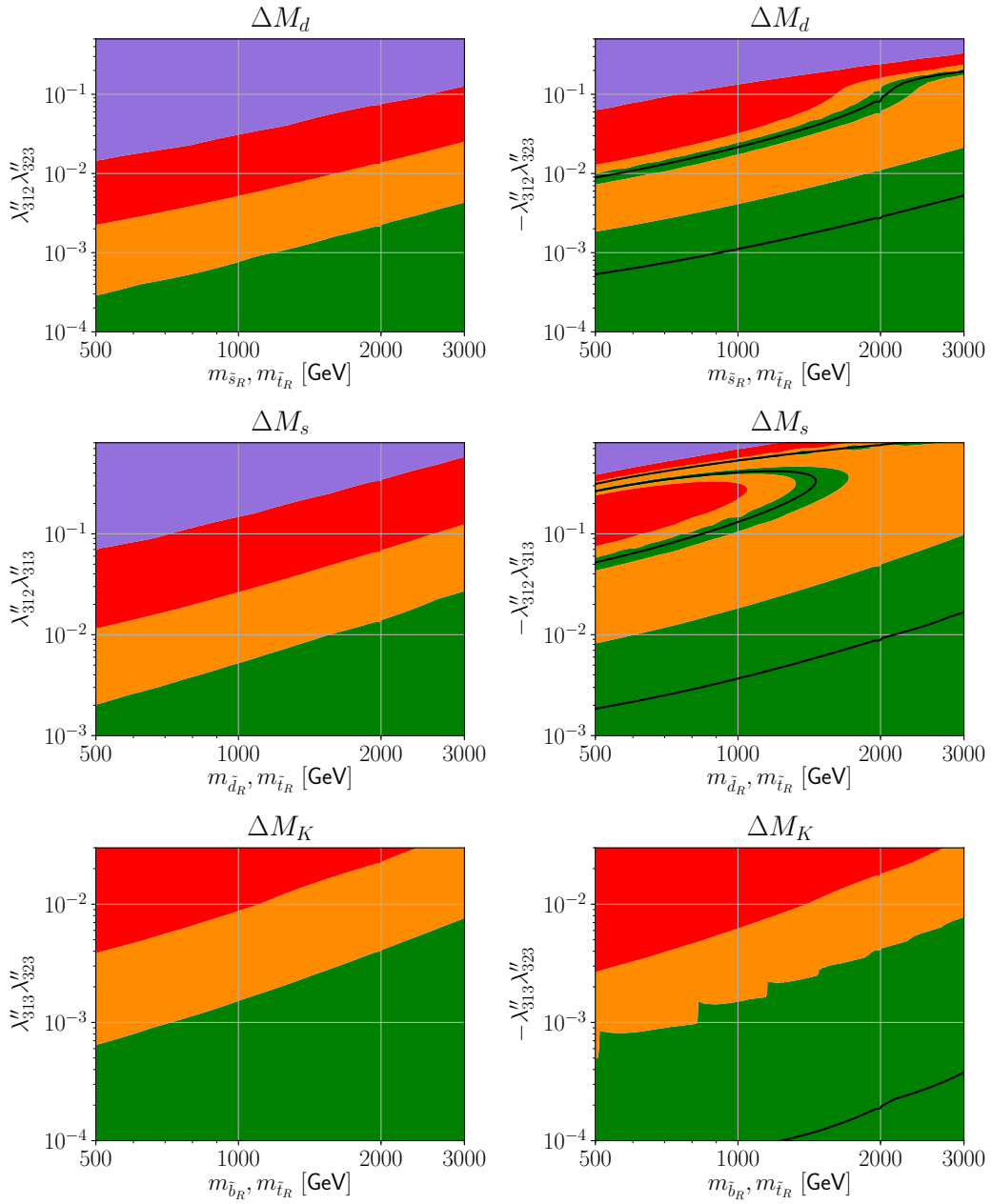
Figure 6. Limits on $\bar{U}_3 \bar{D}_i \bar{D}_j$ couplings from the meson oscillation parameters. Internal (s)top lines are allowed by such couplings. The color code is similar to that of the previous plots. For these plots, the parameter set of the scenario SUSY-RpV(a) of table 1 has been employed except for the squark masses that are scanned over.

indicated by the current status of LHC searches), so that the associated diagrams generally remain subdominant. In this setup, three classes of diagrams compete: (1) boxes including two squarks and two quarks in internal lines, which scale like $(\lambda'' \cdot \lambda'')^2$, (2) boxes including two quarks, one squark and a W-boson, which scale like $\lambda'' \cdot \lambda''$ but involve a CKM-suppression and a quark-chirality flip, and (3) similarly boxes with two squarks, one quark and a chargino, which scale like $\lambda'' \cdot \lambda''$. The matter of the chirality flip can be easily understood as only right-handed quarks couple via λ'' but only left-handed quarks couple to a W. Therefore, such diagrams with an internal W line are mostly relevant when the internal quark line involves a top-quark. As to the boxes with an internal chargino line, we also find that such contributions are mainly relevant for an internal stop line: indeed, the higgsino contribution scales with the Yukawa coupling, hence is suppressed for squarks of first or second generation. In addition, the gaugino contribution relies on left-right squark mixing, which we keep negligible for squarks of the first and second generation — making the assumption that the trilinear soft terms are proportional to the Yukawa couplings [8].

From now on, all the parameters are set to the values of the scenario SUSY-RpV(a) of table 1, except for those that are explicitly scanned over (e.g. the squark masses). In figure 6, we present the 1, 2 and $3\,\sigma$ limits on coupling combinations allowing for internal (s)top lines. The relevant right-handed squarks are assumed to be mass-degenerate. The regime with small λ'' couplings is dominated by the box diagrams involving W bosons and top quarks in the internal lines. We find that, for low mass values, this contribution scales with the squark mass in an intermediate fashion between linear and quadratic, because of the finite top mass effects. These effects largely vanish for squark masses above $\mathcal{O}(1\,\mathrm{TeV})$ and we then recover the scaling with $\frac{\lambda'' \cdot \lambda''}{m_{\tilde{q}}^2}$. The supersymmetrized version of the W boxes, i.e. boxes with internal charginos, are also contributing with a scaling of $\frac{\lambda'' \cdot \lambda''}{m_{\tilde{q}}^2}$. However their impact w.r.t. the W boxes is always reduced. At large values of the couplings and for light squarks, the purely $\bar{U}\bar{D}\bar{D}$-mediated diagrams appear to be the most relevant, scaling with $\frac{(\lambda'' \cdot \lambda'')^2}{m_{\tilde{q}}^2}$ — in analogy to the slepton box-diagrams with non-vanishing $LQ\bar{D}$ coupling — so that the bounds on $\lambda'' \cdot \lambda''$ show a roughly linear dependence with the squark mass. Then, for both large $|\lambda'' \cdot \lambda''|$ and heavier quarks, the W-mediated diagrams and these purely $\bar{U}\bar{D}\bar{D}$ boxes can be of comparable magnitude, hence lead to interference structures. This interplay between various contributions brings about a non-trivial mass dependence of the bounds on the λ'' couplings, with both constructive as well as destructive effects between the individual amplitudes. The plots for negative $\lambda'' \cdot \lambda''$ couplings perfectly illustrate this fact, in particular in the case of ΔM_s. Beyond this interference regime, at sufficiently large squark masses, the contribution from the UDD box with an internal W-line eventually supersedes the pure UDD amplitude.

Since the bounds on the individual coupling combinations do not scale with a simple power law in $m_{\tilde{q}_R}$, we refrain from showing approximate expressions as we did in the scenarios with flavor-violation of $LQ\bar{D}$-type.

In figure 7, by contrast, the choice of non-vanishing λ'' couplings does not allow for internal (s)top lines. Thus the RpV-diagrams with mixed W/squark or chargino/quark internal lines are suppressed, and the scaling of the limits from meson-oscillation parameters
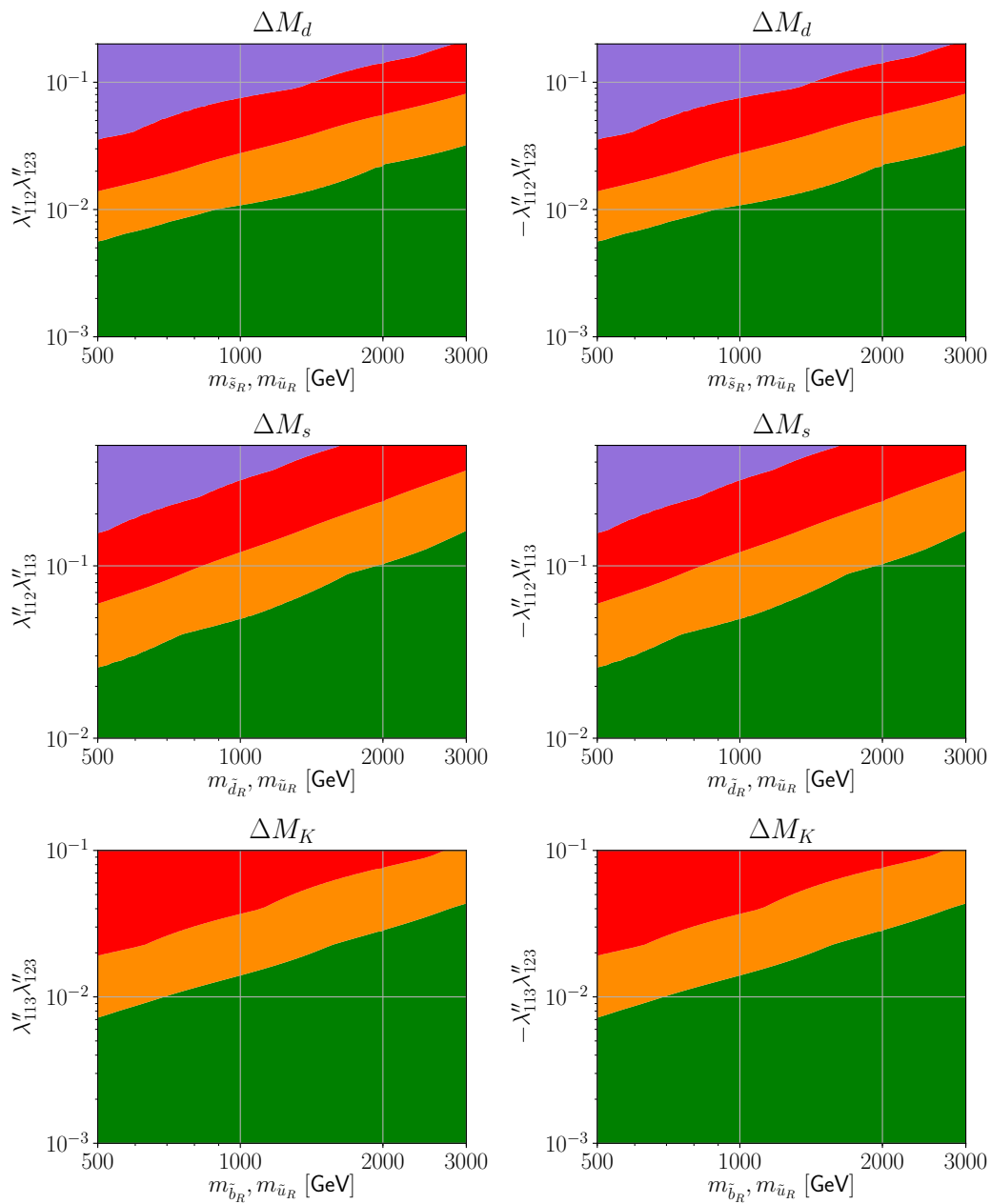
Figure 7. Limits on $\bar{U}_1\bar{D}_i\bar{D}_j$ couplings from the meson oscillation parameters. In this case, amplitudes with internal top lines vanish. The color code is similar to that of the previous plots. For these plots, the parameter set of the scenario SUSY-RpV(a) of table 1 has been employed except for the squark masses that are scanned over.

is closer to linear. In addition, the $2\,\sigma$ bounds are somewhat milder than in the previous case and roughly symmetrical for positive and negative $\lambda'' \cdot \lambda''$ products. Thus, in this case, we extract the approximate bounds on $\bar{U}_1 \bar{D}_i \bar{D}_j$ coupling pairs:

$$\begin{cases} |\lambda''_{112}\lambda''_{123}| \lesssim 2.8 \times 10^{-2} \left(\frac{m_{\tilde{s}_R, \tilde{u}_R}}{1\,\mathrm{TeV}} \right), \\ |\lambda''_{112}\lambda''_{113}| \lesssim 1.2 \times 10^{-1} \left(\frac{m_{\tilde{d}_R, \tilde{u}_R}}{1\,\mathrm{TeV}} \right), \\ |\lambda''_{113}\lambda''_{123}| \lesssim 3.6 \times 10^{-2} \left(\frac{m_{\tilde{b}_R, \tilde{u}_R}}{1\,\mathrm{TeV}} \right), \end{cases} \tag{4.4}$$

Given that the scaling of the bounds on $\lambda'' \cdot \lambda''$ pairs decidedly depends on the specific choice of couplings, we refrain from showing a compilation table as table 2 for the $LQ\bar{D}$ couplings, since it would only be representative of a specific SUSY spectrum.

4.3 Competition among $LQ\bar{D}$-driven contributions

Bounds on individual RpV-coupling products may be misleading, in the sense that several RpV-effects could cancel one another. In fact, the decomposition along the line of the low-energy flavors provides likely-undue attention to these specific directions of RpV, while the latter have no deep specificity from the high-energy perspective. In particular, RGE's are expected to mix the various flavor-directions of non-vanishing RpV-couplings, while the boundary condition at, say, the GUT scale, has no particular reason for alignment with the low-energy flavor directions [87, 104]. Obviously however, the relevant directions in flavor space are highly model-dependent and we have no particular suggestion to make from the low-energy perspective of this work. Instead, we simply wish to illustrate the possibility of allowed directions with large RpV-couplings. To this end, we allow for two non-vanishing $\lambda' \cdot \lambda'$ coupling products and investigate the limits originating in the ΔM measurements.

If we consider figures 3 and 5, the tree-level diagram for $\lambda'_{i31} \cdot \lambda'_{i13} = \mathcal{O}(10^{-6})$ and the RpV-box for $\lambda'_{i31} \cdot \lambda'_{i33} = \mathcal{O}(10^{-4})$ — implying a hierarchy $\lambda'_{i13}/\lambda'_{i33} = \mathcal{O}(10^{-2})$ — naively contribute to ΔM_d by amplitudes of comparable magnitude. Whether these contributions can interfere destructively clearly depends on the form of the amplitudes but also on the sign of the non-vanishing couplings. In figure 8, we complete the results from figures 3 and 5 by now allowing for three non-vanishing couplings. In practice, we set the slepton/sneutrino mass to $1\,\mathrm{TeV}$ and keep one $LQ\bar{D}$ coupling to a constant value: $\lambda'_{131} = 0.01$, $\lambda'_{132} = 0.1$, or $\lambda'_{121} = 0.1$. Then, we vary two independent λ', our choice depending again on the valence quarks of the considered ΔM. However, we stress that this procedure in fact opens three non-trivial $\lambda' \cdot \lambda'$ directions, so that the game is somewhat more complex than just playing one contribution versus the other.

As expected, in the plots of figure 8, the interplay of various RpV-contributions opens funnel-shaped allowed regions for comparatively large values of the $LQ\bar{D}$ couplings, highlighting the possibility of destructive interferences. We note that, considering that the tree-level and radiative contributions do not necessarily have the same scaling with respect to the slepton/sneutrino mass, the 'allowed angle' depends on the sfermion spectrum. Of course, the choice of parameters falling within the allowed funnels appears to be fine-tuned from the perspective of this work, but might be justified from a high-energy approach. On
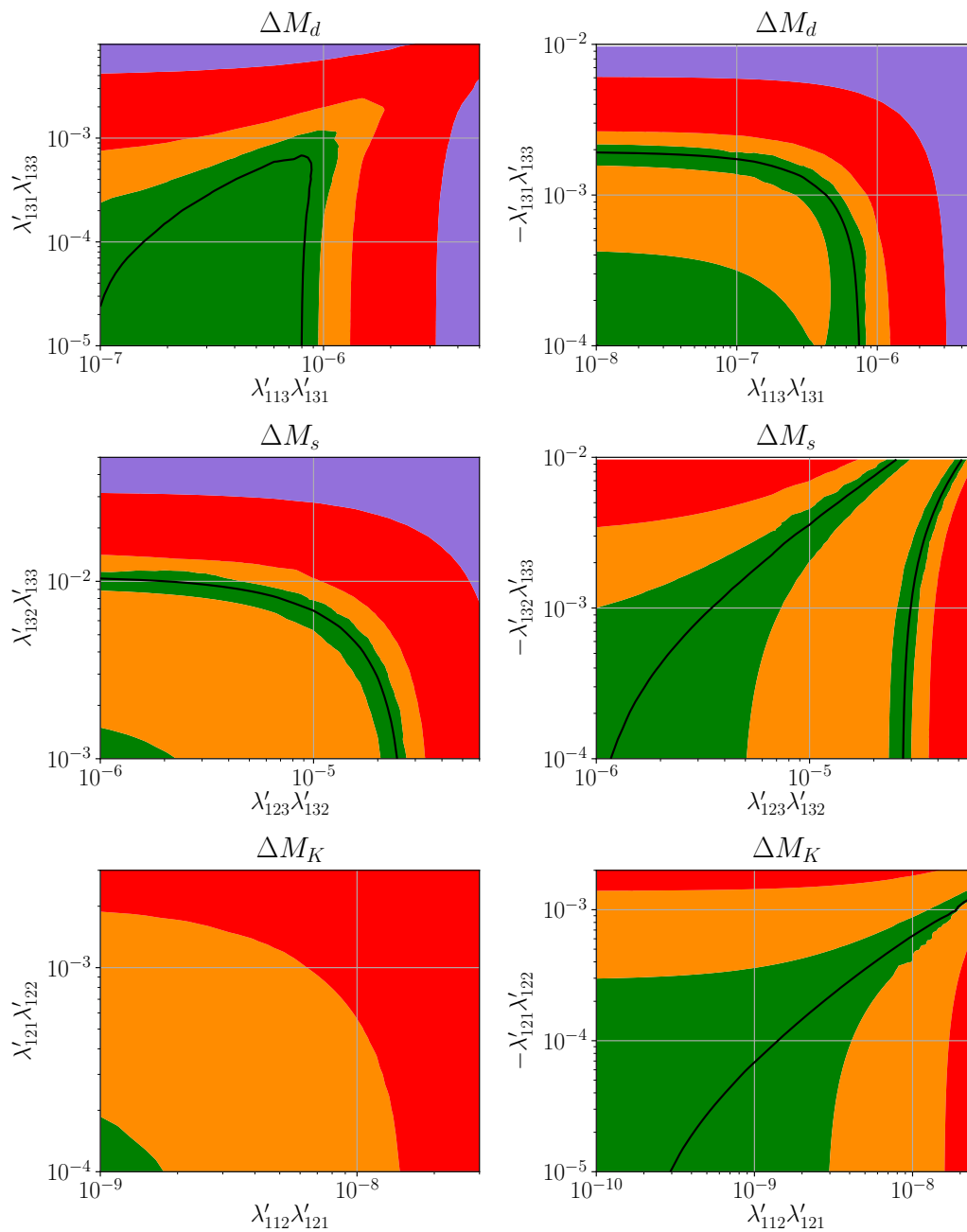
Figure 8. Limits from the meson-oscillation parameters on two RpV-directions of $LQ\bar{D}$-type. The parameters are set to the values in the third row of table 1, with slepton/sneutrinos of 1 TeV. As in the previous plots, the color code reflects the level of tension between our predictions and the experimental measurements.

the other hand, constructive interferences lead to the 'rounded edges' observed in some of the plots.

As mentioned earlier, we will not consider the interplay of $LQ\bar{D}$- and $\bar{U}\bar{D}\bar{D}$-couplings, since such scenarios are of limited relevance without a quantitative analysis of the proton decay rate. On the other hand, our discussion in this subsection points to the relevance of considering a full evaluation of the ΔM's (and other observables), when considering RpV-scenarios beyond the simplistic one-coupling-dominance approach.

4.4 Competition between flavor violation in the R-parity conserving and R-parity violating sectors

RpV-couplings are not the only new sources of flavor violation in SUSY-inspired models. In fact, the large number of possible flavor-violating parameters of the R_p-conserving soft-SUSY-breaking Lagrangian is often perceived as a weakness for this class of model, known as the SUSY Flavor Problem. In particular, the soft quadratic mass-terms in the squark sector $m^2_{Q,\bar{U},\bar{D}}$ and the trilinear soft terms $A_{U,D}$ are matrices in flavor-space that are not necessarily aligned with the flavor-structure of the Yukawa/CKM matrices. In this case, flavor-violation is generated in $L-L$, $R-R$ (for $\tilde{m}^2$) or $L-R$ (for A) squark mixing. Correspondingly, flavor-changing-neutral gluinos or neutralinos, as well as new flavor-changing chargino couplings, could contribute to $\Delta M_{K,d,s}$ in e.g. diagrams of the form of figure 2, (b–d) — see e.g. ref. [55]. Here, we wish to illustrate the potential interplay of R_p-conserving and RpV flavor violation. In particular, we note that the presence of flavor-violating effects in RpV-couplings would likely mediate flavor-violation in the squark sector via the RGE's [104].

We will focus on R_p-conserving flavor-violation in the quadratic squark mass parameters m^2_{ij}, where we assume the diagonal terms to be degenerate for squarks of left-handed and right-handed type (for simplicity): $m^2_{\bar{D}} = m^2_Q \equiv m^2$. Flavor-violation in the trilinear soft terms would lead to comparable effects at the level of the meson-oscillation parameters. However, large A-terms easily produce new (e.g. color- and charge-violating) minima in the scalar potential, that lead to instability of the usual vacuum, with possibly short-time tunnelling. In fact, we find that such stability considerations typically constrain the A-terms much more efficiently than the ΔM's.

In figure 9, we allow for non-vanishing m^2_{13}, m^2_{23} or m^2_{12}, simultaneously with non-zero $\lambda'_{113}\lambda'_{131}$, $\lambda'_{123}\lambda'_{132}$ and $\lambda'_{112}\lambda'_{121}$. The former induce contributions to ΔM_d, ΔM_s and ΔM_K through R_p-conserving squark mixing, while the latter provide RpV tree-level contributions to the same ΔM's. The parameters are set to the scenario SUSY-RpV(a) of table 1, with the slepton/sneutrino mass at 1.5 TeV. In analogy with the results of section 4.3, we observe that R_p-conserving and RpV contributions may interfere destructively or constructively. Thus, allowed funnels with comparatively large values of the RpV-couplings open. In particular, we note that a tiny m^2_{12} is sufficient for relaxing limits from ΔM_K, while the typical values of m^2_{13} and m^2_{23} affecting ΔM_d and ΔM_s are significantly larger.

A similar analysis can be performed with RpV of the $\bar{U}\bar{D}\bar{D}$-type. This is shown in figure 10.
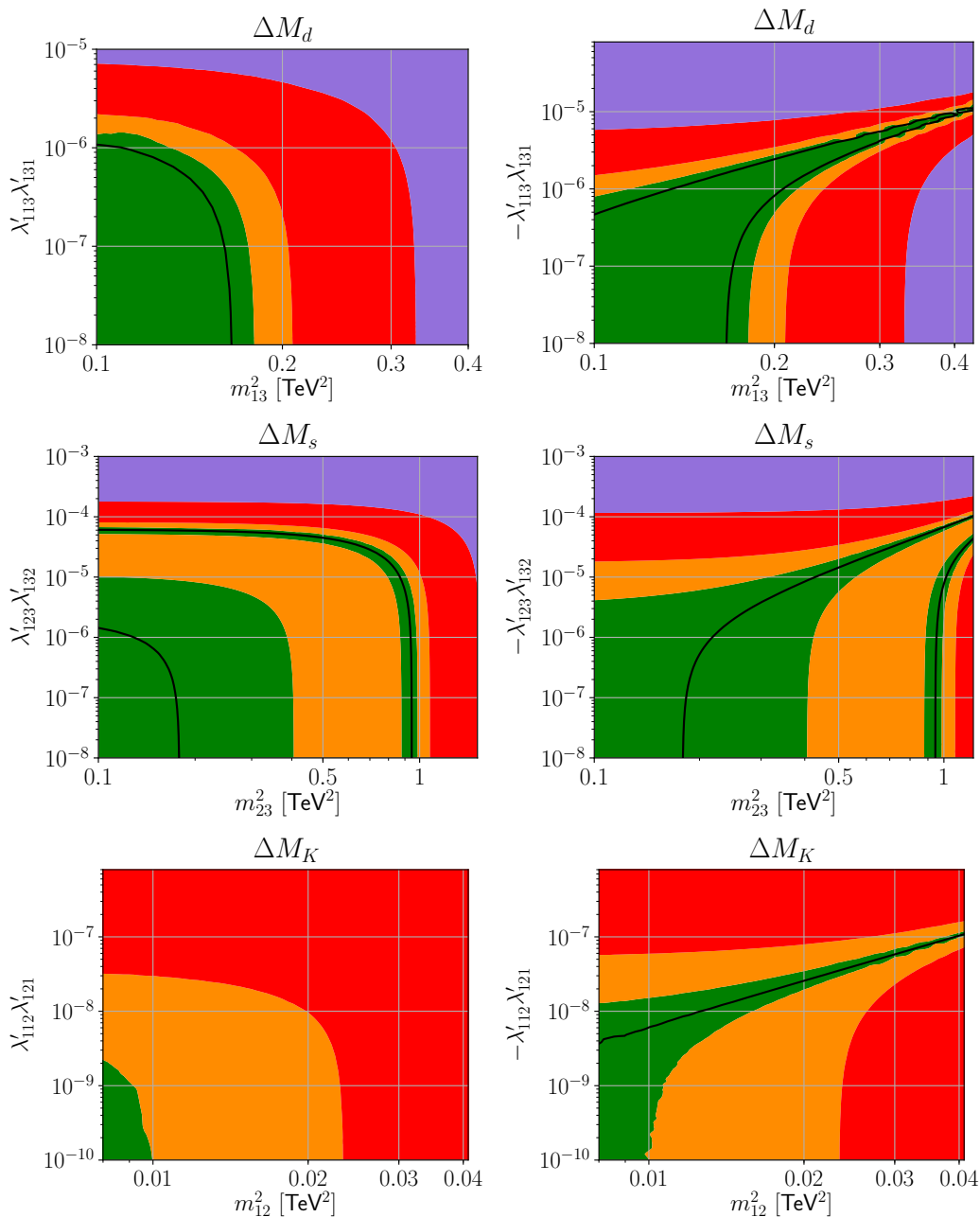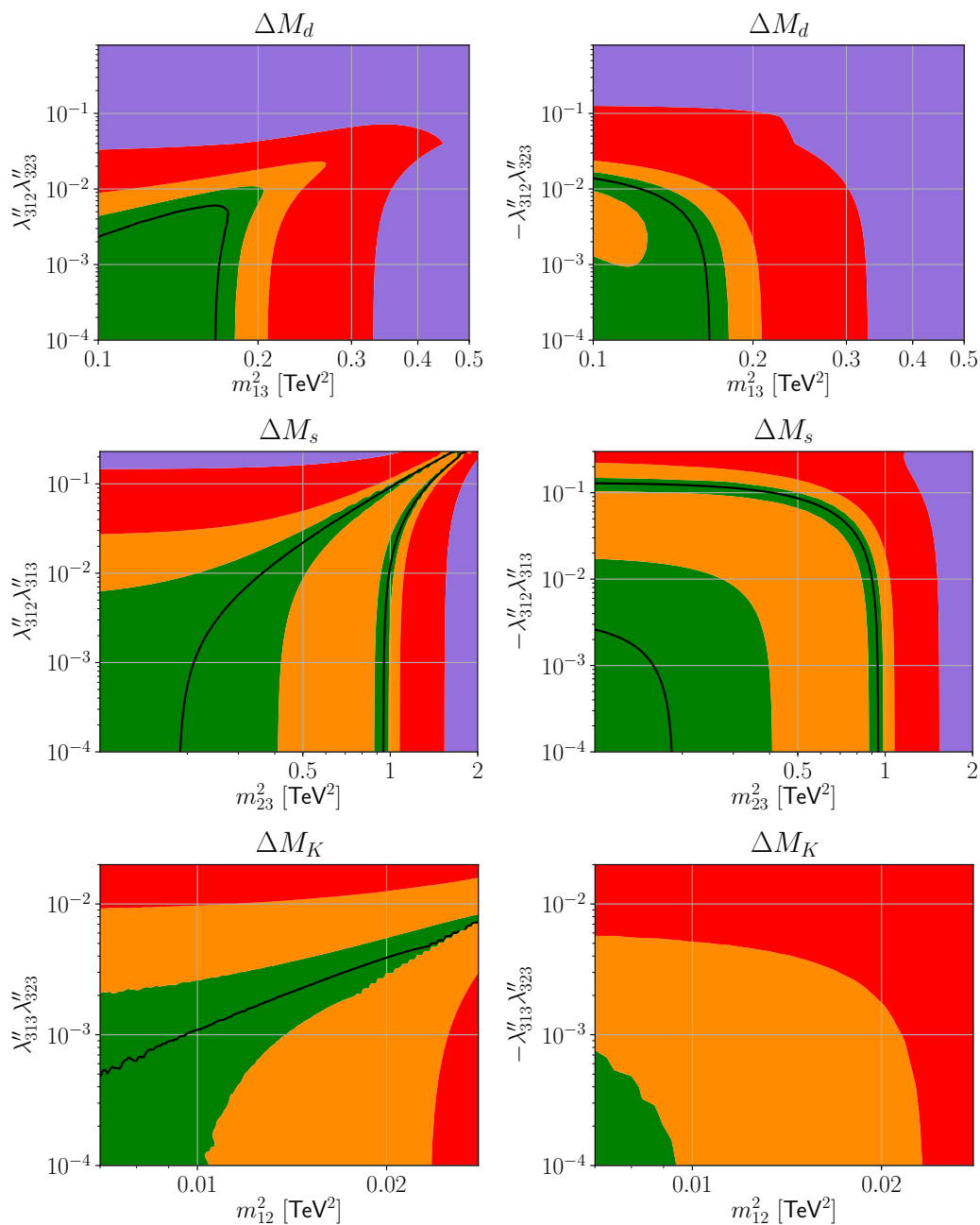
Figure 9. Constraints from the meson-oscillation parameters in the presence of both flavor-violating $LQ\bar{D}$-couplings and (R_p-conserving) flavor-violating mixing in the squark sector. The spectrum is set to the scenario SUSY-RpV(a) of table 1, with the slepton/sneutrino mass at 1.5 TeV. The flavor-violating quadratic soft mass parameters in the squark sector, m_{ij}^2, are chosen to be degenerate for left-handed and right-handed squarks. The color code follows the same conventions as before.

Figure 10. Constraints from the meson-oscillation parameters in the presence of both flavor-violating $\bar{U}\bar{D}\bar{D}$-couplings and flavor-violating squark mixing. The parameters are set to the scenario SUSY-RpV(a) from table 1. The color code is unchanged compared to previous plots.

In this subsection, we have stressed that the limits originating from meson-oscillation parameters are quite sensitive to the possible existence of flavor-violating sources beyond that of the RpV-couplings. A full analysis of these effects thus appears necessary when testing a complete model.

5 Conclusions

In this paper, we have analyzed the meson-mixing parameters $\Delta M_{d,s}$ and ΔM_K at the full one-loop order in the RpV-MSSM. In particular, we have completed earlier calculations in the literature, in which only tree-level and box diagrams were usually considered. We also performed a numerical study based on our results and employing recent experimental and lattice data. The tighter limits that we derive — as compared to older works — illustrate the improvement of the precision in experimental measurements, but also the relevance of some of the new contributions that we consider. In particular, the interplay of SM-like and $LQ\bar{D}$-type flavor-violation modifies the scaling of the bounds with the sneutrino/slepton mass for a whole class of couplings. Finally, we have emphasized the possibility of interference effects amongst new sources of flavor violation, either exclusively in the RpV-sector or in association with R_p-conserving squark mixing. While the appearance of allowed directions with comparatively large couplings largely intervenes as a fine-tuned curiosity in the low-energy perspective of our work, it also stresses the relevance of a detailed analysis of the observables when considering a complete high-energy model, since accidental relations among parameters could affect the picture of low-energy limits.

A Notations

A.1 Mixing matrices

- The squark mass matrices mix left- and right-handed components. We define the mass-eigenstates in terms of a unitary rotation of the gauge/flavor-eigenstates:

$$
\begin{cases}
U_\alpha = X^{U_L}_{\alpha f} \, U^f_L + X^{U_R}_{\alpha f} \, \bar{U}^{f\,*}_R \\[2mm]
D_\alpha = X^{D_L}_{\alpha f} \, D^f_L + X^{D_R}_{\alpha f} \, \bar{D}^{f\,*}_R
\end{cases}
\tag{A.1}
$$

Here, U_α (resp. D_α) represents the scalar-up (resp. sdown) mass state with mass m_{U_α} (resp. m_{D_α}). Summation over the generation index f is implicit.

- R-parity violation leads to a mixing of charged-Higgs and slepton fields. We define the mass-eigenstates $H^\pm_\alpha$ with mass m_{H_α} as:

$$
H^-_\alpha = X^C_{\alpha u} \, H^-_u + X^C_{\alpha d} \, H^-_d + X^C_{\alpha E^f_L} \, E^f_L + X^C_{\alpha E^f_R} \, \bar{E}^{f\,*}_R \,.
\tag{A.2}
$$

- Similarly, the neutral Higgs mass-states involve both the doublet-Higgs, $H^0_u = v_u + \frac{h^0_u + \imath a^0_u}{\sqrt{2}}$ and $H^0_d = v_d + \frac{h^0_d + \imath a^0_d}{\sqrt{2}}$, and the sneutrino fields, $N^f_L = \frac{h^0_{N_f} + \imath a^0_{N_f}}{\sqrt{2}}$; in the CP-violating case, CP-even and CP-odd components mix as well.

$$
S_\alpha = X^R_{\alpha u} h^0_u + X^R_{\alpha d} h^0_d + X^R_{\alpha N_f} h^0_{N_f} + X^I_{\alpha u} a^0_u + X^I_{\alpha d} a^0_d + X^I_{\alpha N_f} a^0_{N_f} \,.
\tag{A.3}
$$

S_α denotes the mass-eigenstate associated with the mass m_{S_α}.

- The charged winos $\tilde{w}^+$, $\tilde{w}^-$, higgsinos $\tilde{h}^+_u$, $\tilde{h}^-_d$ and lepton fields e^f_L, $\bar{e}^f_R$ define the chargino sector. For the mass $m_{\chi^\pm_k}$, the associated eignstate is given by:

$$
\begin{cases}
\chi^+_k = V_{kw} \, \tilde{w}^+ + V_{ku} \, \tilde{h}^+_u + V_{ke_f} \, \bar{e}^f_R \,, \\[2mm]
\chi^-_k = U_{kw} \, \tilde{w}^- + U_{kd} \, \tilde{h}^-_d + U_{ke_f} \, e^f_L \,.
\end{cases}
\tag{A.4}
$$

- The violation of R-parity also mixes neutrino and neutralino states. The eigenstate with mass $m_{\chi^0_k}$ reads:

$$
\chi^0_k = N_{kb} \, \tilde{b}^0 + N_{kw} \, \tilde{w}^0 + N_{ku} \, \tilde{h}^0_u + N_{kd} \, \tilde{h}^0_d + N_{k\nu_f} \, \nu^f_L \,.
\tag{A.5}
$$

A.2 Feynman rules

Here, we list the various couplings that are relevant in our calculation. The combinatorial factors appearing in the lagrangian density in the case of identical coupling particles have been explicitly factored out, e.g. $\mathcal{L} \ni -\frac{g^{S_\alpha ZZ}}{2} S_\alpha ZZ$.

- Neutral-Higgs-sneutrinos / Down quarks:

$$
g^{S_\alpha d_k d_i}_L = -\frac{1}{\sqrt{2}} \left[Y^i_d \delta_{ki} (X^R_{\alpha d} + \imath X^I_{\alpha d}) + \lambda'_{fik} (X^R_{\alpha N^f_L} + \imath X^I_{\alpha N^f_L}) \right] = (g^{S_\alpha d_i d_k}_R)^*
\tag{A.6}
$$

- Charged-Higgs-sleptons / Quarks:

$$g_L^{H_\alpha u_k d_i} = -Y_u^k V_{ki}^{\text{CKM}} X_{\alpha u}^C \; ; \quad g_R^{H_\alpha u_k d_i} = -Y_d^i V_{ki}^{\text{CKM}} X_{\alpha d}^C - \lambda_{fli}'^* V_{kl}^{\text{CKM}} X_{\alpha E_L^f}^C \quad (\text{A.7})$$

- Sdowns / Neutralino-neutrinos / Down quarks:

$$g_L^{D_\alpha \chi_k d_i} = -\frac{1}{\sqrt{2}} \left(\frac{g'}{3} N_{k\tilde{b}}^* - g N_{k\tilde{w}}^* \right) X_{\alpha i}^{D_L} - Y_d^i N_{kd}^* X_{\alpha i}^{D_R} - \lambda_{fi\beta}' N_{k\nu_f}^* X_{\alpha\beta}^{D_R}$$

$$g_R^{D_\alpha \chi_k d_i} = -\frac{\sqrt{2}}{3} g' N_{k\tilde{b}} X_{\alpha i}^{D_R} - Y_d^i N_{kd} X_{\alpha i}^{D_L} - \lambda_{f\beta i}'^* N_{k\nu_f} X_{\alpha\beta}^{D_L} \quad (\text{A.8})$$

- Sdowns / Gluinos / Down quarks (T^A are the colour Gell-Mann matrices):

$$g_L^{D_\alpha^a \tilde{g}^A d_i^b} = -\sqrt{2} g_s e^{-\imath \phi_{M_3}/2} X_{\alpha i}^{D_L} T_{ab}^A \quad ; \quad g_R^{D_\alpha^a \tilde{g}^A d_i^b} = \sqrt{2} g_s e^{\imath \phi_{M_3}/2} X_{\alpha i}^{D_R} T_{ab}^A \quad (\text{A.9})$$

- Scalar-ups / Chargino-leptons / Down quarks:

$$g_L^{U_\alpha \chi_k d_i} = V_{\beta i}^{\text{CKM}} \left[Y_u^\beta V_{ku}^* X_{\alpha\beta}^{U_R} - g V_{k\tilde{w}}^* X_{\alpha\beta}^{U_L} \right]$$

$$g_R^{U_\alpha \chi_k d_i} = V_{\beta f}^{\text{CKM}} \left[Y_d^i \delta_{if} U_{kd} X_{\alpha\beta}^{U_L} + \lambda_{lfi}'^* U_{ke_l} X_{\alpha\beta}^{U_L} \right] \quad (\text{A.10})$$

- Scalar-ups / Down quarks (a, b, c: colour-indices):

$$g_L^{U_\alpha^a d_k^b d_i^c} = 0 \quad ; \quad g_R^{U_\alpha^a d_k^b d_i^c} = \varepsilon_{abc} \lambda_{fki}''^* X_{\alpha f}^{U_R} \quad (\text{A.11})$$

- Sdowns / Up / Down quarks (a, b, c: colour-indices):

$$g_L^{D_\alpha^a u_k^b d_i^c} = 0 \quad ; \quad g_R^{D_\alpha^a u_k^b d_i^c} = \varepsilon_{bac} \lambda_{kfi}''^* X_{\alpha f}^{D_R} \quad (\text{A.12})$$

- W / Up / Down quarks:

$$g_L^{W u_k d_i} = \frac{g}{\sqrt{2}} V_{ki}^{\text{CKM}} \quad ; \quad g_R^{W u_k d_i} = 0 \quad (\text{A.13})$$

- Z / Down quarks:

$$g_L^{Z d_k d_i} = \frac{\sqrt{g'^2 + g^2}}{2} \left(-1 + \frac{2}{3} s_W^2 \right) \delta_{ik} \quad ; \quad g_R^{Z d_k d_i} = \frac{\sqrt{g'^2 + g^2}}{3} s_W^2 \delta_{ik} \quad (\text{A.14})$$

- Neutral-Higgs-sneutrinos / Up quarks:

$$g_L^{S_\alpha u_j u_k} = -\frac{Y_u^j}{\sqrt{2}} \delta_{jk} \left(X_{\alpha u}^R + \imath X_{\alpha u}^I \right) = \left(g_R^{S_\alpha u_k u_j} \right)^* \quad (\text{A.15})$$

- Neutral-Higgs-sneutrinos / Charginos-leptons:

$$
\begin{aligned}
g_L^{S_\alpha \chi_j^+ \chi_k^-} = &-\frac{1}{\sqrt{2}} \Big\{ Y_e^f \Big[\left(X_{\alpha d}^R + \imath X_{\alpha d}^I \right) V_{j e_f}^* U_{k e_f}^* - \left(X_{\alpha \tilde{N}_f}^R + \imath X_{\alpha \tilde{N}_f}^I \right) V_{j e_f}^* U_{kd}^* \Big] \\
&+ g \Big[\left(X_{\alpha u}^R - \imath X_{\alpha u}^I \right) V_{ju}^* U_{kw}^* + \left(X_{\alpha d}^R - \imath X_{\alpha d}^I \right) V_{jw}^* U_{kd}^* \\
&\qquad + \left(X_{\alpha \tilde{N}_f}^R - \imath X_{\alpha \tilde{N}_f}^I \right) V_{jw}^* U_{k e_f}^* \Big] \\
&+ \lambda_{fmn} \left(X_{\alpha \tilde{N}_f}^R + \imath X_{\alpha \tilde{N}_f}^I \right) V_{j e_n}^* U_{k e_m}^* \Big\} \\
= &\left(g_R^{S_\alpha \chi_k^+ \chi_j^-} \right)^*
\end{aligned}
\tag{A.16}
$$

- Neutral-Higgs-sneutrinos / Neutrino-neutralinos:

$$
\begin{aligned}
g_L^{S_\alpha \chi_j^0 \chi_k^0} = &-\frac{g'}{2} \Big[\left(X_{\alpha u}^R - \imath X_{\alpha u}^I \right) \left(N_{ju}^* N_{kb}^* + N_{jb}^* N_{ku}^* \right) \\
&\qquad - \left(X_{\alpha d}^R - \imath X_{\alpha d}^I \right) \left(N_{jd}^* N_{kb}^* + N_{kd}^* N_{jb}^* \right) \\
&\qquad - \left(X_{\alpha \tilde{N}_f}^R - \imath X_{\alpha \tilde{N}_f}^I \right) \left(N_{j\nu_f}^* N_{kb}^* + N_{k\nu_f}^* N_{jb}^* \right) \Big] \\
&+ \frac{g}{2} \Big[\left(X_{\alpha u}^R - \imath X_{\alpha u}^I \right) \left(N_{ju}^* N_{kw}^* + N_{jw}^* N_{ku}^* \right) \\
&\qquad - \left(X_{\alpha d}^R - \imath X_{\alpha d}^I \right) \left(N_{jd}^* N_{kw}^* + N_{kd}^* N_{jw}^* \right) \\
&\qquad - \left(X_{\alpha \tilde{N}_f}^R - \imath X_{\alpha \tilde{N}_f}^I \right) \left(N_{j\nu_f}^* N_{kw}^* + N_{k\nu_f}^* N_{jw}^* \right) \Big] \\
= &\left(g_R^{S_\alpha \chi_k^0 \chi_j^0} \right)^*
\end{aligned}
\tag{A.17}
$$

- Neutral-Higgs-sneutrinos / W's:

$$
g^{S_\alpha WW} = \frac{g^2}{\sqrt{2}} \left(v_u X_{\alpha u}^R + v_d X_{\alpha d}^R \right)
\tag{A.18}
$$

- Neutral-Higgs-sneutrinos / Z's:

$$
g^{S_\alpha ZZ} = \frac{g'^2 + g^2}{\sqrt{2}} \left(v_u X_{\alpha u}^R + v_d X_{\alpha d}^R \right)
\tag{A.19}
$$

- Neutral-Higgs-sneutrinos / W-ghosts $g_W^\pm$'s:

$$
g^{S_\alpha g_W g_W} = -\frac{g^2}{2\sqrt{2}} \left[v_u (X_{\alpha u}^R + \imath X_{\alpha u}^I) + v_d (X_{\alpha d}^R - \imath X_{\alpha d}^I) \right]
\tag{A.20}
$$

- Neutral-Higgs-sneutrinos / Z-ghosts g_Z's:

$$
g^{S_\alpha g_Z g_Z} = -\frac{g'^2 + g^2}{2\sqrt{2}} \left[v_u X_{\alpha u}^R + v_d X_{\alpha d}^R \right]
\tag{A.21}
$$

- Neutral-Higgs-sneutrinos / W / Charged-Higgs-sleptons:

$$g^{S_\alpha W H_k} = \frac{g}{2} \left[(X^R_{\alpha d} - \imath X^I_{\alpha d}) X^{C\,*}_{kd} - (X^R_{\alpha u} + \imath X^I_{\alpha u}) X^{C\,*}_{ku} + (X^R_{\alpha \tilde{N}_f} - \imath X^I_{\alpha \tilde{N}_f}) X^{C\,*}_{k\tilde{E}^f_L} \right] \tag{A.22}$$

- Neutral-Higgs-sneutrinos / Z / Neutral-Higgs-sneutrinos:

$$g^{S_\alpha Z S_k} = \imath \frac{\sqrt{g'^2 + g^2}}{2} \Big[X^R_{\alpha d} X^I_{kd} - X^I_{\alpha d} X^R_{kd} - X^R_{\alpha u} X^I_{ku} + X^I_{\alpha u} X^R_{ku}$$
$$+ X^R_{\alpha \tilde{N}_f} X^I_{k\tilde{N}_f} - X^I_{\alpha \tilde{N}_f} X^R_{k\tilde{N}_f} \Big] \tag{A.23}$$

- Neutral-Higgs-sneutrinos / Scalar-ups:

$$g^{\tilde{U}_k \tilde{U}_l S_\alpha} = - \sqrt{2} \left[Y^{f\,2}_u v_u X^R_{\alpha u} + \frac{1}{4} \left(\frac{g'^2}{3} - g^2 \right) (v_u X^R_{\alpha u} - v_d X^R_{\alpha d}) \right] X^{\tilde{U}_f}_{kL} X^{\tilde{U}_f\,*}_{lL}$$
$$- \sqrt{2} \left[Y^{f\,2}_u v_u X^R_{\alpha u} - \frac{g'^2}{3} (v_u X^R_{\alpha u} - v_d X^R_{\alpha d}) \right] X^{\tilde{U}_f}_{kR} X^{\tilde{U}_f\,*}_{lR}$$
$$- \frac{1}{\sqrt{2}} \left[A^{ff'}_u (X^R_{\alpha u} + \imath X^I_{\alpha u}) - \mu^* Y^f_u \delta_{ff'} (X^R_{\alpha d} - \imath X^I_{\alpha d}) \right] X^{\tilde{U}_{f'}}_{kR} X^{\tilde{U}_f\,*}_{lL}$$
$$- \frac{1}{\sqrt{2}} \left[A^{ff'\,*}_u (X^R_{\alpha u} - \imath X^I_{\alpha u}) - \mu Y^f_u \delta_{ff'} (X^R_{\alpha d} + \imath X^I_{\alpha d}) \right] X^{\tilde{U}_f}_{kL} X^{\tilde{U}_{f'}\,*}_{lR} \tag{A.24}$$

- Neutral-Higgs-sneutrinos / Sdowns:

$$g^{\tilde{D}_k \tilde{D}_l S_\alpha} = - \sqrt{2} \left[Y^{f\,2}_d v_d X^R_{\alpha d} + \frac{1}{4} \left(\frac{g'^2}{3} + g^2 \right) (v_u X^R_{\alpha u} - v_d X^R_{\alpha d}) \right] X^{\tilde{D}_f}_{kL} X^{\tilde{D}_f\,*}_{lL}$$
$$- \frac{v_d}{\sqrt{2}} \left[Y^f_d \lambda'^{*}_{ghf} (X^R_{\alpha \tilde{N}_g} - \imath X^I_{\alpha \tilde{N}_g}) + Y^h_d \lambda'_{gfh} (X^R_{\alpha \tilde{N}_g} + \imath X^I_{\alpha \tilde{N}_g}) \right] X^{\tilde{D}_h}_{kL} X^{\tilde{D}_f\,*}_{lL}$$
$$- \sqrt{2} \left[Y^{f\,2}_d v_d X^R_{\alpha d} + \frac{g'^2}{6} (v_u X^R_{\alpha u} - v_d X^R_{\alpha d}) \right] X^{\tilde{D}_f}_{kR} X^{\tilde{D}_f\,*}_{lR}$$
$$- \frac{v_d}{\sqrt{2}} \left[Y^f_d \lambda'^{*}_{gfh} (X^R_{\alpha \tilde{N}_g} - \imath X^I_{\alpha \tilde{N}_g}) + Y^h_d \lambda'_{ghf} (X^R_{\alpha \tilde{N}_g} + \imath X^I_{\alpha \tilde{N}_g}) \right] X^{\tilde{D}_f}_{kR} X^{\tilde{D}_h\,*}_{lR}$$
$$- \frac{1}{\sqrt{2}} \Big[A^{ff'}_d (X^R_{\alpha d} + \imath X^I_{\alpha d}) - \mu^* Y^f_d \delta_{ff'} (X^R_{\alpha u} - \imath X^I_{\alpha u})$$
$$+ A'_{gff'} (X^R_{\alpha \tilde{N}_g} + \imath X^I_{\alpha \tilde{N}_g}) \Big] X^{\tilde{D}_{f'}}_{kR} X^{\tilde{D}_f\,*}_{lL}$$
$$- \frac{1}{\sqrt{2}} \Big[A^{ff'\,*}_d (X^R_{\alpha d} - \imath X^I_{\alpha d}) - \mu Y^f_d \delta_{ff'} (X^R_{\alpha u} + \imath X^I_{\alpha u})$$
$$+ A'^{*}_{gff'} (X^R_{\alpha \tilde{N}_g} - \imath X^I_{\alpha \tilde{N}_g}) \Big] X^{\tilde{D}_f}_{kL} X^{\tilde{D}_{f'}\,*}_{lR} \tag{A.25}$$

- Neutral-Higgs-sneutrinos / Charged Higgs-sleptons

$$g^{H_k H_l S_\alpha} = - \sqrt{2} \Bigg\{ \left[Y^{f\,2}_e v_d X^R_{\alpha d} + \frac{1}{4} \left(-g'^2 + g^2 \right) (v_u X^R_{\alpha u} - v_d X^R_{\alpha d}) \right] \delta_{ff'}$$
$$- \frac{v_d}{2} \Big[Y^{f'}_e \lambda^*_{fgf'} (X^R_{\alpha \tilde{N}_g} - \imath X^I_{\alpha \tilde{N}_g})$$
$$+ Y^f_e \lambda_{f'gf} (X^R_{\alpha \tilde{N}_g} + \imath X^I_{\alpha \tilde{N}_g}) \Big] \Bigg\} X^C_{k\tilde{E}^f_L} X^{C\,*}_{l\tilde{E}^{f'}_L}$$

$$
-\sqrt{2}\left\{\left[Y_e^{f\,2}v_dX_{\alpha d}^R+\frac{g'^2}{2}(v_uX_{\alpha u}^R-v_dX_{\alpha d}^R)\right]\delta_{ff'}\right.
$$
$$
-\frac{v_d}{2}\left[Y_e^f\lambda_{fgf'}^*(X_{\alpha\tilde N_g}^R-\imath X_{\alpha\tilde N_g}^I)\right.
$$
$$
\left.\left.+Y_e^{f'}\lambda_{f'gf}(X_{\alpha\tilde N_g}^R+\imath X_{\alpha\tilde N_g}^I)\right]\right\}X_{k\tilde E_R^f}^C X_{l\tilde E_R^{f'}}^{C\,*}
$$
$$
-\frac{1}{\sqrt{2}}\left[A_e^{f'f}(X_{\alpha d}^R+\imath X_{\alpha d}^I)-\mu^*Y_e^f\delta_{ff'}(X_{\alpha u}^R-\imath X_{\alpha u}^I)\right.
$$
$$
\left.+A_{gf'f}(X_{\alpha\tilde N_g}^R+\imath X_{\alpha\tilde N_g}^I)\right]X_{k\tilde E_R^f}^C X_{l\tilde E_L^{f'}}^{C\,*}
$$
$$
-\frac{1}{\sqrt{2}}\left[A_e^{ff'\,*}(X_{\alpha d}^R-\imath X_{\alpha d}^I)-\mu Y_e^f\delta_{ff'}(X_{\alpha u}^R+\imath X_{\alpha u}^I)\right.
$$
$$
\left.+A_{gff'}^*(X_{\alpha\tilde N_g}^R-\imath X_{\alpha\tilde N_g}^I)\right]X_{k\tilde E_L^f}^C X_{l\tilde E_R^{f'}}^{C\,*}
$$
$$
-\frac{1}{2\sqrt{2}}\left[g'^2(v_uX_{\alpha u}^R-v_dX_{\alpha d}^R)+g^2(v_uX_{\alpha u}^R+v_dX_{\alpha d}^R)\right]X_{ku}^C X_{lu}^{C\,*}
$$
$$
-\frac{1}{2\sqrt{2}}\left[g'^2(v_dX_{\alpha d}^R-v_uX_{\alpha u}^R)+g^2(v_uX_{\alpha u}^R+v_dX_{\alpha d}^R)\right]X_{kd}^C X_{ld}^{C\,*}
$$
$$
-\frac{g^2}{2\sqrt{2}}\left[v_u(X_{\alpha d}^R-\imath X_{\alpha d}^I)+v_d(X_{\alpha u}^R-\imath X_{\alpha u}^I)\right]X_{ku}^C X_{ld}^{C\,*}
$$
$$
-\frac{g^2}{2\sqrt{2}}\left[v_u(X_{\alpha d}^R+\imath X_{\alpha d}^I)+v_d(X_{\alpha u}^R+\imath X_{\alpha u}^I)\right]X_{kd}^C X_{lu}^{C\,*}
$$
$$
+\frac{1}{\sqrt{2}}\left[A_e^{ff'}(X_{\alpha\tilde N_f}^R+\imath X_{\alpha\tilde N_f}^I)X_{k\tilde E_R^{f'}}^C X_{ld}^{C\,*}\right.
$$
$$
\left.+A_e^{ff'\,*}(X_{\alpha\tilde N_f}^R-\imath X_{\alpha\tilde N_f}^I)X_{kd}^C X_{l\tilde E_R^{f'}}^{C\,*}\right]
$$
$$
+\frac{Y_e^{f\,2}v_d}{\sqrt{2}}\left[(X_{\alpha\tilde N_f}^R-\imath X_{\alpha\tilde N_f}^I)X_{kd}^C X_{l\tilde E_L^f}^{C\,*}+(X_{\alpha\tilde N_f}^R+\imath X_{\alpha\tilde N_f}^I)X_{k\tilde E_L^f}^C X_{ld}^{C\,*}\right]
$$
$$
+\frac{Y_e^f}{\sqrt{2}}\left[\mu^*(X_{\alpha\tilde N_f}^R+\imath X_{\alpha\tilde N_f}^I)X_{k\tilde E_R^f}^C X_{lu}^{C\,*}+\mu(X_{\alpha\tilde N_f}^R-\imath X_{\alpha\tilde N_f}^I)X_{ku}^C X_{l\tilde E_R^f}^{C\,*}\right]
$$
$$
-\frac{g^2}{2\sqrt{2}}\left[(X_{\alpha\tilde N_f}^R+\imath X_{\alpha\tilde N_f}^I)X_{k\tilde E_L^f}^C(v_uX_{lu}^{C\,*}+v_dX_{ld}^{C\,*})\right.
$$
$$
\left.+(X_{\alpha\tilde N_f}^R-\imath X_{\alpha\tilde N_f}^I)(v_uX_{ku}^C+v_dX_{kd}^C)X_{l\tilde E_L^f}^{C\,*}\right] \tag{A.26}
$$

- Cubic Neutral-Higgs-sneutrinos:

$$
g^{S_\alpha S_\beta S_\gamma}=\frac{g'^2+g^2}{4\sqrt{2}}\left[v_u\left(\Pi_{\alpha\beta\gamma}^{S\,uuu}+\Pi_{\alpha\beta\gamma}^{A\,uuu}-\Pi_{\alpha\beta\gamma}^{S\,udd}-\Pi_{\alpha\beta\gamma}^{A\,udd}-\Pi_{\alpha\beta\gamma}^{S\,u\tilde N_f\tilde N_f}-\Pi_{\alpha\beta\gamma}^{A\,u\tilde N_f\tilde N_f}\right)\right.
$$
$$
\left.+v_d\left(\Pi_{\alpha\beta\gamma}^{S\,ddd}+\Pi_{\alpha\beta\gamma}^{A\,ddd}-\Pi_{\alpha\beta\gamma}^{S\,duu}-\Pi_{\alpha\beta\gamma}^{A\,duu}-\Pi_{\alpha\beta\gamma}^{S\,d\tilde N_f\tilde N_f}-\Pi_{\alpha\beta\gamma}^{A\,d\tilde N_f\tilde N_f}\right)\right] \tag{A.27}
$$

where:

$$
\Pi_{\alpha\beta\gamma}^{S\,abc}=X_{\alpha a}^R X_{\beta b}^R X_{\gamma c}^R+X_{\alpha b}^R X_{\beta c}^R X_{\gamma a}^R+X_{\alpha c}^R X_{\beta a}^R X_{\gamma b}^R
$$
$$
+X_{\alpha a}^R X_{\beta c}^R X_{\gamma b}^R+X_{\alpha c}^R X_{\beta b}^R X_{\gamma a}^R+X_{\alpha b}^R X_{\beta a}^R X_{\gamma c}^R
$$

$$\Pi^{A\,abc}_{\alpha\beta\gamma} = X^R_{\alpha a}\left(X^I_{\beta b}X^I_{\gamma c} + X^I_{\beta c}X^I_{\gamma b}\right) + X^R_{\beta a}\left(X^I_{\alpha b}X^I_{\gamma c} + X^I_{\alpha c}X^I_{\gamma b}\right)$$
$$+ X^R_{\gamma a}\left(X^I_{\alpha b}X^I_{\beta c} + X^I_{\alpha c}X^I_{\beta b}\right)$$

- Neutral-Higgs-sneutrinos / W quartic:

$$g^{WWS_\alpha S_\beta} = \frac{g^2}{2}\Big[X^R_{\alpha u}X^R_{\beta u} + X^I_{\alpha u}X^I_{\beta u} + X^R_{\alpha d}X^R_{\beta d}$$
$$+ X^I_{\alpha d}X^I_{\beta d} + X^R_{\alpha\tilde N_f}X^R_{\beta\tilde N_f} + X^I_{\alpha\tilde N_f}X^I_{\beta\tilde N_f}\Big] \tag{A.28}$$

- Neutral-Higgs-sneutrinos / Z quartic:

$$g^{ZZS_\alpha S_\beta} = \frac{g'^2 + g^2}{2}\Big[X^R_{\alpha u}X^R_{\beta u} + X^I_{\alpha u}X^I_{\beta u} + X^R_{\alpha d}X^R_{\beta d}$$
$$+ X^I_{\alpha d}X^I_{\beta d} + X^R_{\alpha\tilde N_f}X^R_{\beta\tilde N_f} + X^I_{\alpha\tilde N_f}X^I_{\beta\tilde N_f}\Big] \tag{A.29}$$

- Neutral-Higgs-sneutrinos / Scalar-ups quartic:

$$g^{\tilde U_k\tilde U_l S_\alpha S_\beta} = -Y_u^{f\,2}\left(X^R_{\alpha u}X^R_{\beta u} + X^I_{\alpha u}X^I_{\beta u}\right)\left(X^{\tilde U_f}_{kL}X^{\tilde U_f\,*}_{lL} + X^{\tilde U_f}_{kR}X^{\tilde U_f\,*}_{lR}\right)$$
$$- \left[\frac{1}{4}\left(\frac{g'^2}{3} - g^2\right)X^{\tilde U_f}_{kL}X^{\tilde U_f\,*}_{lL} - \frac{g'^2}{3}X^{\tilde U_f}_{kR}X^{\tilde U_f\,*}_{lR}\right]$$
$$\times \Big(X^R_{\alpha u}X^R_{\beta u} + X^I_{\alpha u}X^I_{\beta u} - X^R_{\alpha d}X^R_{\beta d} - X^I_{\alpha d}X^I_{\beta d}$$
$$- X^R_{\alpha\tilde N_{f'}}X^R_{\beta\tilde N_{f'}} - X^I_{\alpha\tilde N_{f'}}X^I_{\beta\tilde N_{f'}}\Big) \tag{A.30}$$

- Neutral-Higgs-sneutrinos / Sdowns quartic:

$$g^{\tilde D_k\tilde D_l S_\alpha S_\beta} = -Y_d^{f\,2}\left(X^R_{\alpha d}X^R_{\beta d} + X^I_{\alpha d}X^I_{\beta d}\right)\left(X^{\tilde D_f}_{kL}X^{\tilde D_f\,*}_{lL} + X^{\tilde D_f}_{kR}X^{\tilde D_f\,*}_{lR}\right) \tag{A.31}$$
$$- \left[\frac{1}{4}\left(\frac{g'^2}{3} + g^2\right)X^{\tilde D_f}_{kL}X^{\tilde D_f\,*}_{lL} + \frac{g'^2}{6}X^{\tilde D_f}_{kR}X^{\tilde D_f\,*}_{lR}\right]$$
$$\times \Big(X^R_{\alpha u}X^R_{\beta u} + X^I_{\alpha u}X^I_{\beta u} - X^R_{\alpha d}X^R_{\beta d}$$
$$- X^I_{\alpha d}X^I_{\beta d}X^R_{\alpha\tilde N_{f'}}X^R_{\beta\tilde N_{f'}} - X^I_{\alpha\tilde N_{f'}}X^I_{\beta\tilde N_{f'}}\Big)$$
$$- \frac{Y_d^f}{2}\left(\lambda'^*_{ghf}X^{\tilde D_h}_{kL}X^{\tilde D_f\,*}_{lL} + \lambda'^*_{gfh}X^{\tilde D_f}_{kR}X^{\tilde D_h\,*}_{lR}\right)$$
$$\times \left[(X^R_{\alpha d} + \imath X^I_{\alpha d})(X^R_{\beta\tilde N_g} - \imath X^I_{\beta\tilde N_g}) + (\alpha\leftrightarrow\beta)\right]$$
$$- \frac{Y_d^f}{2}\left(\lambda'_{ghf}X^{\tilde D_f}_{kL}X^{\tilde D_h\,*}_{lL} + \lambda'_{gfh}X^{\tilde D_h}_{kR}X^{\tilde D_f\,*}_{lR}\right)$$
$$\times \left[(X^R_{\alpha d} - \imath X^I_{\alpha d})(X^R_{\beta\tilde N_g} + \imath X^I_{\beta\tilde N_g}) + (\alpha\leftrightarrow\beta)\right]$$
$$- \frac{1}{2}\left(\lambda'_{ghf}\lambda'^*_{mnf}X^{\tilde D_n}_{kL}X^{\tilde D_h\,*}_{lL} + \lambda'_{gfh}\lambda'^*_{mfn}X^{\tilde D_h}_{kR}X^{\tilde D_n\,*}_{lR}\right)$$
$$\times \left[(X^R_{\alpha\tilde N_g} + \imath X^I_{\alpha\tilde N_g})(X^R_{\beta\tilde N_m} - \imath X^I_{\beta\tilde N_m}) + (\alpha\leftrightarrow\beta)\right] \tag{A.32}$$

- Neutral-Higgs-sneutrinos / Charged Higgs-sleptons quartic:

$$
\begin{aligned}
\mathcal{L} \ni & -Y_e^{f\,2}\left[|H_d^0|^2\left(|E_L^f|^2+|E_R^{c\,f}|^2\right)+|N_L^f|^2 H_d^+ H_d^- -H_d^0 N_L^{f\,*} H_d^+ E_L^f -H_d^{0*} N_L^f E_L^{f\,*} H_d^-\right] \\
& -\lambda_{jki}\lambda_{mni}^* N_L^j N_L^{m\,*} E_L^{n\,*} E_L^k -\lambda_{ijk}\lambda_{imn}^* N_L^j N_L^{m\,*} E_R^{c\,k} E_R^{c\,n\,*} -Y_e^f Y_e^{f'} N_L^f N_L^{f'\,*} E_R^{c\,f} E_R^{c\,f'\,*} \\
& +Y_e^f\left[\lambda_{fij}^* H_d^0 N_L^{i\,*} E_R^{c\,f} E_R^{c\,j\,*} +\lambda_{ijf}^* H_d^0 N_L^{j\,*} E_L^{i\,*} E_L^f +\lambda_{ijf} N_L^f N_L^{i\,*} E_L^{j\,*} H_d^- +cc\right] \\
& -\frac{g'^2}{4}\left[|H_u^0|^2-|H_d^0|^2-|N_L^f|^2\right]\left[H_u^+ H_u^- -H_d^+ H_d^- -|E_L^{f'}|^2 +2|E_R^{c\,f'}|^2\right] \\
& -\frac{g^2}{4}\left[\left(|H_u^0|^2+|H_d^0|^2+|N_L^f|^2\right)H_u^+ H_u^- +\left(|H_d^0|^2+|H_u^0|^2-|N_L^f|^2\right)H_d^+ H_d^-\right. \\
& \qquad +2N_L^f N_L^{f'\,*} E_L^{f\,*} E_L^{f'} +\left(|H_u^0|^2-|H_d^0|^2-|N_L^f|^2\right)|E_L^f|^2 +2H_u^{0\,*}H_d^{0\,*}H_u^+ H_d^- \\
& \qquad +2H_u^0 H_d^0 H_d^+ H_u^- +2N_L^{f\,*}H_u^{0\,*}H_u^+ E_L^f +2N_L^f H_u^0 E_L^{f\,*} H_u^- \\
& \qquad \left.+2N_L^{f\,*}H_d^0 H_d^+ E_L^f +2N_L^f H_d^{0\,*} E_L^{f\,*} H_d^-\right]
\end{aligned}
\tag{A.33}
$$

The coupling $g^{H_k H_l S_\alpha S_\beta}$ is obtained through the replacements $H_u^+ \to X_{ku}^C$, $H_d^+ \to X_{kd}^C$, $E_L^{f\,*} \to X_{k\tilde{E}_L^f}^C$, $E_R^{c\,f} \to X_{k\tilde{E}_R^f}^C$, $H_u^- \to X_{lu}^{C\,*}$, $H_d^- \to X_{ld}^{C\,*}$, $E_L^f \to X_{l\tilde{E}_L^f}^{C\,*}$, $E_R^{c\,f\,*} \to X_{l\tilde{E}_R^f}^{C\,*}$, $H_u^0 \to X_{.u}^R + \imath X_{.u}^I$, $H_d^0 \to X_{.d}^R + \imath X_{.d}^I$, and $N_L^f \to X_{.\tilde{N}_f}^R + \imath X_{.\tilde{N}_f}^I$ (. $=\alpha,\ \beta$ indifferently, such that the coupling is symmetric over the exchange $\alpha \leftrightarrow \beta$ in the end).

- Neutral-Higgs-sneutrinos quartic:

$$
\begin{aligned}
g^{S_\alpha S_\beta S_\gamma S_\delta} = \frac{g'^2+g^2}{32}\bigg[& \Pi_{\alpha\beta\gamma\delta}^{S\,uuuu} +\Pi_{\alpha\beta\gamma\delta}^{S\,dddd} -2\Pi_{\alpha\beta\gamma\delta}^{S\,uudd} -2\Pi_{\alpha\beta\gamma\delta}^{S\,uu\tilde{N}_f\tilde{N}_f} +2\Pi_{\alpha\beta\gamma\delta}^{S\,dd\tilde{N}_f\tilde{N}_f} \\
& +\Pi_{\alpha\beta\gamma\delta}^{S\,\tilde{N}_f\tilde{N}_f\tilde{N}_{f'}\tilde{N}_{f'}} +\Pi_{\alpha\beta\gamma\delta}^{P\,uuuu} +\Pi_{\alpha\beta\gamma\delta}^{P\,dddd} -2\Pi_{\alpha\beta\gamma\delta}^{P\,uudd} \\
& -2\Pi_{\alpha\beta\gamma\delta}^{P\,uu\tilde{N}_f\tilde{N}_f} +2\Pi_{\alpha\beta\gamma\delta}^{P\,dd\tilde{N}_f\tilde{N}_f} +\Pi_{\alpha\beta\gamma\delta}^{P\,\tilde{N}_f\tilde{N}_f\tilde{N}_{f'}\tilde{N}_{f'}} +2\Pi_{\alpha\beta\gamma\delta}^{S\,uu\,P\,uu} \\
& +2\Pi_{\alpha\beta\gamma\delta}^{S\,dd\,P\,dd} -2\Pi_{\alpha\beta\gamma\delta}^{S\,uu\,P\,dd} -2\Pi_{\alpha\beta\gamma\delta}^{S\,dd\,P\,uu} -2\Pi_{\alpha\beta\gamma\delta}^{S\,uu\,P\,\tilde{N}_f\tilde{N}_f} \\
& -2\Pi_{\alpha\beta\gamma\delta}^{S\,\tilde{N}_f\tilde{N}_f\,P\,uu} +2\Pi_{\alpha\beta\gamma\delta}^{S\,dd\,P\,\tilde{N}_f\tilde{N}_f} +2\Pi_{\alpha\beta\gamma\delta}^{S\,\tilde{N}_f\tilde{N}_f\,P\,dd} \\
& +2\Pi_{\alpha\beta\gamma\delta}^{S\,\tilde{N}_f\tilde{N}_f\,P\,\tilde{N}_{f'}\tilde{N}_{f'}} \bigg]
\end{aligned}
\tag{A.34}
$$

where:

$$
\begin{aligned}
\Pi_{ijkl}^{S\,abcd} &= \sum_{\sigma\in S_4} X_{\sigma(i)a}^R X_{\sigma(j)b}^R X_{\sigma(k)c}^R X_{\sigma(l)d}^R\,; \\
\Pi_{ijkl}^{P\,abcd} &= \sum_{\sigma\in S_4} X_{\sigma(i)a}^I X_{\sigma(j)b}^I X_{\sigma(k)c}^I X_{\sigma(l)d}^I \\
\Pi_{ijkl}^{S\,ab\,P\,cd} &= \sum_{\sigma\in S_4} X_{\sigma(i)a}^R X_{\sigma(j)b}^R X_{\sigma(k)c}^I X_{\sigma(l)d}^I
\end{aligned}
$$

A.3 Loop-functions

The loop functions relevant for our computations are

- $A_0(m) = -16\pi^2 \imath \int \frac{d^D k}{(2\pi)^D} \frac{1}{k^2 - m^2}$.

- $B_0(p, m_1, m_2) = -16\pi^2 \imath \int \frac{d^D k}{(2\pi)^D} \frac{1}{[k^2 - m_1^2][(k+p)^2 - m_2^2]}$.

- $p^\mu B_1(p, m_1, m_2) = -16\pi^2 \imath \int \frac{d^D k}{(2\pi)^D} \frac{k^\mu}{[k^2 - m_1^2][(k+p)^2 - m_2^2]}$.

- $[g^{\mu\nu} B_{22} + p^\mu p^\nu B_{21}](p, m_1, m_2) = -16\pi^2 \imath \int \frac{d^D k}{(2\pi)^D} \frac{k^\mu k^\nu}{[k^2 - m_1^2][(k+p)^2 - m_2^2]}$.

- $C_0(p_1, p_2, m_1, m_2, m_3) = -16\pi^2 \imath \int \frac{d^D k}{(2\pi)^D} \frac{1}{[k^2 - m_1^2][(k+p_1)^2 - m_2^2][(k+p_1+p_2)^2 - m_3^2]}$.

- $[p_1^\mu C_{11} + p_2^\mu C_{12}](p_1, p_2, m_1, m_2, m_3)$
$$= -16\pi^2 \imath \int \frac{d^D k}{(2\pi)^D} \frac{k^\mu}{[k^2 - m_1^2][(k+p_1)^2 - m_2^2][(k+p_1+p_2)^2 - m_3^2]} .$$

- $[g^{\mu\nu} C_{24} + p_1^\mu p_1^\nu C_{21} + p_2^\mu p_2^\nu C_{22} + (p_1^\mu p_2^\nu + p_2^\mu p_1^\nu) C_{23}](p_1, p_2, m_1, m_2, m_3)$
$$= -16\pi^2 \imath \int \frac{d^D k}{(2\pi)^D} \frac{k^\mu k^\nu}{[k^2 - m_1^2][(k+p_1)^2 - m_2^2][(k+p_1+p_2)^2 - m_3^2]} .$$

- $D_0(m_1, m_2, m_3, m_4) = -16\pi^2 \imath \int \frac{d^D k}{(2\pi)^D} \frac{1}{[k^2 - m_1^2][k^2 - m_2^2][k^2 - m_3^2][k^2 - m_4^2]}$.

- $D_2(m_1, m_2, m_3, m_4) = -16\pi^2 \imath \int \frac{d^D k}{(2\pi)^D} \frac{k^2}{[k^2 - m_1^2][k^2 - m_2^2][k^2 - m_3^2][k^2 - m_4^2]}$.

Explicit expressions for these functions in the limit of vanishing external momenta can e.g. be found in ref. [105].

B Tree level contributions

The tree-level contribution to the $d_i \bar{d}_j \to d_j \bar{d}_i$ amplitudes corresponds to the topology of figure 1a and is mediated by a sneutrino internal line. It generates the following terms in the EFT:

$$\mathcal{L}_{\text{EFT}} \ni \frac{1}{2m_{S_\alpha}^2} \left[\left(g_L^{S_\alpha d_j d_i} \right)^2 O_2 + \left(g_R^{S_\alpha d_j d_i} \right)^2 \tilde{O}_2 + 2 g_L^{S_\alpha d_j d_i} g_R^{S_\alpha d_j d_i} O_4 \right] \tag{B.1}$$

where the couplings $g_{L,R}^{S_\alpha d_j d_i}$ are defined in eq. (A.6). The sum over sneutrino/neutral-Higgs mixed states S_α with mass m_{S_α} is implicit. The operators O_2, $\tilde{O}_2$, etc, are defined in eq. (2.2).

C $d_i - d_j$ self-energy contributions

Loop corrections on the external d-fermion legs are determined by the LSZ reduction. Defining the matrix of renormalized $d_i - d_j$ self energies as: $\hat{\Sigma}^{ij}(\not{p}) = \hat{\Sigma}_L^{ij}(\not{p}) P_L + \hat{\Sigma}_R^{ij}(\not{p}) P_R =$

$P_L \tilde{\Sigma}_L^{ij}(\not{p}) + P_R \tilde{\Sigma}_R^{ij}(\not{p})$, we derive the contribution to the EFT:

$$
\begin{aligned}
\mathcal{L}_{\text{EFT}} \ni \frac{1}{2m_{S_\alpha}^2} \Bigg\{ & g_L^{S_\alpha d_j d_i} \Bigg[\frac{1}{2} g_L^{S_\alpha d_j d_i} \left(\left.\frac{d\hat{\Sigma}_L^{jj}}{d\not{p}}\right|_{\not{p}_{d_j}} + \left.\frac{d\hat{\Sigma}_L^{jj}}{d\not{p}}\right|_{\not{p}'_{d_j}} + \left.\frac{d\tilde{\Sigma}_L^{ii}}{d\not{p}}\right|_{\not{p}_{d_i}} + \left.\frac{d\tilde{\Sigma}_L^{ii}}{d\not{p}}\right|_{\not{p}'_{d_i}} \right) \\
& + \sum_{k\neq j} g_L^{S_\alpha d_k d_i} \left(\left.\frac{m_{d_k}\hat{\Sigma}_L^{jk} + \not{p}_{d_j}\hat{\Sigma}_R^{jk}}{m_{d_j}^2 - m_{d_k}^2}\right|_{\not{p}_{d_j}} + \left.\frac{m_{d_k}\hat{\Sigma}_L^{jk} + \not{p}'_{d_j}\hat{\Sigma}_R^{jk}}{m_{d_j}^2 - m_{d_k}^2}\right|_{\not{p}'_{d_j}} \right) \\
& + \sum_{k\neq i} g_L^{S_\alpha d_j d_k} \left(\left.\frac{m_{d_k}\tilde{\Sigma}_L^{ki} + \not{p}_{d_i}\tilde{\Sigma}_R^{ki}}{m_{d_i}^2 - m_{d_k}^2}\right|_{\not{p}_{d_i}} + \left.\frac{m_{d_k}\tilde{\Sigma}_L^{ki} + \not{p}'_{d_i}\tilde{\Sigma}_R^{ki}}{m_{d_i}^2 - m_{d_k}^2}\right|_{\not{p}'_{d_i}} \right) \Bigg] O_2 \\
+ & g_R^{S_\alpha d_j d_i} \Bigg[\frac{1}{2} g_R^{S_\alpha d_j d_i} \left(\left.\frac{d\hat{\Sigma}_R^{jj}}{d\not{p}}\right|_{\not{p}_{d_j}} + \left.\frac{d\hat{\Sigma}_R^{jj}}{d\not{p}}\right|_{\not{p}'_{d_j}} + \left.\frac{d\tilde{\Sigma}_R^{ii}}{d\not{p}}\right|_{\not{p}_{d_i}} + \left.\frac{d\tilde{\Sigma}_R^{ii}}{d\not{p}}\right|_{\not{p}'_{d_i}} \right) \\
& + \sum_{k\neq j} g_R^{S_\alpha d_k d_i} \left(\left.\frac{m_{d_k}\hat{\Sigma}_R^{jk} + \not{p}_{d_j}\hat{\Sigma}_L^{jk}}{m_{d_j}^2 - m_{d_k}^2}\right|_{\not{p}_{d_j}} + \left.\frac{m_{d_k}\hat{\Sigma}_R^{jk} + \not{p}'_{d_j}\hat{\Sigma}_L^{jk}}{m_{d_j}^2 - m_{d_k}^2}\right|_{\not{p}'_{d_j}} \right) \\
& + \sum_{k\neq i} g_R^{S_\alpha d_j d_k} \left(\left.\frac{m_{d_k}\tilde{\Sigma}_R^{ki} + \not{p}_{d_i}\tilde{\Sigma}_L^{ki}}{m_{d_i}^2 - m_{d_k}^2}\right|_{\not{p}_{d_i}} + \left.\frac{m_{d_k}\tilde{\Sigma}_R^{ki} + \not{p}'_{d_i}\tilde{\Sigma}_L^{ki}}{m_{d_i}^2 - m_{d_k}^2}\right|_{\not{p}'_{d_i}} \right) \Bigg] \tilde{O}_2 \\
+ & \Bigg(g_L^{S_\alpha d_j d_i} \Bigg[\frac{1}{2} g_R^{S_\alpha d_j d_i} \left(\left.\frac{d\hat{\Sigma}_R^{jj}}{d\not{p}}\right|_{\not{p}_{d_j}} + \left.\frac{d\hat{\Sigma}_R^{jj}}{d\not{p}}\right|_{\not{p}'_{d_j}} + \left.\frac{d\tilde{\Sigma}_R^{ii}}{d\not{p}}\right|_{\not{p}_{d_i}} + \left.\frac{d\tilde{\Sigma}_R^{ii}}{d\not{p}}\right|_{\not{p}'_{d_i}} \right) \\
& + \sum_{k\neq j} g_R^{S_\alpha d_k d_i} \left(\left.\frac{m_{d_k}\hat{\Sigma}_R^{jk} + \not{p}_{d_j}\hat{\Sigma}_L^{jk}}{m_{d_j}^2 - m_{d_k}^2}\right|_{\not{p}_{d_j}} + \left.\frac{m_{d_k}\hat{\Sigma}_R^{jk} + \not{p}'_{d_j}\hat{\Sigma}_L^{jk}}{m_{d_j}^2 - m_{d_k}^2}\right|_{\not{p}'_{d_j}} \right) \\
& + \sum_{k\neq i} g_R^{S_\alpha d_j d_k} \left(\left.\frac{m_{d_k}\tilde{\Sigma}_R^{ki} + \not{p}_{d_i}\tilde{\Sigma}_L^{ki}}{m_{d_i}^2 - m_{d_k}^2}\right|_{\not{p}_{d_i}} + \left.\frac{m_{d_k}\tilde{\Sigma}_R^{ki} + \not{p}'_{d_i}\tilde{\Sigma}_L^{ki}}{m_{d_i}^2 - m_{d_k}^2}\right|_{\not{p}'_{d_i}} \right) \Bigg] \\
+ & g_R^{S_\alpha d_j d_i} \Bigg[\frac{1}{2} g_L^{S_\alpha d_j d_i} \left(\left.\frac{d\hat{\Sigma}_L^{jj}}{d\not{p}}\right|_{\not{p}_{d_j}} + \left.\frac{d\hat{\Sigma}_L^{jj}}{d\not{p}}\right|_{\not{p}'_{d_j}} + \left.\frac{d\tilde{\Sigma}_L^{ii}}{d\not{p}}\right|_{\not{p}_{d_i}} + \left.\frac{d\tilde{\Sigma}_L^{ii}}{d\not{p}}\right|_{\not{p}'_{d_i}} \right) \\
& + \sum_{k\neq j} g_L^{S_\alpha d_k d_i} \left(\left.\frac{m_{d_k}\hat{\Sigma}_L^{jk} + \not{p}_{d_j}\hat{\Sigma}_R^{jk}}{m_{d_j}^2 - m_{d_k}^2}\right|_{\not{p}_{d_j}} + \left.\frac{m_{d_k}\hat{\Sigma}_L^{jk} + \not{p}'_{d_j}\hat{\Sigma}_R^{jk}}{m_{d_j}^2 - m_{d_k}^2}\right|_{\not{p}'_{d_j}} \right) \\
& + \sum_{k\neq i} g_L^{S_\alpha d_j d_k} \left(\left.\frac{m_{d_k}\tilde{\Sigma}_L^{ki} + \not{p}_{d_i}\tilde{\Sigma}_R^{ki}}{m_{d_i}^2 - m_{d_k}^2}\right|_{\not{p}_{d_i}} + \left.\frac{m_{d_k}\tilde{\Sigma}_L^{ki} + \not{p}'_{d_i}\tilde{\Sigma}_R^{ki}}{m_{d_i}^2 - m_{d_k}^2}\right|_{\not{p}'_{d_i}} \right) \Bigg] \Bigg) O_4 \Bigg\},
\end{aligned}
$$

(C.1)

where the momenta $\not{p}_{d_j}$, $\not{p}'_{d_j}$, $\not{p}_{d_i}$ and $\not{p}'_{d_i}$ are evaluated at the values m_{d_j}, $-m_{d_j}$, m_{d_i} and $-m_{d_i}$. We list below the contributions to the self-energies.

C.1 Scalar/fermion loop

$$-i\Sigma_{d_j d_i}^{S/f}(\not{p}) = \frac{i}{16\pi^2}\Big\{ -\not{p}\left[g_L^{Sfd_j\,*}g_L^{Sfd_i}P_L + g_R^{Sfd_j\,*}g_R^{Sfd_i}P_R\right]B_1$$
$$+ m_f\left[g_R^{Sfd_j\,*}g_L^{Sfd_i}P_L + g_L^{Sfd_j\,*}g_R^{Sfd_i}P_R\right]B_0\Big\}(-p,m_f,m_S) \quad (C.2)$$

The scalar/fermion pair (S/f) is summed over the following list of particles:

- Higgs-sneutrino/down: couplings from eq. (A.6).

- Charged Higgs-slepton/up: couplings from eq. (A.7).

- sdown/neutralino-neutrino: couplings from eq. (A.8).

- sdown/gluino: couplings from eq. (A.9); color-factor $C_2(3) = 4/3$.

- sup/chargino-lepton: couplings from eq. (A.10).

- sup/down: couplings from eq. (A.11); color factor: $\varepsilon_{abc}\varepsilon_{abd} = 2\delta_{cd}$.

- sdown/up: couplings from eq. (A.12); color factor: $\varepsilon_{abc}\varepsilon_{abd} = 2\delta_{cd}$.

C.2 Vector/fermion loop

$$-i\Sigma_{d_j d_i}^{V/f}(p) = -\frac{i}{16\pi^2}\Big\{(D-2)\not{p}\left[g_L^{Vfd_j\,*}g_L^{Vfd_i}P_L + g_R^{Vfd_j\,*}g_R^{Vfd_i}P_R\right]B_1$$
$$+ Dm_f\left[g_R^{Vfd_j\,*}g_L^{Vfd_i}P_L + g_L^{Vfd_j\,*}g_R^{Vfd_i}P_R\right]B_0\Big\}(-p,m_f,m_V) \quad (C.3)$$

The vector/fermion pair (S/f) is summed over the following list of particles:

- W/up: eq. (A.13).

- Z/down: eq. (A.14).

C.3 Counterterm

Defining the generic d-mass counterterm $\delta m_{d\,ji} = \delta m_{d\,ji}^L P_L + \delta m_{d\,ji}^R P_R$ as well as the d-wave-function counterterm $\delta Z_{d\,ji} = \delta Z_{d\,ji}^L P_L + \delta Z_{d\,ji}^R P_R$, we arrive at the following contribution:

$$-i\Sigma_{d_j d_i}^{CT}(p) = i\frac{\not{p}}{2}\left[\left(\delta Z_{d\,ji}^L + \delta Z_{d\,ij}^{L\,*}\right)P_L + \left(\delta Z_{d\,ji}^R + \delta Z_{d\,ij}^{R\,*}\right)P_R\right]$$
$$- i\left[\left(\delta m_{d\,ji}^L + \frac{1}{2}\left(m_{d_i}\delta Z_{d\,ij}^{R\,*} + m_{d_j}\delta Z_{d\,ji}^L\right)\right)P_L\right.$$
$$\left. + \left(\delta m_{d\,ji}^R + \frac{1}{2}\left(m_{d_i}\delta Z_{d\,ij}^{L\,*} + m_{d_j}\delta Z_{d\,ji}^R\right)\right)P_R\right] \quad (C.4)$$

In principle, $\delta m_{d\,ji}^L = \left(\delta m_{d\,ij}^R\right)^* = \delta Y_{d\,ji}^L v_d + Y_d^i \delta_{ij}\delta v_d$.

D Sneutrino-Higgs self-energies

We assume that the tadpoles (Higgs, gauge bosons) vanish, which supposes certain relations at the loop-level between vevs and tree-level parameters. Then, defining the renormalized neutral-scalar self-energy matrix $\hat{\Sigma}_{\alpha\beta}^S$, we derive the following contribution to the EFT:

$$\mathcal{L}_{\text{EFT}} \ni \frac{-1}{2m_{S_\alpha}^2 m_{S_\beta}^2} \left[g_L^{S_\alpha d_j d_i} \hat{\Sigma}_{\alpha\beta}^S g_L^{S_\beta d_j d_i} O_2 + g_R^{S_\alpha d_j d_i} \hat{\Sigma}_{\alpha\beta}^S g_R^{S_\beta d_j d_i} \tilde{O}_2 + 2 g_L^{S_\alpha d_j d_i} \hat{\Sigma}_{\alpha\beta}^S g_R^{S_\beta d_j d_i} O_4 \right] . \tag{D.1}$$

The various contributions to the neutral-scalar self-energies are listed below.

D.1 Scalar A_0-loop

$$-\imath \Sigma_{\alpha\beta}^{S\,A_S} = -\frac{\imath}{16\pi^2} g^{\tilde{S}\tilde{S}S_\alpha S_\beta} A_0(m_{\tilde{S}}) . \tag{D.2}$$

This contribution is summed over the scalar $\tilde{S}$, taking value in the following list of particles:

- scalar-ups: couplings from eq. (A.30). 3 colors contributing.

- sdowns: couplings from eq. (A.31). 3 colors contributing.

- Charged Higgs-sleptons: couplings from eq. (A.33).

- Higgs-sneutrinos: couplings from eq. (A.34); symmetry-factor 1/2.

D.2 Vector A_0-loop

$$-\imath \Sigma_{\alpha\beta}^{S\,A_V} = \frac{\imath}{16\pi^2} g^{VVS_\alpha S_\beta} D\, A_0(m_V) \tag{D.3}$$

The vector V belongs to the following list of particles:

- W's: couplings from eq. (A.28).

- Z's: couplings from eq. (A.29); symmetry-factor 1/2.

D.3 Scalar B-loop

$$-\imath \Sigma_{\alpha\beta}^{S\,B_S} == \frac{\imath}{16\pi^2} g^{S_\delta S_\gamma S_\alpha} g^{S_\gamma S_\delta S_\beta} B_0(m_{S_\gamma}, m_{S_\delta}) \tag{D.4}$$

The scalar pair (S_γ, S_δ) is summed over the particles:

- scalar-ups: couplings from eq. (A.24). 3 colors contributing.

- sdowns: couplings from eq. (A.25). 3 colors contributing.

- Charged Higgs-sleptons: couplings from eq. (A.26).

- Higgs-sneutrinos: couplings from eq. (A.27).

D.4 Fermion B-loop

$$-\imath\Sigma^{S\,B_f}_{\alpha\beta} = \frac{-2\imath}{16\pi^2}\Bigg\{ \left[g_L^{S_\alpha\tilde{f}f}g_L^{S_\beta\tilde{f}f\,*} + g_R^{S_\alpha\tilde{f}f}g_R^{S_\beta\tilde{f}f\,*} \right] DB_{22}$$

$$+ \left[g_L^{S_\alpha\tilde{f}f}g_R^{S_\beta\tilde{f}f\,*} + g_R^{S_\alpha\tilde{f}f}g_L^{S_\beta\tilde{f}f\,*} \right] m_f m_{\tilde{f}} B_0 \Bigg\}(m_f, m_{\tilde{f}}) \qquad \text{(D.5)}$$

List of particles for the fermion pair $(f, \tilde{f})$:

- ups: couplings of eq. (A.15). 3 colors contributing.

- downs: couplings of eq. (A.6). 3 colors contributing.

- charginos-leptons: couplings of eq. (A.16).

- neutrino-neutralinos: couplings of eq. (A.17); symmetry-factor 1/2.

D.5 Vector B-loop

$$-\imath\Sigma^{S\,B_V}_{\alpha\beta} = \frac{\imath}{16\pi^2} g^{S_\alpha VV} g^{S_\beta VV} DB_0(m_V, m_V) \qquad \text{(D.6)}$$

The vector V is summed over:

- W's: couplings of eq. (A.18).

- Z's: couplings of eq. (A.19); symmetry-factor 1/2

D.6 Ghost B-loop

$$-\imath\Sigma^{S\,B_g}_{\alpha\beta} = -\frac{\imath}{16\pi^2} g^{S_\alpha gg} g^{S_\beta gg} B_0(m_g, m_g) \qquad \text{(D.7)}$$

The contribution is summed over the ghost fields g:

- g_W's: couplings of eq. (A.20).

- g_Z: couplings of eq. (A.21).

D.7 Scalar/vector B-loop

$$-\imath\Sigma^{S\,B_{SV}}_{\alpha\beta} = \frac{\imath}{16\pi^2} g^{S_\alpha VS\,*} g^{S_\beta VS} DB_{22}(m_V, m_S) \qquad \text{(D.8)}$$

List of particles for the scalar/vector pair (S/V):

- Charged Higgs-slepton / W: couplings of eq. (A.22).

- Higgs - sneutrino / Z: couplings of eq. (A.23).

D.8 Counterterms

Defining the neutral scalar mass and wave-function counterterms $\delta m^2_{\alpha\beta}$ and $\delta Z^S_{\alpha\beta}$:

$$-\imath\Sigma^{S\,CT}_{\alpha\beta} = -\imath\left[\delta m^2_{\alpha\beta} + \frac{1}{2}\delta Z^S_{\alpha\beta}\left(m^2_{S_\alpha} + m^2_{S_\beta} \right) \right] \qquad \text{(D.9)}$$

E Vertex corrections

The vertex corrections to the EFT are obtained as:

$$\mathcal{L}_{\text{EFT}} \ni \frac{1}{2m_{S_\alpha}^2} \Big[g_L^{S_\alpha d_j d_i} \hat{V}_L^{S_\alpha d_j d_i} O_2 + g_R^{S_\alpha d_j d_i} \hat{V}_R^{S_\alpha d_j d_i} \tilde{O}_2$$
$$+ \Big(g_R^{S_\alpha d_j d_i} \hat{V}_L^{S_\alpha d_j d_i} + g_L^{S_\alpha d_j d_i} \hat{V}_R^{S_\alpha d_j d_i} \Big) O_4 \Big] \tag{E.1}$$

where the $\bar{d}_j d_i$-neutral-Higgs renormalized vertex function $\hat{V}^{S_\alpha d_j d_i} = \hat{V}_L^{S_\alpha d_j d_i} P_L + \hat{V}_L^{S_\alpha d_j d_i} P_R$ receives the contributions listed below.

E.1 Scalar/fermion loop with cubic scalar coupling

$$-i\hat{V}^{S_\alpha d_j d_i}[Sff, S^3] = -\frac{i}{16\pi^2} g^{S_\alpha S_k S_l}$$
$$\times \Big[g_R^{S_l f d_j \, *} g_L^{S_k f d_i} P_L + g_L^{S_l f d_j \, *} g_R^{S_k f d_i} P_R \Big] m_f C_0(m_f, m_{S_k}, m_{S_l}) \tag{E.2}$$

List of particles for the scalar/fermion triplet $(S_k, S_l/f)$:

- Higgs-sneutrino/down: couplings from eqs. (A.6), (A.27).

- Charged Higgs-slepton/up: couplings from eqs. (A.7), (A.26).

- sdown/neutralino-neutrino: couplings from eqs. (A.8), (A.25).

- sdown/gluino: couplings from eqs. (A.9), (A.25); color-factor $C_2(3) = 4/3$.

- sup/chargino-lepton: couplings from eqs. (A.10), (A.24).

- sup/down: couplings from eqs. (A.11), (A.24).

- sdown/up: couplings from eqs. (A.12), (A.25).

E.2 Scalar/fermion loop without cubic scalar coupling

$$-i\hat{V}^{S_\alpha d_j d_i}[Sff] = -\frac{i}{16\pi^2} \Big\{ \Big[g_R^{S f_l d_j \, *} g_R^{S_\alpha f_l f_k} g_L^{S f_k d_i} P_L + g_L^{S f_l d_j \, *} g_L^{S_\alpha f_l f_k} g_R^{S f_k d_i} P_R \Big] D\, C_{24}$$
$$+ \Big[g_R^{S f_l d_j \, *} g_L^{S_\alpha f_l f_k} g_L^{S f_k d_i} P_L + g_L^{S f_l d_j \, *} g_R^{S_\alpha f_l f_k} g_R^{S f_k d_i} P_R \Big] m_{f_k} m_{f_l} C_0 \Big\}$$
$$\times (m_S, m_{f_k}, m_{f_l}) \tag{E.3}$$

List of particles for the scalar/fermion triplet $(S/f_k, f_l)$:

- Higgs-sneutrino/down: couplings from eq. (A.6).

- Charged Higgs-slepton/up: couplings from eqs. (A.7), (A.15).

- sdown/neutralino-neutrino: couplings from eqs. (A.8), (A.17).

- sup/chargino-lepton: couplings from eqs. (A.10), (A.16).

- sup/down: couplings from eqs. (A.11), (A.6).

- sdown/up: couplings from eqs. (A.12), (A.15).

E.3 Vector/fermion loop with scalar-vector coupling

$$-\imath \hat{V}^{S_\alpha d_j d_i}[SVV, Vff] = -\frac{\imath}{16\pi^2} g^{S_\alpha V_k V_l} \left[g_R^{V_l f d_j *} g_L^{V_k f d_i} P_L + g_L^{V_l f d_j *} g_R^{V_k f d_i} P_R \right]$$
$$\times D m_f \, C_0(m_f, m_{V_k}, m_{V_l}) \tag{E.4}$$

The vector/fermion triplet $(V_k, V_l/f)$ takes the following values:

- W/up: couplings from eqs. (A.13), (A.18).

- Z/down: couplings from eqs. (A.14), (A.19).

E.4 Vector/fermion loop with scalar-fermion coupling

$$- \imath \hat{V}^{S_\alpha d_j d_i}[SVV, Sff]$$
$$= \frac{\imath}{16\pi^2} \left\{ \left[g_R^{V f_l d_j *} g_L^{S_\alpha f_l f_k} g_L^{V f_k d_i} P_L + g_L^{V f_l d_j *} g_R^{S_\alpha f_l f_k} g_R^{V f_k d_i} P_R \right] D^2 C_{24} \right.$$
$$\left. + \left[g_R^{V f_l d_j *} g_R^{S_\alpha f_l f_k} g_L^{V f_k d_i} P_L + g_L^{V f_l d_j *} g_L^{S_\alpha f_l f_k} g_R^{V f_k d_i} P_R \right] D m_{f_k} m_{f_l} C_0 \right\}$$
$$\times (m_V, m_{f_k}, m_{f_l}) \tag{E.5}$$

The vector/fermion triplet $(V/f_k, f_l)$ takes the following values:

- W/up: couplings from eqs. (A.13), (A.15).

- Z/down: couplings from eqs. (A.14), (A.6).

E.5 Vector/Scalar/fermion loops

$$-\imath \hat{V}^{S_\alpha d_j d_i}[VSf] = -\frac{\imath}{16\pi^2} \left\{ g^{VSS_\alpha} \left[g_R^{S f d_j *} g_L^{V f d_i} P_L + g_L^{S f d_j *} g_R^{V f d_i} P_R \right] \right.$$
$$\left. + g^{SVS_\alpha} \left[g_R^{V f d_j *} g_L^{S f d_i} P_L + g_L^{V f d_j *} g_R^{S f d_i} P_R \right] \right\}$$
$$\times D \, C_{24}(m_f, m_S, m_V) \tag{E.6}$$

List of particles for the scalar/vector/fermion triplet $(S/V/f)$:

- charged-Higgs-slepton/W/up: couplings from eqs. (A.13), (A.7), (A.22).

- neutral-Higgs-sneutrino/Z/down: couplings from eqs. (A.14), (A.6), (A.23).

E.6 Counterterms

The counterterm contribution $-\imath \hat{V}^{S_\alpha d_j d_i}[CT]$ reads:

$$\imath \left\{ -\frac{1}{\sqrt{2}} \left[\delta Y_{dji}^L (X_{kd}^R + \imath X_{kd}^I) + \delta \lambda_{fij}^{\prime L} (X_{k\tilde{N}_f}^R + \imath X_{k\tilde{N}_f}^I) \right] \right.$$
$$\left. + \frac{1}{2} \left[\delta Z_{djl}^{R *} g_L^{S_\alpha d_l d_i} + \delta Z_{dil}^L g_L^{S_\alpha d_j d_l} + \delta Z_{k\alpha}^S g_L^{S_\alpha d_j d_i} \right] \right\} P_L$$
$$+ \imath \left\{ -\frac{1}{\sqrt{2}} \left[\delta Y_{dji}^R (X_{kd}^R - \imath X_{kd}^I) + \delta \lambda_{fji}^{\prime R} (X_{k\tilde{N}_f}^R - \imath X_{k\tilde{N}_f}^I) \right] \right.$$
$$\left. + \frac{1}{2} \left[\delta Z_{djl}^{L *} g_R^{S_\alpha d_l d_i} + \delta Z_{dil}^R g_R^{S_\alpha d_j d_l} + \delta Z_{k\alpha}^S g_R^{S_\alpha d_j d_i} \right] \right\} P_R \tag{E.7}$$

where $\delta Y^R_{dji} = \left(\delta Y^L_{dij}\right)^*$ is the counterterm to the Yukawa coupling and $\delta \lambda'^R_{fji} = \left(\delta \lambda'^L_{fji}\right)^*$ is the counterterm to the λ' coupling.

F Box diagrams

Here, we collect the box-diagram contributions to the $d_i \bar{d}_j \to d_j \bar{d}_i$ amplitude. The results are listed according to the topologies of figure 2.

F.1 Vector/fermion/vector/fermion "straight" box

Case $V_{\alpha,\beta}$ colour-singlets:

$$
\begin{aligned}
\mathcal{L}_{\text{EFT}} \ni \frac{1}{32\pi^2} & \left\{ g^{V_\alpha f_k d_j *}_L g^{V_\beta f_k d_i}_L g^{V_\beta f_l d_j *}_L g^{V_\alpha f_l d_i}_L D_2 O_1 + g^{V_\alpha f_k d_j *}_R g^{V_\beta f_k d_i}_R g^{V_\beta f_l d_j *}_R g^{V_\alpha f_l d_i}_R D_2 \tilde{O}_1 \right. \\
& + 16 g^{V_\alpha f_k d_j *}_R g^{V_\beta f_k d_i}_L g^{V_\beta f_l d_j *}_R g^{V_\alpha f_l d_i}_L m_{f_k} m_{f_l} D_0 O_2 \\
& + 16 g^{V_\alpha f_k d_j *}_L g^{V_\beta f_k d_i}_R g^{V_\beta f_l d_j *}_L g^{V_\alpha f_l d_i}_R m_{f_k} m_{f_l} D_0 \tilde{O}_2 \\
& + 16 \left[g^{V_\alpha f_k d_j *}_R g^{V_\beta f_k d_i}_L g^{V_\beta f_l d_j *}_L g^{V_\alpha f_l d_i}_R + g^{V_\alpha f_k d_j *}_L g^{V_\beta f_k d_i}_R g^{V_\beta f_l d_j *}_R g^{V_\alpha f_l d_i}_L \right] m_{f_k} m_{f_l} D_0 O_4 \\
& \left. - 2 \left[g^{V_\alpha f_k d_j *}_L g^{V_\beta f_k d_i}_L g^{V_\beta f_l d_j *}_R g^{V_\alpha f_l d_i}_R + g^{V_\alpha f_k d_j *}_R g^{V_\beta f_k d_i}_R g^{V_\beta f_l d_j *}_L g^{V_\alpha f_l d_i}_L \right] D_2 O_5 \right\} \\
& \times (m_{S_\alpha}, m_{f_k}, m_{S_\beta}, m_{f_l})
\end{aligned}
\tag{F.1}
$$

List of particles:

- W / up: couplings from eq. (A.13).

F.2 Scalar/fermion/scalar/fermion "straight" box

Case 1: $S_{\alpha,\beta}$ colour-singlets:

$$
\begin{aligned}
\mathcal{L}_{\text{EFT}} \ni \frac{1}{32\pi^2} & \left\{ g^{S_\alpha f_k d_j *}_L g^{S_\beta f_k d_i}_L g^{S_\beta f_l d_j *}_L g^{S_\alpha f_l d_i}_L \frac{D_2}{4} O_1 \right. \\
& + g^{S_\alpha f_k d_j *}_R g^{S_\beta f_k d_i}_R g^{S_\beta f_l d_j *}_R g^{S_\alpha f_l d_i}_R \frac{D_2}{4} \tilde{O}_1 \\
& + g^{S_\alpha f_k d_j *}_R g^{S_\beta f_k d_i}_L g^{S_\beta f_l d_j *}_R g^{S_\alpha f_l d_i}_L m_{f_k} m_{f_l} D_0 O_2 \\
& + g^{S_\alpha f_k d_j *}_L g^{S_\beta f_k d_i}_R g^{S_\beta f_l d_j *}_L g^{S_\alpha f_l d_i}_R m_{f_k} m_{f_l} D_0 \tilde{O}_2 \\
& + \left[g^{S_\alpha f_k d_j *}_R g^{S_\beta f_k d_i}_L g^{S_\beta f_l d_j *}_L g^{S_\alpha f_l d_i}_R + g^{S_\alpha f_k d_j *}_L g^{S_\beta f_k d_i}_R g^{S_\beta f_l d_j *}_R g^{S_\alpha f_l d_i}_L \right] m_{f_k} m_{f_l} D_0 O_4 \\
& \left. - \left[g^{S_\alpha f_k d_j *}_L g^{S_\beta f_k d_i}_L g^{S_\beta f_l d_j *}_R g^{S_\alpha f_l d_i}_R + g^{S_\alpha f_k d_j *}_R g^{S_\beta f_k d_i}_R g^{S_\beta f_l d_j *}_L g^{S_\alpha f_l d_i}_L \right] \frac{D_2}{2} O_5 \right\} \\
& \times (m_{S_\alpha}, m_{f_k}, m_{S_\beta}, m_{f_l})
\end{aligned}
\tag{F.2}
$$

List of particles:

- Higgs-sneutrino / down: couplings from eq. (A.6).

- Charged Higgs-slepton / up: couplings from eq. (A.7).

Case 2: $f_{k,l}$ colour-singlets:

$$\mathcal{L}_{\text{EFT}} \ni \frac{1}{32\pi^2} \left\{ g_L^{S_\alpha f_k d_j *} g_L^{S_\beta f_k d_i} g_L^{S_\beta f_l d_j *} g_L^{S_\alpha f_l d_i} \frac{D_2}{4} O_1 + g_R^{S_\alpha f_k d_j *} g_R^{S_\beta f_k d_i} g_R^{S_\beta f_l d_j *} g_R^{S_\alpha f_l d_i} \frac{D_2}{4} \tilde{O}_1 \right.$$

$$+ g_R^{S_\alpha f_k d_j *} g_L^{S_\beta f_k d_i} g_R^{S_\beta f_l d_j *} g_L^{S_\alpha f_l d_i} m_{f_k} m_{f_l} D_0 \, O_3$$

$$+ g_L^{S_\alpha f_k d_j *} g_R^{S_\beta f_k d_i} g_L^{S_\beta f_l d_j *} g_R^{S_\alpha f_l d_i} m_{f_k} m_{f_l} D_0 \, \tilde{O}_3$$

$$- \left[g_L^{S_\alpha f_k d_j *} g_L^{S_\beta f_k d_i} g_R^{S_\beta f_l d_j *} g_R^{S_\alpha f_l d_i} + g_R^{S_\alpha f_k d_j *} g_R^{S_\beta f_k d_i} g_L^{S_\beta f_l d_j *} g_L^{S_\alpha f_l d_i} \right] \frac{D_2}{2} O_4$$

$$+ \left. \left[g_R^{S_\alpha f_k d_j *} g_L^{S_\beta f_k d_i} g_L^{S_\beta f_l d_j *} g_R^{S_\alpha f_l d_i} + g_L^{S_\alpha f_k d_j *} g_R^{S_\beta f_k d_i} g_R^{S_\beta f_l d_j *} g_L^{S_\alpha f_l d_i} \right] m_{f_k} m_{f_l} D_0 \, O_5 \right\}$$

$$\times \, (m_{S_\alpha}, m_{f_k}, m_{S_\beta}, m_{f_l}) \tag{F.3}$$

List of particles:

- sdown / neutrino-neutralino: couplings from eq. (A.8).

- sup / chargino-lepton: couplings from eq. (A.10).

Case 3: all fields colour-triplets:

$$\mathcal{L}_{\text{EFT}} \ni \frac{1}{32\pi^2} \left\{ g_L^{S_\alpha f_k d_j *} g_L^{S_\beta f_k d_i} g_L^{S_\beta f_l d_j *} g_L^{S_\alpha f_l d_i} \frac{D_2}{2} O_1 + g_R^{S_\alpha f_k d_j *} g_R^{S_\beta f_k d_i} g_R^{S_\beta f_l d_j *} g_R^{S_\alpha f_l d_i} \frac{D_2}{2} \tilde{O}_1 \right.$$

$$+ g_R^{S_\alpha f_k d_j *} g_L^{S_\beta f_k d_i} g_R^{S_\beta f_l d_j *} g_L^{S_\alpha f_l d_i} m_{f_k} m_{f_l} D_0 (O_2 + O_3)$$

$$+ g_L^{S_\alpha f_k d_j *} g_R^{S_\beta f_k d_i} g_L^{S_\beta f_l d_j *} g_R^{S_\alpha f_l d_i} m_{f_k} m_{f_l} D_0 (\tilde{O}_2 + \tilde{O}_3)$$

$$+ (O_4 + O_5) \left(\left[g_R^{S_\alpha f_k d_j *} g_L^{S_\beta f_k d_i} g_L^{S_\beta f_l d_j *} g_R^{S_\alpha f_l d_i} \right. \right.$$

$$\left. + g_L^{S_\alpha f_k d_j *} g_R^{S_\beta f_k d_i} g_R^{S_\beta f_l d_j *} g_L^{S_\alpha f_l d_i} \right] m_{f_k} m_{f_l} D_0$$

$$\left. \left. - \left[g_L^{S_\alpha f_k d_j *} g_L^{S_\beta f_k d_i} g_R^{S_\beta f_l d_j *} g_R^{S_\alpha f_l d_i} + g_R^{S_\alpha f_k d_j *} g_R^{S_\beta f_k d_i} g_L^{S_\beta f_l d_j *} g_L^{S_\alpha f_l d_i} \right] \frac{D_2}{2} \right) \right\}$$

$$\times \, (m_{S_\alpha}, m_{f_k}, m_{S_\beta}, m_{f_l}) \tag{F.4}$$

List of particles:

- sdown / up: couplings from eq. (A.12).

- sup / down: couplings from eq. (A.11).

Case 4: $f_{k,l}$ colour-octets:

$$\mathcal{L}_{\text{EFT}} \ni \frac{1}{32\pi^2} \left\{ \frac{11}{18} g_L^{S_\alpha f_k d_j *} g_L^{S_\beta f_k d_i} g_L^{S_\beta f_l d_j *} g_L^{S_\alpha f_l d_i} \frac{D_2}{4} O_1 \right.$$

$$+ \frac{11}{18} g_R^{S_\alpha f_k d_j *} g_R^{S_\beta f_k d_i} g_R^{S_\beta f_l d_j *} g_R^{S_\alpha f_l d_i} \frac{D_2}{4} \tilde{O}_1$$

$$+ g_R^{S_\alpha f_k d_j *} g_L^{S_\beta f_k d_i} g_R^{S_\beta f_l d_j *} g_L^{S_\alpha f_l d_i} m_{f_k} m_{f_l} D_0 \left(\frac{7}{12} O_2 + \frac{1}{36} O_3 \right)$$

$$+ g_L^{S_\alpha f_k d_j *} g_R^{S_\beta f_k d_i} g_L^{S_\beta f_l d_j *} g_R^{S_\alpha f_l d_i} m_{f_k} m_{f_l} D_0 \left(\frac{7}{12} \tilde{O}_2 + \frac{1}{36} \tilde{O}_3 \right)$$

$$+ \left[g_R^{S_\alpha f_k d_j *} g_L^{S_\beta f_k d_i} g_L^{S_\beta f_l d_j *} g_R^{S_\alpha f_l d_i} \right.$$

$$\left. + g_L^{S_\alpha f_k d_j *} g_R^{S_\beta f_k d_i} g_R^{S_\beta f_l d_j *} g_L^{S_\alpha f_l d_i} \right] m_{f_k} m_{f_l} D_0 \left(\frac{7}{12} O_4 + \frac{1}{36} O_5 \right)$$

$$- \left[g_L^{S_\alpha f_k d_j *} g_L^{S_\beta f_k d_i} g_R^{S_\beta f_l d_j *} g_R^{S_\alpha f_l d_i} \right.$$

$$\left. + g_R^{S_\alpha f_k d_j *} g_R^{S_\beta f_k d_i} g_L^{S_\beta f_l d_j *} g_L^{S_\alpha f_l d_i} \right] \frac{D_2}{4} \left(\frac{1}{18} O_4 + \frac{7}{6} O_5 \right) \Bigg\}$$

$$\times (m_{S_\alpha}, m_{f_k}, m_{S_\beta}, m_{f_l}) \tag{F.5}$$

List of particles:

- sdown / gluino: couplings from eq. (A.9) (stripped from Gell-Mann matrix element).

Case 5: $f_{k,l}$ colour-octet+singlet:

$$\mathcal{L}_{\text{EFT}} \ni \frac{1}{32\pi^2} \Bigg\{ \frac{1}{3} g_L^{S_\alpha f_k d_j *} g_L^{S_\beta f_k d_i} g_L^{S_\beta f_l d_j *} g_L^{S_\alpha f_l d_i} \frac{D_2}{4} O_1$$

$$+ \frac{1}{3} g_R^{S_\alpha f_k d_j *} g_R^{S_\beta f_k d_i} g_R^{S_\beta f_l d_j *} g_R^{S_\alpha f_l d_i} \frac{D_2}{4} \tilde{O}_1$$

$$+ g_R^{S_\alpha f_k d_j *} g_L^{S_\beta f_k d_i} g_R^{S_\beta f_l d_j *} g_L^{S_\alpha f_l d_i} m_{f_k} m_{f_l} D_0 \frac{1}{2} \left(O_2 - \frac{1}{3} O_3 \right)$$

$$+ g_L^{S_\alpha f_k d_j *} g_R^{S_\beta f_k d_i} g_L^{S_\beta f_l d_j *} g_R^{S_\alpha f_l d_i} m_{f_k} m_{f_l} D_0 \frac{1}{2} \left(\tilde{O}_2 - \frac{1}{3} \tilde{O}_3 \right)$$

$$+ \left[g_R^{S_\alpha f_k d_j *} g_L^{S_\beta f_k d_i} g_L^{S_\beta f_l d_j *} g_R^{S_\alpha f_l d_i} \right.$$

$$\left. + g_L^{S_\alpha f_k d_j *} g_R^{S_\beta f_k d_i} g_R^{S_\beta f_l d_j *} g_L^{S_\alpha f_l d_i} \right] m_{f_k} m_{f_l} D_0 \left(O_4 - \frac{1}{3} O_5 \right)$$

$$+ \left[g_L^{S_\alpha f_k d_j *} g_L^{S_\beta f_k d_i} g_R^{S_\beta f_l d_j *} g_R^{S_\alpha f_l d_i} \right.$$

$$\left. + g_R^{S_\alpha f_k d_j *} g_R^{S_\beta f_k d_i} g_L^{S_\beta f_l d_j *} g_L^{S_\alpha f_l d_i} \right] \frac{D_2}{4} \left(\frac{1}{3} O_4 - O_5 \right) \Bigg\}$$

$$\times (m_{S_\alpha}, m_{f_k}, m_{S_\beta}, m_{f_l}) \tag{F.6}$$

List of particles:

- sdown / gluino / sdown / neutralino-neutrino: couplings from eqs. (A.8), (A.9) (stripped from Gell-Mann matrix element); ×2 (π-rotated diagram).

F.3 Scalar/fermion/scalar/fermion "scalar-cross" box

Case 1: $S_{\alpha,\beta}$ colour-singlets:

$$\mathcal{L}_{\text{EFT}} \ni \frac{1}{32\pi^2} \Bigg\{ - g_L^{S_\alpha f_k d_j *} g_L^{S_\beta f_k d_i} g_L^{S_\alpha f_l d_j *} g_L^{S_\beta f_l d_i} \frac{D_2}{4} O_1$$

$$- g_R^{S_\alpha f_k d_j *} g_R^{S_\beta f_k d_i} g_R^{S_\alpha f_l d_j *} g_R^{S_\beta f_l d_i} \frac{D_2}{4} \tilde{O}_1$$

$$+ g_R^{S_\alpha f_k d_j *} g_L^{S_\beta f_k d_i} g_R^{S_\alpha f_l d_j *} g_L^{S_\beta f_l d_i} m_{f_k} m_{f_l} D_0 O_2$$

$$+ g_L^{S_\alpha f_k d_j *} g_R^{S_\beta f_k d_i} g_L^{S_\alpha f_l d_j *} g_R^{S_\beta f_l d_i} m_{f_k} m_{f_l} D_0 \, \tilde{O}_2$$

$$+ \left[g_R^{S_\alpha f_k d_j *} g_L^{S_\beta f_k d_i} g_L^{S_\alpha f_l d_j *} g_R^{S_\beta f_l d_i} + g_L^{S_\alpha f_k d_j *} g_R^{S_\beta f_k d_i} g_R^{S_\alpha f_l d_j *} g_L^{S_\beta f_l d_i} \right] m_{f_k} m_{f_l} D_0 \, O_4$$

$$+ \left[g_L^{S_\alpha f_k d_j *} g_L^{S_\beta f_k d_i} g_R^{S_\alpha f_l d_j *} g_R^{S_\beta f_l d_i} + g_R^{S_\alpha f_k d_j *} g_R^{S_\beta f_k d_i} g_L^{S_\alpha f_l d_j *} g_L^{S_\beta f_l d_i} \right] \frac{D_2}{2} \, O_5 \Bigg\}$$

$$\times \, (m_{S_\alpha}, m_{f_k}, m_{S_\beta}, m_{f_l}) \tag{F.7}$$

List of particles:

- Higgs-sneutrino / down: couplings from eq. (A.6).

Case 2: f_k colour-singlet:

$$\mathcal{L}_{\text{EFT}} \ni \frac{1}{32\pi^2} \Bigg\{ g_R^{S_\alpha f_k d_j *} g_L^{S_\beta f_k d_i} g_R^{S_\alpha f_l d_j *} g_L^{S_\beta f_l d_i} m_{f_k} m_{f_l} D_0 (O_2 - O_3)$$

$$+ g_L^{S_\alpha f_k d_j *} g_R^{S_\beta f_k d_i} g_L^{S_\alpha f_l d_j *} g_R^{S_\beta f_l d_i} m_{f_k} m_{f_l} D_0 (\tilde{O}_2 - \tilde{O}_3)$$

$$+ (O_4 - O_5) \bigg(\Big[g_R^{S_\alpha f_k d_j *} g_L^{S_\beta f_k d_i} g_L^{S_\alpha f_l d_j *} g_R^{S_\beta f_l d_i}$$

$$+ g_L^{S_\alpha f_k d_j *} g_R^{S_\beta f_k d_i} g_R^{S_\alpha f_l d_j *} g_L^{S_\beta f_l d_i} \Big] m_{f_k} m_{f_l} D_0$$

$$- \Big[g_L^{S_\alpha f_k d_j *} g_L^{S_\beta f_k d_i} g_R^{S_\alpha f_l d_j *} g_R^{S_\beta f_l d_i} + g_R^{S_\alpha f_k d_j *} g_R^{S_\beta f_k d_i} g_L^{S_\alpha f_l d_j *} g_L^{S_\beta f_l d_i} \Big] \frac{D_2}{2} \bigg) \Bigg\}$$

$$\times \, (m_{S_\alpha}, m_{f_k}, m_{S_\beta}, m_{f_l}) \tag{F.8}$$

List of particles:

- sup / chargino-lepton / sup / down: couplings from eqs. (A.10), (A.11).

- sdown / neutralino-neutrino / sdown / up: couplings from eqs. (A.8), (A.12).

Case 3: f_k colour-triplet:

$$\mathcal{L}_{\text{EFT}} \ni \frac{1}{32\pi^2} \Bigg\{ - g_L^{S_\alpha f_k d_j *} g_L^{S_\beta f_k d_i} g_L^{S_\alpha f_l d_j *} g_L^{S_\beta f_l d_i} \frac{D_2}{4} \, O_1$$

$$- g_R^{S_\alpha f_k d_j *} g_R^{S_\beta f_k d_i} g_R^{S_\alpha f_l d_j *} g_R^{S_\beta f_l d_i} \frac{D_2}{4} \, \tilde{O}_1$$

$$+ g_R^{S_\alpha f_k d_j *} g_L^{S_\beta f_k d_i} g_R^{S_\alpha f_l d_j *} g_L^{S_\beta f_l d_i} m_{f_k} m_{f_l} D_0 \frac{1}{6} (5 O_2 + O_3)$$

$$+ g_L^{S_\alpha f_k d_j *} g_R^{S_\beta f_k d_i} g_L^{S_\alpha f_l d_j *} g_R^{S_\beta f_l d_i} m_{f_k} m_{f_l} D_0 \frac{1}{6} (5 \tilde{O}_2 + \tilde{O}_3)$$

$$+ \Big[g_R^{S_\alpha f_k d_j *} g_L^{S_\beta f_k d_i} g_L^{S_\alpha f_l d_j *} g_R^{S_\beta f_l d_i}$$

$$+ g_L^{S_\alpha f_k d_j *} g_R^{S_\beta f_k d_i} g_R^{S_\alpha f_l d_j *} g_L^{S_\beta f_l d_i} \Big] m_{f_k} m_{f_l} D_0 \frac{1}{6} (5 O_4 + O_5)$$

$$+ \Big[g_L^{S_\alpha f_k d_j *} g_L^{S_\beta f_k d_i} g_R^{S_\alpha f_l d_j *} g_R^{S_\beta f_l d_i}$$

$$+ g_R^{S_\alpha f_k d_j *} g_R^{S_\beta f_k d_i} g_L^{S_\alpha f_l d_j *} g_L^{S_\beta f_l d_i} \Big] \frac{D_2}{4} \frac{1}{3} (O_4 + 5 O_5) \Bigg\}$$

$$\times \, (m_{S_\alpha}, m_{f_k}, m_{S_\beta}, m_{f_l}) \tag{F.9}$$

List of particles:

- sdown / gluino / sdown / up: couplings from eqs. (A.12), (A.9) (stripped from Gell-Mann matrix element); $\times 2$ (π-rotated diagram).

F.4 Scalar/fermion/scalar/fermion "fermion-cross" box

Case 1: f_k colour-singlet:

$$
\begin{aligned}
\mathcal{L}_{\text{EFT}} \ni \frac{1}{32\pi^2} \Big\{ & g_L^{S_\alpha f_k d_j\,*} g_L^{S_\beta f_k d_j\,*} g_L^{S_\alpha f_l d_i} g_L^{S_\beta f_l d_i} \frac{m_{f_k} m_{f_l}}{2} D_0\, O_1 \\
& + g_R^{S_\alpha f_k d_j\,*} g_R^{S_\beta f_k d_j\,*} g_R^{S_\alpha f_l d_i} g_R^{S_\beta f_l d_i} \frac{m_{f_k} m_{f_l}}{2} D_0\, \tilde{O}_1 \\
& - g_R^{S_\alpha f_k d_j\,*} g_R^{S_\beta f_k d_j\,*} g_L^{S_\alpha f_l d_i} g_L^{S_\beta f_l d_i} m_{f_k} m_{f_l} D_0 (O_2 + O_3) \\
& - g_L^{S_\alpha f_k d_j\,*} g_L^{S_\beta f_k d_j\,*} g_R^{S_\alpha f_l d_i} g_R^{S_\beta f_l d_i} m_{f_k} m_{f_l} D_0 (\tilde{O}_2 + \tilde{O}_3) \\
& - \Big[g_L^{S_\alpha f_k d_j\,*} g_R^{S_\beta f_k d_j\,*} g_R^{S_\alpha f_l d_i} g_L^{S_\beta f_l d_i} + g_R^{S_\alpha f_k d_j\,*} g_L^{S_\beta f_k d_j\,*} g_L^{S_\alpha f_l d_i} g_R^{S_\beta f_l d_i} \Big] \frac{D_2}{2} O_4 \\
& + \Big[g_R^{S_\alpha f_k d_j\,*} g_L^{S_\beta f_k d_j\,*} g_R^{S_\alpha f_l d_i} g_L^{S_\beta f_l d_i} + g_L^{S_\alpha f_k d_j\,*} g_R^{S_\beta f_k d_j\,*} g_L^{S_\alpha f_l d_i} g_R^{S_\beta f_l d_i} \Big] \frac{D_2}{2} O_5 \Big\} \\
& \times (m_{S_\alpha}, m_{f_k}, m_{S_\beta}, m_{f_l})
\end{aligned}
\tag{F.10}
$$

List of particles:

- sdown / neutrino-neutralino: couplings from eq. (A.8).

Case 2: S_α colour-singlet:

$$
\begin{aligned}
\mathcal{L}_{\text{EFT}} \ni \frac{1}{32\pi^2} \Big\{ & - g_R^{S_\alpha f_k d_j\,*} g_R^{S_\beta f_k d_j\,*} g_L^{S_\alpha f_l d_i} g_L^{S_\beta f_l d_i} m_{f_k} m_{f_l} D_0\, O_3 \\
& - g_L^{S_\alpha f_k d_j\,*} g_L^{S_\beta f_k d_j\,*} g_R^{S_\alpha f_l d_i} g_R^{S_\beta f_l d_i} m_{f_k} m_{f_l} D_0\, \tilde{O}_3 \\
& - (O_4 - O_5) \Big(\Big[g_R^{S_\alpha f_k d_j\,*} g_L^{S_\beta f_k d_j\,*} g_R^{S_\alpha f_l d_i} g_L^{S_\beta f_l d_i} + g_L^{S_\alpha f_k d_j\,*} g_R^{S_\beta f_k d_j\,*} g_L^{S_\alpha f_l d_i} g_R^{S_\beta f_l d_i} \Big] \\
& + \Big[g_L^{S_\alpha f_k d_j\,*} g_R^{S_\beta f_k d_j\,*} g_R^{S_\alpha f_l d_i} g_L^{S_\beta f_l d_i} + g_R^{S_\alpha f_k d_j\,*} g_L^{S_\beta f_k d_j\,*} g_L^{S_\alpha f_l d_i} g_R^{S_\beta f_l d_i} \Big] \Big) \frac{D_2}{2} \Big\} \\
& \times (m_{S_\alpha}, m_{f_k}, m_{S_\beta}, m_{f_l})
\end{aligned}
\tag{F.11}
$$

List of particles:

- Charged Higgs-slepton / up / sdown / up: couplings from eqs. (A.7), (A.12).

- Higgs-sneutrino / down / sup / down: couplings from eqs. (A.6), (A.11).

Case 3: $f_{k,l}$ colour-octets:

$$
\begin{aligned}
\mathcal{L}_{\text{EFT}} \ni \frac{1}{32\pi^2} \Big\{ & \frac{1}{18} g_L^{S_\alpha f_k d_j\,*} g_L^{S_\beta f_k d_j\,*} g_L^{S_\alpha f_l d_i} g_L^{S_\beta f_l d_i} m_{f_k} m_{f_l} D_0\, O_1 \\
& + \frac{1}{18} g_R^{S_\alpha f_k d_j\,*} g_R^{S_\beta f_k d_j\,*} g_R^{S_\alpha f_l d_i} g_R^{S_\beta f_l d_i} m_{f_k} m_{f_l} D_0\, \tilde{O}_1
\end{aligned}
$$

$$
\begin{aligned}
&- \frac{1}{9} g_R^{S_\alpha f_k d_j *} g_R^{S_\beta f_k d_j *} g_L^{S_\alpha f_l d_i} g_L^{S_\beta f_l d_i} m_{f_k} m_{f_l} D_0 (O_2 + O_3) \\
&- \frac{1}{9} g_L^{S_\alpha f_k d_j *} g_L^{S_\beta f_k d_j *} g_R^{S_\alpha f_l d_i} g_R^{S_\beta f_l d_i} m_{f_k} m_{f_l} D_0 (\tilde{O}_2 + \tilde{O}_3) \\
&- \frac{1}{9} \Big[g_R^{S_\alpha f_k d_j *} g_L^{S_\beta f_k d_j *} g_R^{S_\alpha f_l d_i} g_L^{S_\beta f_l d_i} \\
&\qquad\quad + g_L^{S_\alpha f_k d_j *} g_R^{S_\beta f_k d_j *} g_L^{S_\alpha f_l d_i} g_R^{S_\beta f_l d_i} \Big] \frac{D_2}{4} (5 O_4 - 3 O_5) \\
&- \frac{1}{9} \Big[g_L^{S_\alpha f_k d_j *} g_R^{S_\beta f_k d_j *} g_R^{S_\alpha f_l d_i} g_L^{S_\beta f_l d_i} \\
&\qquad\quad + g_R^{S_\alpha f_k d_j *} g_L^{S_\beta f_k d_j *} g_L^{S_\alpha f_l d_i} g_R^{S_\beta f_l d_i} \Big] \frac{D_2}{4} (3 O_4 - 5 O_5) \Big\} \\
&\times (m_{S_\alpha}, m_{f_k}, m_{S_\beta}, m_{f_l})
\end{aligned}
\tag{F.12}
$$

List of particles:

- sdown / gluinos: couplings from eq. (A.9) (stripped from Gell-Mann matrix element).

Case 4: $f_{k,l}$ colour-octet+singlet:

$$
\begin{aligned}
\mathcal{L}_{\mathrm{EFT}} \ni \frac{1}{32\pi^2} \Big\{ &\frac{1}{6} g_L^{S_\alpha f_k d_j *} g_L^{S_\beta f_k d_j *} g_L^{S_\alpha f_l d_i} g_L^{S_\beta f_l d_i} m_{f_k} m_{f_l} D_0 \, O_1 \\
&+ \frac{1}{6} g_R^{S_\alpha f_k d_j *} g_R^{S_\beta f_k d_j *} g_R^{S_\alpha f_l d_i} g_R^{S_\beta f_l d_i} m_{f_k} m_{f_l} D_0 \, \tilde{O}_1 \\
&- \frac{1}{3} g_R^{S_\alpha f_k d_j *} g_R^{S_\beta f_k d_j *} g_L^{S_\alpha f_l d_i} g_L^{S_\beta f_l d_i} m_{f_k} m_{f_l} D_0 (O_2 + O_3) \\
&- \frac{1}{3} g_L^{S_\alpha f_k d_j *} g_L^{S_\beta f_k d_j *} g_R^{S_\alpha f_l d_i} g_R^{S_\beta f_l d_i} m_{f_k} m_{f_l} D_0 (\tilde{O}_2 + \tilde{O}_3) \\
&+ \frac{1}{3} \Big[g_R^{S_\alpha f_k d_j *} g_L^{S_\beta f_k d_j *} g_R^{S_\alpha f_l d_i} g_L^{S_\beta f_l d_i} \\
&\qquad\quad + g_L^{S_\alpha f_k d_j *} g_R^{S_\beta f_k d_j *} g_L^{S_\alpha f_l d_i} g_R^{S_\beta f_l d_i} \Big] \frac{D_2}{4} (O_4 - 3 O_5) \\
&+ \frac{1}{3} \Big[g_L^{S_\alpha f_k d_j *} g_R^{S_\beta f_k d_j *} g_R^{S_\alpha f_l d_i} g_L^{S_\beta f_l d_i} \\
&\qquad\quad + g_R^{S_\alpha f_k d_j *} g_L^{S_\beta f_k d_j *} g_L^{S_\alpha f_l d_i} g_R^{S_\beta f_l d_i} \Big] \frac{D_2}{4} (3 O_4 - O_5) \Big\} \\
&\times (m_{S_\alpha}, m_{f_k}, m_{S_\beta}, m_{f_l})
\end{aligned}
\tag{F.13}
$$

List of particles:

- sdown / gluino / sdown / neutralino-neutrino: couplings from eqs. (A.8), (A.9) (stripped from Gell-Mann matrix element); + diagram with $\chi^0 \leftrightarrow \tilde{g}$.

F.5 Vector/fermion/scalar/fermion "straight" box

Case S colour-singlet:

$$
\begin{aligned}
\mathcal{L}_{\mathrm{EFT}} \ni \frac{1}{32\pi^2} \Big\{ &- g_L^{V f_k d_j *} g_L^{S f_k d_i} g_L^{S f_l d_j *} g_L^{V f_l d_i} m_{f_k} m_{f_l} D_0 \, O_1 \\
&- g_R^{V f_k d_j *} g_R^{S f_k d_i} g_R^{S f_l d_j *} g_R^{V f_l d_i} m_{f_k} m_{f_l} D_0 \, \tilde{O}_1
\end{aligned}
$$

$$- 2 g_R^{V f_k d_j *} g_L^{S f_k d_i} g_R^{S f_l d_j *} g_L^{V f_l d_i} D_2 (O_2 + O_3)$$

$$- 2 g_L^{V f_k d_j *} g_R^{S f_k d_i} g_L^{S f_l d_j *} g_R^{V f_l d_i} D_2 (\tilde{O}_2 + \tilde{O}_3)$$

$$- \left[g_L^{V f_k d_j *} g_R^{S f_k d_i} g_R^{S f_l d_j *} g_L^{V f_l d_i} + g_R^{V f_k d_j *} g_L^{S f_k d_i} g_L^{S f_l d_j *} g_R^{V f_l d_i} \right] D_2 O_4$$

$$+ 2 \left[g_L^{V f_k d_j *} g_L^{S f_k d_i} g_R^{S f_l d_j *} g_R^{V f_l d_i} + g_R^{V f_k d_j *} g_R^{S f_k d_i} g_L^{S f_l d_j *} g_L^{V f_l d_i} \right] m_{f_k} m_{f_l} D_0 O_5 \Big\}$$

$$\times (m_V, m_{f_k}, m_S, m_{f_l}) \tag{F.14}$$

List of particles:

- Z / down / sneutrino-neutral Higgs /down: couplings from eqs. (A.6), (A.14); $\times 2$ (π-rotated diagram).

- W / up / charged Higgs-slepton / up: couplings from eqs. (A.7), (A.13); $\times 2$ (π-rotated diagram).

F.6 Vector/fermion/scalar/fermion "cross" boxes

Case S colour-singlet:

$$\mathcal{L}_{\text{EFT}} \ni \frac{1}{32\pi^2} \Big\{ - \left(g_L^{V f_k d_j *} g_L^{S f_k d_i} g_L^{V f_l d_j *} g_L^{S f_l d_i} m_{f_k} m_{f_l} \right.$$

$$\left. + g_L^{S f_k d_j *} g_L^{V f_k d_i} g_L^{S f_l d_j *} g_L^{V f_l d_i} \right) m_{f_k} m_{f_l} D_0 O_1$$

$$- \left(g_R^{V f_k d_j *} g_R^{S f_k d_i} g_R^{V f_l d_j *} g_R^{S f_l d_i} + g_R^{S f_k d_j *} g_R^{V f_k d_i} g_R^{S f_l d_j *} g_R^{V f_l d_i} \right) m_{f_k} m_{f_l} D_0 \tilde{O}_1$$

$$- 2 \left(g_R^{V f_k d_j *} g_L^{S f_k d_i} g_R^{V f_l d_j *} g_L^{S f_l d_i} + g_R^{S f_k d_j *} g_L^{V f_k d_i} g_R^{S f_l d_j *} g_L^{V f_l d_i} \right) D_2 O_3$$

$$- 2 \left(g_L^{V f_k d_j *} g_R^{S f_k d_i} g_L^{V f_l d_j *} g_R^{S f_l d_i} + g_L^{S f_k d_j *} g_R^{V f_k d_i} g_L^{S f_l d_j *} g_R^{V f_l d_i} \right) D_2 \tilde{O}_3$$

$$+ \Big[g_L^{V f_k d_j *} g_R^{S f_k d_i} g_R^{V f_l d_j *} g_L^{S f_l d_i} + g_R^{V f_k d_j *} g_L^{S f_k d_i} g_L^{V f_l d_j *} g_R^{S f_l d_i}$$

$$+ g_L^{S f_k d_j *} g_R^{V f_k d_i} g_R^{S f_l d_j *} g_L^{V f_l d_i} + g_R^{S f_k d_j *} g_L^{V f_k d_i} g_L^{S f_l d_j *} g_R^{V f_l d_i} \Big] D_2 O_4$$

$$+ 2 \Big[g_L^{V f_k d_j *} g_L^{S f_k d_i} g_R^{V f_l d_j *} g_R^{S f_l d_i} + g_R^{V f_k d_j *} g_R^{S f_k d_i} g_L^{V f_l d_j *} g_L^{S f_l d_i}$$

$$+ g_L^{S f_k d_j *} g_L^{V f_k d_i} g_R^{S f_l d_j *} g_R^{V f_l d_i} + g_R^{S f_k d_j *} g_R^{V f_k d_i} g_L^{S f_l d_j *} g_L^{V f_l d_i} \Big] m_{f_k} m_{f_l} D_0 O_5 \Big\}$$

$$\times (m_V, m_{f_k}, m_S, m_{f_l}) \tag{F.15}$$

List of particles:

- Z / down / sneutrino-neutral Higgs / down: couplings from eqs. (A.6), (A.14).

F.7 Vector/fermion/scalar/fermion "fermion-cross" box

Case S colour-triplet:

$$\mathcal{L}_{\text{EFT}} \ni \frac{1}{32\pi^2} \Big\{ g_R^{V f_k d_j *} g_R^{S f_k d_j *} g_L^{S f_l d_i} g_L^{V f_l d_i} \frac{D_2}{4} (O_2 - O_3)$$

$$- g_L^{V f_k d_j *} g_L^{S f_k d_j *} g_R^{S f_l d_i} g_R^{V f_l d_i} \frac{D_2}{4} (\tilde{O}_2 - \tilde{O}_3)$$

$$+ 2 \left(g_L^{V f_k d_j *} g_R^{S f_k d_j *} + g_R^{V f_k d_j *} g_L^{S f_k d_j *} \right) \left(g_R^{S f_l d_i} g_L^{V f_l d_i} + g_L^{S f_l d_i} g_R^{V f_l d_i} \right)$$

$$\times m_{f_k} m_{f_l} D_0 (O_4 - O_5) \bigg\} (m_V, m_{f_k}, m_S, m_{f_l}) \tag{F.16}$$

List of particles:

- W / up / sdown / up: couplings from eqs. (A.13), (A.12); $\times 2$ (π-rotated diagram).

- Z / down / sup / down: couplings from eqs. (A.14), (A.11); vanishes from antisymmetry of λ''; $\times 2$ (π-rotated diagram).

References

[1] S. Strandberg, *Searches for SUSY*, https://indico.cern.ch/event/686555/contributions/ 3028076/attachments/1683895/2706865/SUSYPlenaryICHEP2018.pdf.

[2] https://twiki.cern.ch/AtlasPublic/SupersymmetryPublicResults

[3] https://twiki.cern.ch/CMSPublic/PhysicsResultsSUS

[4] https://twiki.cern.ch/AtlasPublic/ExoticsPublicResults

[5] https://twiki.cern.ch/CMSPublic/PhysicsResultsEXO

[6] ATLAS collaboration, *Search for electroweak production of supersymmetric particles in final states with two or three leptons at $\sqrt{s} = 13\,TeV$ with the ATLAS detector*, *Eur. Phys. J.* **C 78** (2018) 995 [arXiv:1803.02762] [INSPIRE].

[7] P. Bechtle et al., *Killing the CMSSM softly*, *Eur. Phys. J.* **C 76** (2016) 96 [arXiv:1508.05951] [INSPIRE].

[8] H.P. Nilles, *Supersymmetry, supergravity and particle physics*, *Phys. Rept.* **110** (1984) 1 [INSPIRE].

[9] H.E. Haber and G.L. Kane, *The search for supersymmetry: probing physics beyond the standard model*, *Phys. Rept.* **117** (1985) 75 [INSPIRE].

[10] E. Gildener, *Gauge symmetry hierarchies*, *Phys. Rev.* **D 14** (1976) 1667 [INSPIRE].

[11] G.R. Farrar and P. Fayet, *Phenomenology of the production, decay, and detection of new hadronic states associated with supersymmetry*, *Phys. Lett.* **B 76** (1978) 575.

[12] G. Jungman, M. Kamionkowski and K. Griest, *Supersymmetric dark matter*, *Phys. Rept.* **267** (1996) 195 [hep-ph/9506380] [INSPIRE].

[13] H.K. Dreiner, *An Introduction to explicit R-parity violation*, hep-ph/9707435 [INSPIRE].

[14] R. Barbier et al., *R-parity violating supersymmetry*, *Phys. Rept.* **420** (2005) 1 [hep-ph/0406039] [INSPIRE].

[15] A.H. Chamseddine and H.K. Dreiner, *Anomaly free gauged R symmetry in local supersymmetry*, *Nucl. Phys.* **B 458** (1996) 65 [hep-ph/9504337] [INSPIRE].

[16] H.K. Dreiner, C. Luhn and M. Thormeier, *What is the discrete gauge symmetry of the MSSM?*, *Phys. Rev.* **D 73** (2006) 075007 [`hep-ph/0512163`] [INSPIRE].

[17] H.K. Dreiner, C. Luhn, H. Murayama and M. Thormeier, *Proton hexality from an anomalous flavor* U(1) *and neutrino masses: linking to the string scale*, *Nucl. Phys.* **B 795** (2008) 172 [`arXiv:0708.0989`] [INSPIRE].

[18] H.K. Dreiner, T. Opferkuch and C. Luhn, *Froggatt-Nielsen models with a residual* $\mathbb{Z}_4^R$ *symmetry*, *Phys. Rev.* **D 88** (2013) 115005 [`arXiv:1308.0332`] [INSPIRE].

[19] M. Hanussek and J.S. Kim, *Testing neutrino masses in the R-parity violating minimal supersymmetric standard model with LHC results*, *Phys. Rev.* **D 85** (2012) 115021 [`arXiv:1205.0019`] [INSPIRE].

[20] D. Dercks et al., *R-parity violation at the LHC*, *Eur. Phys. J.* **C 77** (2017) 856 [`arXiv:1706.09418`] [INSPIRE].

[21] S. Weinberg, *Supersymmetry at ordinary energies. 1. Masses and conservation laws*, *Phys. Rev.* **D 26** (1982) 287 [INSPIRE].

[22] J.-H. Jang, J.K. Kim and J.S. Lee, *Constraints on the R-parity and lepton flavor violating couplings from B0 decays to two charged leptons*, *Phys. Rev.* **D 55** (1997) 7296 [`hep-ph/9701283`] [INSPIRE].

[23] K.-m. Cheung and O.C.W. Kong, $\mu \to e\gamma$ *from supersymmetry without R-parity*, *Phys. Rev.* **D 64** (2001) 095007 [`hep-ph/0101347`] [INSPIRE].

[24] A. Vicente, *Charged lepton flavor violation beyond minimal supersymmetry*, *Nucl. Phys. Proc. Suppl.* **248-250** (2014) 20 [`arXiv:1310.8162`] [INSPIRE].

[25] D.F. Carvalho, M.E. Gomez and J.C. Romao, *Charged lepton flavor violation in supersymmetry with bilinear R-parity violation*, *Phys. Rev.* **D 65** (2002) 093013 [`hep-ph/0202054`] [INSPIRE].

[26] M. Endo, K. Hamaguchi and S. Iwamoto, *Lepton flavor violation and cosmological constraints on R-parity violation*, *JCAP* **02** (2010) 032 [`arXiv:0912.0585`] [INSPIRE].

[27] K. Choi, E.J. Chun and K. Hwang, *Lepton flavor violation and bilinear R-parity violation*, *Phys. Lett.* **B 488** (2000) 145 [`hep-ph/0005262`] [INSPIRE].

[28] A. de Gouvêa, S. Lola and K. Tobe, *Lepton flavor violation in supersymmetric models with trilinear R-parity violation*, *Phys. Rev.* **D 63** (2001) 035004 [`hep-ph/0008085`] [INSPIRE].

[29] A. Vicente, *Lepton flavor violation beyond the MSSM*, *Adv. High Energy Phys.* **2015** (2015) 686572 [`arXiv:1503.08622`] [INSPIRE].

[30] A. Gemintern, S. Bar-Shalom, G. Eilam and F. Krauss, *Lepton flavor violating decays* $L \to l\gamma\gamma$ *as a new probe of supersymmetry with broken R parity*, *Phys. Rev.* **D 67** (2003) 115012 [`hep-ph/0302186`] [INSPIRE].

[31] C.-Y. Chen and O.C.W. Kong, *Leptonic radiative decay in supersymmetry without R parity*, *Phys. Rev.* **D 79** (2009) 115013 [`arXiv:0901.3371`] [INSPIRE].

[32] Y. Cheng and O.C.W. Kong, *Leptonic flavor violating Higgs to* $\mu + \tau$ *decay in supersymmetry without R parity*, in the proceedings of the 20th *International Conference on Supersymmetry and Unification of Fundamental Interactions (SUSY 2012)*, August 13–17, Beijing, China (2012), `arXiv:1211.0365` [INSPIRE].

[33] A. Arhrib, Y. Cheng and O.C.W. Kong, *Comprehensive analysis on lepton flavor violating Higgs boson to $\mu^{\mp}\tau^{\pm}$ decay in supersymmetry without R parity*, *Phys. Rev.* **D 87** (2013) 015025 [arXiv:1210.8241] [INSPIRE].

[34] A. Arhrib, Y. Cheng and O.C.W. Kong, *Higgs to $\mu + \tau$ decay in supersymmetry without R-parity*, *EPL* **101** (2013) 31003 [arXiv:1208.4669] [INSPIRE].

[35] J. Cao, L. Wu and J.M. Yang, *Lepton flavor-changing processes in R-parity violating MSSM: $Z \to l_i \bar{l}_j$ and $\gamma\gamma \to l_i \bar{l}_j$ under new bounds from $l_i \to l_j\gamma$*, *Nucl. Phys.* **B 829** (2010) 370 [arXiv:0908.4556] [INSPIRE].

[36] M. Gomez and D.F. Carvalho, *Lepton flavor violation in SUSY with and without R parity*, in the proceedings of the *Corfu Summer Institute on Elementary Particle Physics (Corfu 2001)*, August 31–September 20, Corfu, Greece (2001), hep-ph/0204133 [INSPIRE].

[37] H.K. Dreiner, M. Krämer and B. O'Leary, *Bounds on R-parity violating supersymmetric couplings from leptonic and semi-leptonic meson decays*, *Phys. Rev.* **D 75** (2007) 114016 [hep-ph/0612278] [INSPIRE].

[38] H.K. Dreiner, K. Nickel, F. Staub and A. Vicente, *New bounds on trilinear R-parity violation from lepton flavor violating observables*, *Phys. Rev.* **D 86** (2012) 015003 [arXiv:1204.5925] [INSPIRE].

[39] W.-j. Li, Y.-d. Yang and X.-d. Zhang, *$\tau^- \to \mu^- \pi^0 (\eta, \eta')$ decays in new physics scenarios beyond the standard model*, *Phys. Rev.* **D 73** (2006) 073005 [hep-ph/0511273] [INSPIRE].

[40] W. Li, X.-Q. Nie, Y.-Y. Fan, M.-Q. Lu and Y.-w. Guo, *RPV SUSY effects in $\tau^- \to e^- (\mu^-) K\bar{K}$ Decays*, *Int. J. Mod. Phys.* **A 29** (2014) 1450063 [arXiv:1312.2231] [INSPIRE].

[41] G.-C. Cho and H. Matsuo, *Constraints on R-parity violating interactions in supersymmetric standard model from leptonic decays of D_s and B^+ mesons*, *Phys. Lett.* **B 703** (2011) 318 [arXiv:1107.3004] [INSPIRE].

[42] R. Bose, *Rare τ decays in R-parity violating supersymmetry*, *J. Phys.* **G 38** (2011) 065003 [arXiv:1012.1736] [INSPIRE].

[43] Y. Grossman and H.E. Haber, *(S)neutrino properties in R-parity violating supersymmetry. 1. CP conserving phenomena*, *Phys. Rev.* **D 59** (1999) 093008 [hep-ph/9810536] [INSPIRE].

[44] H.K. Dreiner, M. Hanussek, J.-S. Kim and C.H. Kom, *Neutrino masses and mixings in the baryon triality constrained minimal supersymmetric standard model*, *Phys. Rev.* **D 84** (2011) 113005 [arXiv:1106.4338] [INSPIRE].

[45] H.K. Dreiner, J. Soo Kim and M. Thormeier, *A simple baryon triality model for neutrino masses*, arXiv:0711.4315 [INSPIRE].

[46] M. Hirsch, M.A. Diaz, W. Porod, J.C. Romao and J.W.F. Valle, *Neutrino masses and mixings from supersymmetry with bilinear R parity violation: a theory for solar and atmospheric neutrino oscillations*, *Phys. Rev.* **D 62** (2000) 113008 [*Erratum ibid.* **D 65** (2002) 119901] [hep-ph/0004115] [INSPIRE].

[47] B. de Carlos and P.L. White, *R-parity violation and quark flavor violation*, *Phys. Rev.* **D 55** (1997) 4222 [hep-ph/9609443] [INSPIRE].

[48] H.K. Dreiner, G. Polesello and M. Thormeier, *Bounds on broken R parity from leptonic meson decays*, *Phys. Rev.* **D 65** (2002) 115006 [hep-ph/0112228] [INSPIRE].

[49] H.K. Dreiner, K. Nickel and F. Staub, $B^0_{s,d} \to \mu\bar{\mu}$ and $B \to X_s\gamma$ in the R-parity violating MSSM, *Phys. Rev.* **D 88** (2013) 115001 [arXiv:1309.1735] [ɪɴSPIRE].

[50] W. Altmannshofer, A.J. Buras and D. Guadagnoli, *The MFV limit of the MSSM for low* $\tan\beta$: *meson mixings revisited*, *JHEP* **11** (2007) 065 [hep-ph/0703200] [ɪɴSPIRE].

[51] F. Gabbiani, E. Gabrielli, A. Masiero and L. Silvestrini, *A complete analysis of FCNC and CP constraints in general SUSY extensions of the standard model*, *Nucl. Phys.* **B 477** (1996) 321 [hep-ph/9604387] [ɪɴSPIRE].

[52] K. Agashe and M. Graesser, *R-parity violation in flavor changing neutral current processes and top quark decays*, *Phys. Rev.* **D 54** (1996) 4445 [hep-ph/9510439] [ɪɴSPIRE].

[53] D. Choudhury and P. Roy, *New constraints on lepton nonconserving R-parity violating couplings*, *Phys. Lett.* **B 378** (1996) 153 [hep-ph/9603363] [ɪɴSPIRE].

[54] G. Bhattacharyya and A. Raychaudhuri, *New constraints on R-parity violation from K and B systems*, *Phys. Rev.* **D 57** (1998) 3837 [hep-ph/9712245] [ɪɴSPIRE].

[55] J.P. Saha and A. Kundu, *Reevaluating bounds on flavor changing neutral current parameters in R parity conserving and R parity violating supersymmetry from B^0-$\bar{B}^0$ mixing*, *Phys. Rev.* **D 69** (2004) 016004 [hep-ph/0307259] [ɪɴSPIRE].

[56] A. Kundu and J.P. Saha, *Constraints on R-parity violating supersymmetry from neutral meson mixing*, *Phys. Rev.* **D 70** (2004) 096002 [hep-ph/0403154] [ɪɴSPIRE].

[57] S. Nandi and J.P. Saha, B_s-$\bar{B}_s$ *mixing, B decays and R-parity violating supersymmetry*, *Phys. Rev.* **D 74** (2006) 095007 [hep-ph/0608341] [ɪɴSPIRE].

[58] R.-M. Wang, G.R. Lu, E.-K. Wang and Y.-D. Yang, *Probe the R-parity violating supersymmetry effects in the B^0_s-$\bar{B}^0_s$ mixing*, *HEPNP* **31** (2007) 332 [hep-ph/0609276] [ɪɴSPIRE].

[59] R.-M. Wang, Y.-G. Xu, M.-L. Liu and B.-Z. Li, *Reevaluating R-parity violating supersymmetry effects in B^0_s-$\bar{B}^0_s$ mixing*, *JHEP* **12** (2010) 034 [arXiv:1007.2944] [ɪɴSPIRE].

[60] HFLAV collaboration, *Averages of b-hadron, c-hadron and τ-lepton properties as of summer 2016*, *Eur. Phys. J.* **C 77** (2017) 895 [arXiv:1612.07233] [ɪɴSPIRE].

[61] A. Lenz et al., *Anatomy of New Physics in B-$\bar{B}$ mixing*, *Phys. Rev.* **D 83** (2011) 036004 [arXiv:1008.1593] [ɪɴSPIRE].

[62] A. Lenz and U. Nierste, *Numerical updates of lifetimes and mixing parameters of B mesons*, in the proceedings of *CKM unitarity triangle. 6*th *International Workshop (CKM 2010)*, Spetember 6–10, Warwick, U.K. (2011), arXiv:1102.4274 [ɪɴSPIRE].

[63] M. Artuso, G. Borissov and A. Lenz, *CP violation in the B^0_s system*, *Rev. Mod. Phys.* **88** (2016) 045002 [arXiv:1511.09466] [ɪɴSPIRE].

[64] L. Di Luzio, M. Kirk and A. Lenz, *Updated B_s-mixing constraints on new physics models for $b \to s\ell^+\ell^-$ anomalies*, *Phys. Rev.* **D 97** (2018) 095035 [arXiv:1712.06572] [ɪɴSPIRE].

[65] FERMILAB LATTICE, MILC collaboration, $B^0_{(s)}$-*mixing matrix elements from lattice QCD for the Standard Model and beyond*, *Phys. Rev.* **D 93** (2016) 113016 [arXiv:1602.03560] [ɪɴSPIRE].

[66] PARTICLE DATA GROUP collaboration, *Review of particle physics*, *Chin. Phys.* **C 40** (2016) 100001.

[67] J. Bijnens, J.M. Gerard and G. Klein, *The K_L-K_S mass difference*, *Phys. Lett.* **B 257** (1991) 191 [INSPIRE].

[68] Z. Bai et al., *K_L-K_S mass difference from lattice QCD*, *Phys. Rev. Lett.* **113** (2014) 112003 [arXiv:1406.0916] [INSPIRE].

[69] A.J. Buras and J. Girrbach, *Stringent tests of constrained Minimal Flavor Violation through $\Delta F = 2$ transitions*, *Eur. Phys. J.* **C 73** (2013) 2560 [arXiv:1304.6835] [INSPIRE].

[70] J. Brod and M. Gorbahn, *Next-to-next-to-leading-order charm-quark contribution to the CP-violation parameter ϵ_K and ΔM_K*, *Phys. Rev. Lett.* **108** (2012) 121801 [arXiv:1108.2036] [INSPIRE].

[71] G. Buchalla, A.J. Buras and M.E. Lautenbacher, *Weak decays beyond leading logarithms*, *Rev. Mod. Phys.* **68** (1996) 1125 [hep-ph/9512380] [INSPIRE].

[72] A.J. Buras, S. Jager and J. Urban, *Master formulae for $\Delta F = 2$ NLO QCD factors in the standard model and beyond*, *Nucl. Phys.* **B 605** (2001) 600 [hep-ph/0102316] [INSPIRE].

[73] W. Porod, *SPheno, a program for calculating supersymmetric spectra, SUSY particle decays and SUSY particle production at e^+e^- colliders*, *Comput. Phys. Commun.* **153** (2003) 275 [hep-ph/0301101] [INSPIRE].

[74] W. Porod and F. Staub, *SPheno 3.1: extensions including flavour, CP-phases and models beyond the MSSM*, *Comput. Phys. Commun.* **183** (2012) 2458 [arXiv:1104.1573] [INSPIRE].

[75] F. Staub, *SARAH*, arXiv:0806.0538 [INSPIRE].

[76] F. Staub, *From Superpotential to model files for FeynArts and CalcHep/CompHEP*, *Comput. Phys. Commun.* **181** (2010) 1077 [arXiv:0909.2863] [INSPIRE].

[77] F. Staub, *Automatic calculation of supersymmetric renormalization group equations and self energies*, *Comput. Phys. Commun.* **182** (2011) 808 [arXiv:1002.0840] [INSPIRE].

[78] F. Staub, *SARAH 3.2: Dirac gauginos, UFO output and more*, *Comput. Phys. Commun.* **184** (2013) 1792 [arXiv:1207.0906] [INSPIRE].

[79] F. Staub, *SARAH 4 : A tool for (not only SUSY) model builders*, *Comput. Phys. Commun.* **185** (2014) 1773 [arXiv:1309.7223] [INSPIRE].

[80] F. Staub, *Exploring new models in all detail with SARAH*, *Adv. High Energy Phys.* **2015** (2015) 840780 [arXiv:1503.04200] [INSPIRE].

[81] W. Porod, F. Staub and A. Vicente, *A flavor kit for BSM models*, *Eur. Phys. J.* **C 74** (2014) 2992 [arXiv:1405.1434] [INSPIRE].

[82] D. Straub et al., *flav-io/flavio v0.23*, (2017).

[83] K. Fujikawa, B.W. Lee and A.I. Sanda, *Generalized renormalizable gauge formulation of spontaneously broken gauge theories*, *Phys. Rev.* **D 6** (1972) 2923 [INSPIRE].

[84] W. Siegel, *Supersymmetric dimensional regularization via dimensional reduction*, *Phys. Lett.* **B 84** (1979) 193.

[85] D.M. Capper, D.R.T. Jones and P. van Nieuwenhuizen, *Regularization by dimensional reduction of supersymmetric and nonsupersymmetric gauge theories*, *Nucl. Phys.* **B 167** (1980) 479 [INSPIRE].

[86] H.K. Dreiner and M. Thormeier, *Supersymmetric Froggatt-Nielsen models with baryon and lepton number violation*, *Phys. Rev.* **D 69** (2004) 053002 [`hep-ph/0305270`] [ɪɴSPIRE].

[87] B.C. Allanach, A. Dedes and H.K. Dreiner, *R parity violating minimal supergravity model*, *Phys. Rev.* **D 69** (2004) 115002 [*Erratum ibid.* **D 72** (2005) 079902] [`hep-ph/0309196`] [ɪɴSPIRE].

[88] H.K. Dreiner, H.E. Haber and S.P. Martin, *Two-component spinor techniques and Feynman rules for quantum field theory and supersymmetry*, *Phys. Rept.* **494** (2010) 1 [`arXiv:0812.1594`] [ɪɴSPIRE].

[89] S.P. Martin, *Two loop scalar self energies in a general renormalizable theory at leading order in gauge couplings*, *Phys. Rev.* **D 70** (2004) 016005 [`hep-ph/0312092`] [ɪɴSPIRE].

[90] F. Staub and W. Porod, *Improved predictions for intermediate and heavy Supersymmetry in the MSSM and beyond*, *Eur. Phys. J.* **C 77** (2017) 338 [`arXiv:1703.03267`] [ɪɴSPIRE].

[91] M. Goodsell, K. Nickel and F. Staub, *Generic two-loop Higgs mass calculation from a diagrammatic approach*, *Eur. Phys. J.* **C 75** (2015) 290 [`arXiv:1503.03098`] [ɪɴSPIRE].

[92] T. Hahn and M. Pérez-Victoria, *Automatized one loop calculations in four-dimensions and D-dimensions*, *Comput. Phys. Commun.* **118** (1999) 153 [`hep-ph/9807565`] [ɪɴSPIRE].

[93] T. Hahn, *Generating Feynman diagrams and amplitudes with FeynArts 3*, *Comput. Phys. Commun.* **140** (2001) 418 [`hep-ph/0012260`] [ɪɴSPIRE].

[94] B. Chokoufe Nejad, T. Hahn, J.N. Lang and E. Mirabella, *FormCalc 8: better algebra and vectorization*, *J. Phys. Conf. Ser.* **523** (2014) 012050 [`arXiv:1310.0274`] [ɪɴSPIRE].

[95] F. Mahmoudi et al., *Flavour Les Houches accord: interfacing flavour related codes*, *Comput. Phys. Commun.* **183** (2012) 285 [`arXiv:1008.0762`] [ɪɴSPIRE].

[96] J. Brod and M. Gorbahn, ε_K *at next-to-next-to-leading order: the charm-top-quark contribution*, *Phys. Rev.* **D 82** (2010) 094026 [`arXiv:1007.0684`] [ɪɴSPIRE].

[97] ETM collaboration, $\Delta S = 2$ *and* $\Delta C = 2$ *bag parameters in the standard model and beyond from* $N_f = 2 + 1 + 1$ *twisted-mass lattice QCD*, *Phys. Rev.* **D 92** (2015) 034516 [`arXiv:1505.06639`] [ɪɴSPIRE].

[98] HPQCD collaboration, *B-Meson decay constants from improved lattice nonrelativistic QCD with physical u, d, s and c quarks*, *Phys. Rev. Lett.* **110** (2013) 222003 [`arXiv:1302.2644`] [ɪɴSPIRE].

[99] A.J. Buras, M. Jamin and P.H. Weisz, *Leading and next-to-leading QCD corrections to ϵ parameter and* B^0-$\bar{B}^0$ *mixing in the presence of a heavy top quark*, *Nucl. Phys.* **B 347** (1990) 491 [ɪɴSPIRE].

[100] G. D'Ambrosio, G.F. Giudice, G. Isidori and A. Strumia, *Minimal flavor violation: an effective field theory approach*, *Nucl. Phys.* **B 645** (2002) 155 [`hep-ph/0207036`] [ɪɴSPIRE].

[101] J.E. Camargo-Molina, B. O'Leary, W. Porod and F. Staub, *Vevacious: a tool for finding the global minima of one-loop effective potentials with many scalars*, *Eur. Phys. J.* **C 73** (2013) 2588 [`arXiv:1307.1477`] [ɪɴSPIRE].

[102] C.L. Wainwright, *CosmoTransitions: computing cosmological phase transition temperatures and bubble profiles with multiple fields*, *Comput. Phys. Commun.* **183** (2012) 2006 [`arXiv:1109.4189`] [ɪɴSPIRE].

[103] B.C. Allanach, A. Dedes and H.K. Dreiner, *Bounds on R-parity violating couplings at the weak scale and at the GUT scale*, *Phys. Rev.* **D 60** (1999) 075014 [`hep-ph/9906209`] [ɪɴSPIRE].

[104] B.C. Allanach, A. Dedes and H.K. Dreiner, *Two loop supersymmetric renormalization group equations including R-parity violation and aspects of unification*, *Phys. Rev.* **D 60** (1999) 056002 [*Erratum ibid.* **D 86** (2012) 039906] [`hep-ph/9902251`] [ɪɴSPIRE].

[105] A. Abada et al., *Lepton flavor violation in low-scale seesaw models: SUSY and non-SUSY contributions*, *JHEP* **11** (2014) 048 [`arXiv:1408.0138`] [ɪɴSPIRE].